MATERIALS

in

Electronics

Edited by

M. M. Ristić and V. Đ. Mikijelj

INTERNATIONAL INSTITUTE FOR THE
SCIENCE OF SINTERING

and

INSTITUTE OF TECHNICAL SCIENCES
OF THE
SERBIAN ACADEMY OF THE SCIENCES AND ARTS

BEOGRAD/YUGOSLAVIA 1977.

The International Summer School "Materials in Electronics" took place in June 1975, in Hercegnovi, Yugoslavia. Most of lectures which had been received before the beginning of the School were published in short or full versions in No.2, Vol.7 of the Journal "Science of Sintering".

Some of these lectures, being even most interesting, were available, as usually, in the last moment, and some were received after the very beginning of the School or even after its end, so that we couldn't include the same in the School program.

Such papers, as well as some lectures, the final versions of which we found much more interesting than those published in the Journal, are now printed in this book.

We believe that this collection, together with mentioned issue of the Journal "Science of Sintering" can illustrate the School work, as well as some contemporary efforts in researching into the electronic materials science and technology.

EDITORS

Publishing of this Book is supported by the grant of the Republican Community for Science of SR Serbia.

Printed in Yugoslavia
at Faculty for Technology and Metallurgy,
Institute for Printing Tecnology,
Beograd, Karnegijeva 4

C O N T E N T S

PROBLEMS OF OBTAINING MATERIALS WITH DEFINITE PROPERTIES

BY
G.V. SAMSONOV
Institut problem materialovedeniya
AN USSR
Kiev, USSR

Energetics, automatization and materials are the basis of the contemporary scientific and technical progress. In this triad materials occupy a special place, because without their development it is impossible to develop either energetics or automatization in an intensive way. The incessant rise in the working temperature, pressure, rate, then the aggressive influence of external media and radiations more and more reject uses of traditional materials of types such as steel and iron are, and also other metal alloys and ceramic materials, and they require now materials possessing a combined complex of physical, mechanical and chemical properties, able to operate both in superhigh and superlow temperatures under the most complex conditions. Further, if traditional materials took a thousand years to develop and get improved and this procecess is still going on today, new materials must be obtained in the shortest time possible.

The synthesis of new materials requires, in most cases, long and hard experimental work. In order to shorten this process and choose the most effective and the most perspective methods of obtaining the required materials, as well as for the establishment of the possibility of their existence in principle, numerous new

methods have been developed and applied. First of all, one should mention the prognostication of possible chemical compounds by using a computer, which has developed the school of E.M. Savicky, Corresponding Member of AN SSSR[1,2]. The essence of this method is in training an electronic computer of the existing experimental material by using the concord between the composition and the properties of inorganic compounds. Here it appeared that, when the establishment of the concordance and training are concerned, the best results were not obtained by using physical and thermodynamical properties, but by the use of data on the electronic structure of isolated atoms which contain the most complete information on the possibility of formation of compounds. It appeared that the number of prognosticated compounds was by far greater than one could intuitively expect, most likely because up to now all the external conditions (pressure, temperatures, magnetic fields, gravitation) have not been used in experimental work, but which may discover some functions of interatom bonds unknown so far. Although, as Savicki said, "The attempt of the use of an electronic computer for progostications of new compounds was more a question of a postulate than of a solution", the attempt is important because it imposes re-investigations of the fundamental basis of chemistry and physico-chemical analysis - the notions of valency, stoichiometry and thermodynamic equilibrium. Regardless to this problem, the method has already made the creation of new materials possible; further more, it indicates that there are a great number of compounds that have not been synthetized yet but which could be obtained under conditions of intensive excitations of the electronic peripheries.

One of the important ways for shortening the time needed for experiments is the theoretical construction of diagrams of

states and their prognostication by the use of the methods of analogy, statistics and kybernetics (identification by means of an electronic computer[3]). Thermodynamic calculations of state diagrams, developed by D.S. Kamenecka, J.G. Ponyatowsky , I. Aptekar and Kaufmann, are based on model conceptions of physico-chemical or quantum-statistical character: the approximation of ordinary and ideal dissolutions, as presentation of a solid dissolution by means of an abstract model system.

By the application of the method of similarity, developed by the school of Academician G.S. Pisarenko, AN USSR[45], enables determinations of temperature ranges in which the similarity of structural changes is possible and as a result of this - similarity of diagrams of lasting strength; during prognosticating of the characteristics of lasting strength up to looooo hours, the variable change of the stress value can be established, in a pretty reliable way, from the results of the examination of materials by carrying out only a few meetings during loooo hours, as a total number. This includes extrapolation in the case of uniform dependence of properties on the composition or the external factors.

The essential shortening of experiments also makes the use of the method of mathematical programming possible[6].

Quite a number of the prognostication methods of obtaining material with predicted properties are based on the technique of multivariation analysis - discovery of a definite limited number of parameters, by means of which could be expressed the majority of physico-chemical properties of elements, alloys and compounds. Important results have been obtained by the multi-variation analysis, based on the use of the system of the non polarized ion radii, developed by E.V. Prihodko[7] as well as of notions of the contact potential, as the most important parameter of a multi-

compnet system, especially in a solid dissolution (A.K. Beskrovny[8]) that is to say,the application of the notion of discretion of electronic potentials, developed by V.M. Karashchuk[9], according to whom electronic concentrations in which the qualities, changed jumpingly, can have only one of the values of a definite discrete order of numbers. A very useful and productive variant of the multivariation analysis, worked out by S.A. Kutolin[10], with the application of N.I. Kobozev's ideas, is a system of notions, based on the disorder of the physico-chemical system. By means of this system it is possible to characterize the system thermodynamic state: order-disorder, the measure characterizing the equilibrium between the ordered (vectorial - free energy and its application) and disordered (the Brownian-temperature production and changes in entropy) energy forms which characterize the physico-chemical properties of inorganic materials.

In spite of the enormous usefulness of the methods of multivariation analysis for the creation of new substances and materials as well as for the shortening of the time needed for experiments, all of them are based on the already obtained experimental material and mainly respond to the question "how", but not to "why"; and this characterizes the very nature of their limitation, independently of the fact that by their application it is possible to link the composition and the technology of materials with their properties in a direct way (Fig. 1., fuction Ø).

The task of the material prognostication, in a general case, consists of finding out functional bonds between the technology, composition and properties. The difficulty in solving it is in the following:

a) even some simpler F function of a direct bond (properties= Ø (technology)) is often complicated and insufficitently studied;

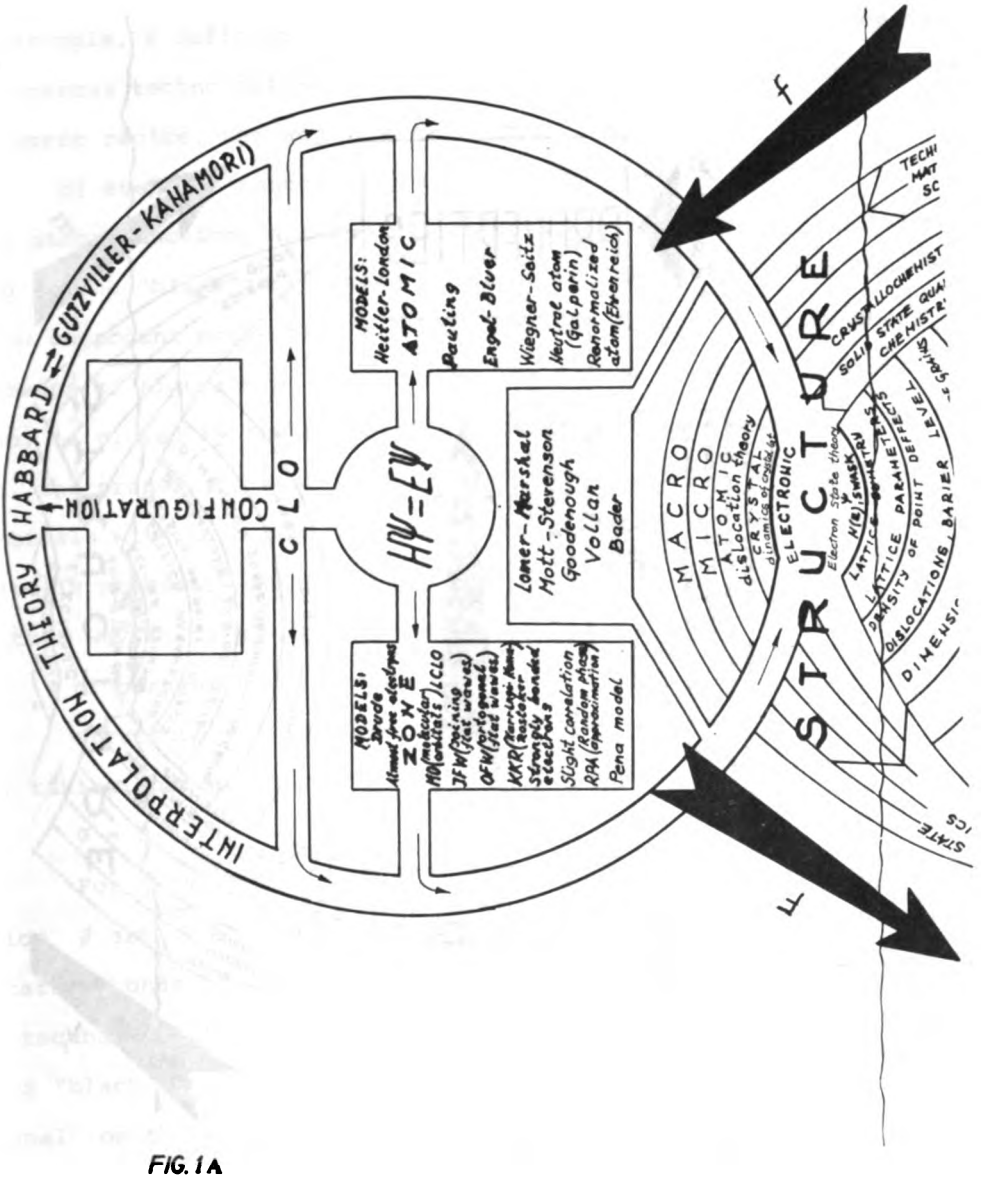

FIG. 1A

PRINCIPLES OF PROGNOSTICATION OF MATERIAL PROPERTIES

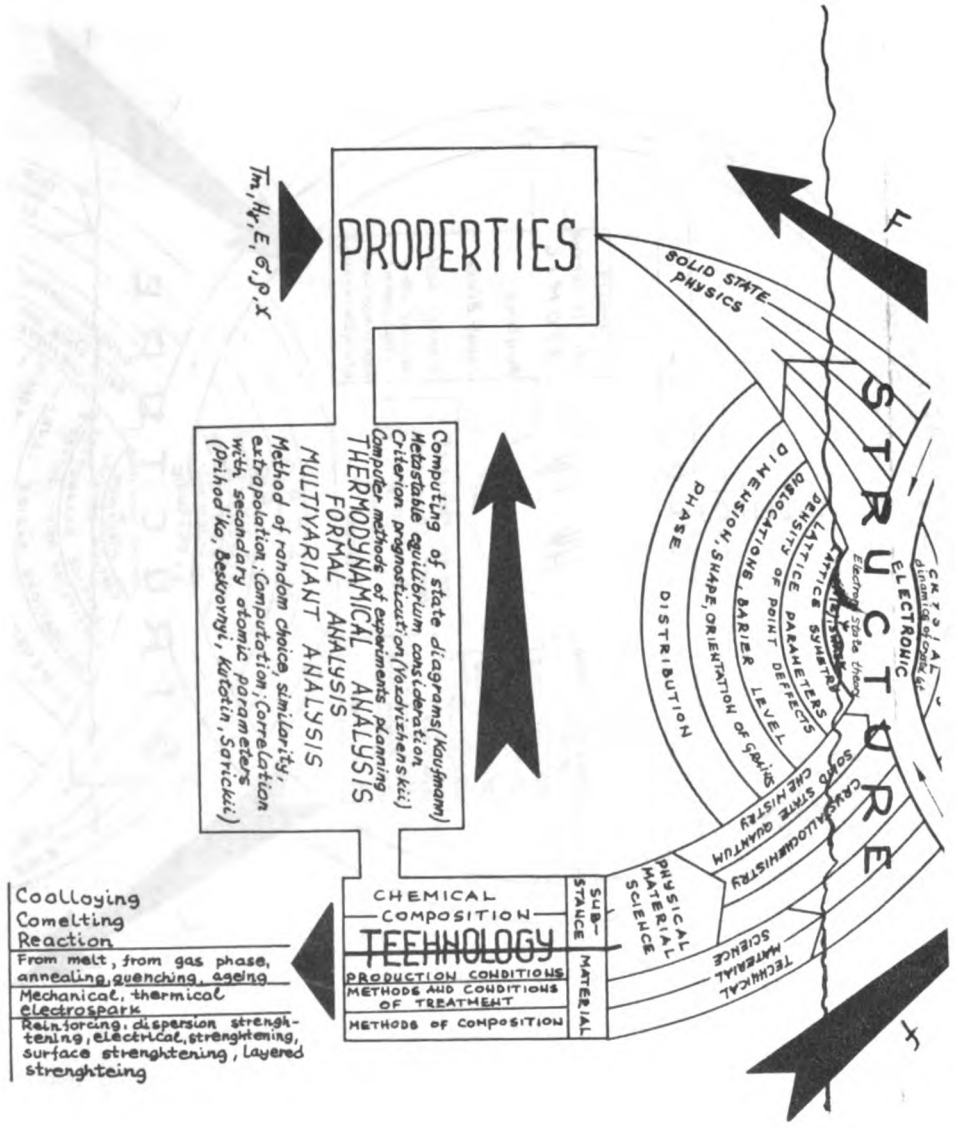

FIG. 1B

PRINCIPLES OF PROGNOSTICATION OF MATERIAL PROPERTIES

b) the inverse function $\emptyset$ is most frequently equivocal as, for example, a definite material strength may be obtained by means of numerous technological processes - by varying of composition, the treatment régime, the way of obtaining);

c) even the function $\emptyset$, in a general case,is the term of some other function, and for its determination there is only the method of the "black case", when no model of interaction is given, but a few component properties are used and the final result is obtained by means of algorithms. The role of the "black case", in a given case, is played by the material structure through which, in principle, the properties must be expressed (for example, for obtaining materials with high temperatures of transition into super-conductive state is necessary to increase the state density at the Fermi level). In this way it is possible to write:

properties = F (structure)

structure = f (technology),

or, taking into account that the properties= $\emptyset$ (technology):

$$\emptyset = F \cdot f.$$

For this reason, possibilities of investigations of the function $\emptyset$ are limited by the establishment of the correlative, quantitative bonds "property-property", "property-composition", "property-technology" if the structure is not considered concretely, but as a "black case" for which only the dependence of the "coming-in signal" on the "coming-out Signal" is known). Such an approach is characteristic only for the earliest stage of the development of the materials science; during further stages of the evolution of the materials science the category "structure" gains an important role, through which, as through a parameter, the function $\emptyset$ is obtained. The notion structure has the central position in the scheme

Fig. 1., because it is the structure that is determined from the "first principles", for example, from the laws of the quantum mechanics (the equations of Schrödinger and Dirack) and the quantum statistics. Of no less importance is the fact that the structure is not only some theoretical abstraction but can also be controlled experimentally, similar to the technological parameters and properties.

In a general case "structure" may be presented in the form of a hierarchy succession of "substructures", the roughest stage of which one must take to be macrostructure, then follow microstructure (grain boundaries), atomic structure (impurities, defects, dislocations) and crystal structure; the basis of all these is the electronic structure (Fig. 1.) The dependence of each substructure on technological parameters may be expressed only in terms of definite values referzing to the substructures of the deeper level: microstructure is the function of atomic structure, atomic one is the function of the crystal, the crystal is the function of the electronic structure. The electronic structure is the deepest level of the knowledge of matter, its nature, and the research into it symbolizes the beginning of the final stage of the development of the contemporary materials science. The electronic structure itself, at the existing lavel of knowledge, cannot be reduced to some deeper substructure (although "the electron is inexhaustible as well as the atom") and must be derived from the "first principles" - the most basic laws describing the motion of matter. Schrödinger´s equation is such a principle for the electronic structure.

This equation cannot be solved exactly and is necessary to develop the system of approximations for theoretical consideration of the electronic structure and the establishment of the whole

chain: property-structure-technology. Two, in principle, possible ways of describing the multiatomic system are based on the presentation of its composition from atoms or electrons and ions; this corresponds to the atomic and zone interpretations of the electronic structure. Each of these interpretations, with a rather great approximation, should lead to a regular picture of the crystal; however, some of the properties (chemical ones and diffusion) may be described in a simpler and more productive way within the atomic theory, while some other (for example, kinetic ones) are simpler comprised by the zone concept.

At the very beginning of the development of the solid state physics, this physics was based on the principle of the translative symmetry and the thesis of the particular role of the point group of symmetries of the Brave lattice, and also on the monoelectronic approach to the solution of Schrödinger´s equation for crystal. This has lead to some very important results - to the comprehension of the complex n-p conductivity, to the comprehension of the nature of dielectrical, semi-conductive and metal properties of the solids; the analysis of the interaction between conductive electrons and phonons made the interpretation of the phenomenon of the superconductivity as well as of numerous accompaning laws possible. Still, while we are waiting for the creation of a theory by which the construction of substances with prognosticated properties would be possible, the contemporary technology of the materials science, as a basic instrument, does not use physics but the chemistry of the solid state. Obviously the reason for this is not the simplicity of chemical conception operating with eviden comprehensions of the chemical bond types, when compared with more strict quantum-chemical concepts, but because the level of the application of the notion of any complexity is determined by the

degree of their use in the practice. The situation can partly be explained by the complicated operation of computer calculations of the monoelectronic energetic spectrum of the solid body, but the most important fact is, however, that any precision, no matter how high it is, of the monoelectronic zone calculations of the interpretation of a series of notions within the zone theory is either impossible or very complicated. This refers, first of all, to the chemical properties, because during the transition to the monoelectronic zone picture, the basic quantum numeral becomes the wave vector which is determined by the translative symmetry, and the atomic quantum numerals lose their importance completely; at the same time the spin bond scheme of Hund's rule is vanished, i.e. vanishes a great part of the internal atomic interactions that characterize the chemical individuality of elements. Formally, the zone concept (which is very attractive because of its development and because it is based on the non-model conceptions of the group theory) will completely lose its own importance if only one place of the structure of its translative invariant is disturbed. In other words, such a theory could hardly be applied, even with some unknown degree of the interpolation accuracy, to real crystals with defects, dislocations and impurities (if crystals are not of medium size) as well as to compounds within their homogeneity. For the same reason within this theory is much more difucult the interpolation of many qualities which are called atomic - catalytic activities, contact interactions, and the adsorption abilities, whose disappearance is connected with the existence of the surface and derangement of the crystal translative symmetry.

Contrary to the zone theories, the atomic theories do not

have majority of the quoted disadvantages. They apriori take into account the chemical individuality of elements, as for them the conception of isolated atom is the starting one. They do not exaggerate the role of the translative symmetry in the formation of the electronic structure and properties of crystals, and finally, the conception of "from an isolated atom - towards a solid body" is the most consitent from the standpoint of the theoretical aspect and the most useful for the practice. It contains the genetic bond of atoms both in the isolated and condensed states, and it can be the basis for the prognostication of qualities of complex systems.

It would be the most useful obviously if the best principles of the both approach could be united, and this can be fulfilled by the configuration model which establishes the genetic unification of these approaches - the zone approach and the atomic one and reflects the qualities of the space localization and the energetic collectivization of electrons.

In each of the three directions (atomic, zone, configuration) a series of models have been developed which either exclude or determine or complete one another. There are also a number of models whose basic postulates do not directly follow from the laws of the quantum physics or from the physics of the solids. In Fig. 1. they were inserted in the square which has no direct graphic way out towards Schrödinger's equation, but it is topologically connected with the area that is marked as "the electronic structure" (models of Lomer- Marshal, Mott-Stivenson and others).

In Fig. 2, is given the scheme that illustrates the genetic bond between the energetic spectra (zone structures) of the transient metal within the configuration and zone models. In this

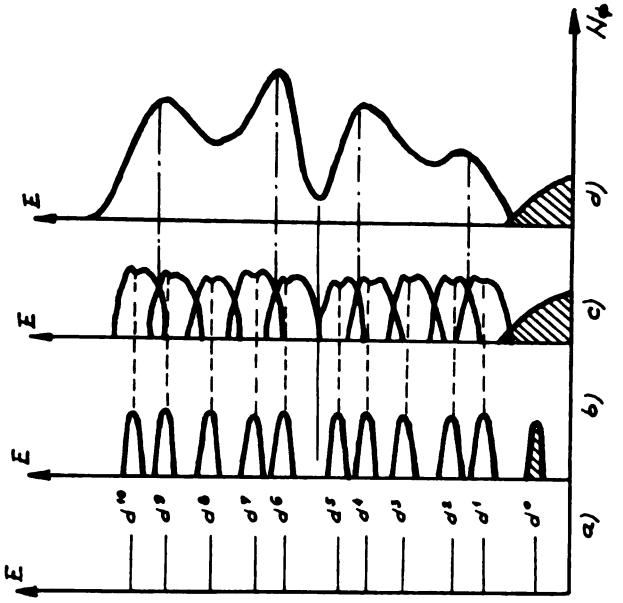

Fig. 2. Transition of the isolated atom electronic configurations towards the Fermi density in the order d-metals.

picture the part a) shows the arrangement of levels on d-orbital, which correspond to different configurations of the isolated atom. During the transition from isolated atoms towards solid bodies, the levels d^n stretch into quasi-particle zones, and this is conditioned by the fluctuation of configurations on the lattice knots (Fig. 2b); during further approach of atoms occurs covering of the levels (Fig. 2c), but not uniformely, in dependence on the configuration energetic stability; in Fig. 2d is shown the law of the state density change at the Fermi level in the order d-metals in the function of the number of completing of d-orbital or energy corresponding to d-states, experimentally observed. One can see that it is a typically zone characteristic, which is determined experimentally.

One of the variants of the matter configuration models in condensed state is the model based on the following assumptions[12]:

1. The existence of two sub-systems of valent elctrons -

partly localized and collectivized - is possible in the condensed matter state.

2. The electrons of the first of the quoted sub-systems (in distinction from the other) should not be described in the crystal in the approximation of the Bloch monoelectronic waves, but in the approximation of configuration fluctuations at each knot of the lattice, from one state to another, within short periods of time (10^{-14}sec. starting from the principle of indeterminacy).

3. Energetically the most stable states in the spectrum of configurations are free, semi-completed and fully completed configurations (the atomic stability); semi-completed configurations (d^5, f^7, sp^3) are the most effective in the sense of the formation of the interatomic bond (binding stability).

4. The stability of the electronic configurations is the function of the principal quantum number of electrons out of which they are formed.

For determination of the localization degree of valent electrons in the energetically stable configuration may be used the results of the X-ray spectral examinations of the valent electron distribution in localized and unlocalized zones; these results were obtained by the school of M.I. Korsunski [13,14]. According to these results, for example, out of 4 zirconium valent electrons 2.6 electrons can be considered as localized, but 1.4 electrons are free; of 5 niobium electrons 3.8 are localized, and 1.2 electrons are collectivized.

If we assume that in the configuration spectrum energetically the most stable configurations prevail and neglecting, in this way, other configurations of the spectrum, it is possible to define the statistical weights of the energetically stable configurations (Tab.I).

Table I d^5 SWASC in transient metals

Group III		Group IV		Group V		Group VI	
Element	Weight	Element	Weight	Element	Weight	Element	Weight
Sc	16	Ti	43	V	63	Cr	73
Y	23	Zr	52	Nb	76	Mo	88
La	24	Hf	55	Ta	81	W	96

When which belonging to groups III-V are concerned, with the increasing temperature increases the localization degree in stable configurations due to the reduced portion of unlocalized s-electrons (s-d-transition; with metals of molydbenum and tungsten types, which have great weight of d^5-configurations, the localization decreases with the increasing temperature (d-s-transitions are mainly realized). This is directly connected with the explanation of the nature of the polymorphism. It is known, for example, that the transient metals of gropu IV (Ti, Zr, Hf) have SC-lattice at ordinary temperatures, but at definite temperatures they endure a phase transformation, passing into VC-phases (α-β transition), while the metals from groups V and VI get crystalized only in the VC-lattice. Such a transition from SC-VC-metals into CC-metals occurs aproximately at the localization degree which is 60%. M.I.Korsunski, with his collaborators, has examined the increasing localization degree during heating of zirconium; however, if the portion of the localized electrons for α-Zr is, according to the results of the X-ray spectrum analysis, 2, 6 out of 4 valent electrons, then for β - Zr at 1500°K is 3. 3, from which follows that the localization degree in α-β - transition increases from 52 up to 66%.

In this way, in order to decrease the temperature of α-β transition of metals from group IV, it is necessary to introduce acceptor impurities which help binding of free electrons, but for

Table II

Statistical Weight of stable electron configurations in transient metals (neglecting intermediary spectrum)

Metal	Configuration of the valent electrons of isolated atom	Degree of localization in metal				Statistical weight of the stable configuration SWASC		
		quantity of electrons localized in configuration d^5	quantity of electrons localized in configuration d^{10}	general quantity of localized electrons	quantity of collectivized electrons	d^0	d^5	d^{10}
Sc	$3d^1 4s^2$	0,8	0	0,8	2,2	84	16	0
Ti	$3d^2 4s^2$	2,2	0	2,2	1,8	57	43	0
V	$3d^3 4s^2$	3,2	0	3,2	1,8	37	63	0
Cr	$3d^5 4s^1$	3,5	0	3,5	2,5	27	73	0
Fe	$3d^6 4s^2$	2,7	4,6	7,3	0,7	0	54	46
Co	$3d^7 4s^2$	1,4	7,2	8,6	0,4	0	28	72
Ni	$3d^8 4s^2$	0,6	8,8	9,4	0,6	0	12	88
Cu	$3d^{10} 4s^1$	0,4	9,2	9,6	1,4	0	8	92
X	$4d^1 5s^2$	1,4	0	1,4	1,6	73	27	0
Zr	$4d^2 5s^2$	2,6	0	2,6	1,4	48	52	0
Nb	$4d^4 5s^1$	3,8	0	3,8	1,2	24	76	0
Mo	$4d^5 5s^1$	4,5	0	4,5	1,5	12	88	0
Ru	$4d^7 5s^1$	4,0	2,0	6,0	2,0	0	80	20
Rh	$4d^8 5s^1$	3,0	4,0	7,0	2,0	0	60	40
Pd	$4d^{10} 5s^0$	0,9	8,2	9,1	0,9	0	18	82
Ag	$4d^{10} 5s^1$	0,2	9,6	9,8	1,2	0	4	96
La	$5d^1 6s^2$	1,2	0	1,2	1,8	76	24	0
Hf	$5d^2 6s^2$	2,7	0	2,7	1,3	45	55	0
Ta	$5d^3 6s^2$	4,1	0	4,1	0,9	19	81	0
W	$5d^4 6s^2$	4,8	0	4,8	0,2	4	96	0
Re	$5d^5 6s^2$	4,7	0,6	5,3	1,7	0	94	6
Os	$5d^6 6s^2$	4,2	1,6	5,8	2,2	0	84	16
Ir	$5d^7 6s^2$	3,4	3,2	6,6	2,4	0	68	32
Pt	$5d^9 6s^1$	2,0	6,0	8,0	2,0	0	40	60
Au	$5d^{10} 6s^1$	0,5	9,0	9,5	1,5	0	10	90

the decrease - the introduction of donor impurities, "deluting agents", that have d^5-configurations. This gives an opportunity of the directed alloying of titanium, zirconium and hafnium together with the obtaining of the prognosticated properties. It is interesting that vanadium, which is by its weight a d^5-configuration, is almost at the border of the phase transition SC-VC, because, being in pure from a VC-metal, during slight contamination by donor impurities, may pass into VZ-form, but by its other properties it seems to be on the border between IV and V groups, and this is also expressed in the other properties of its inorganic compounds.

The model may be used for the evaluation of compositions alloys with the extreme properties and which are conditioned by the maximum localization of valent electron of components in the most stable d^5 - states:

$$\frac{X_B}{X_A} = \frac{5-n_A}{n_B}$$

where n_A, n_B are the quantities of the localized electrons of A and B alloy components, X_A, X_B the conents of components in the alloy.

As shown in Fig. 3., in alloys W - Re, for example, the maximum localization of valent electrons in d^5-states correspond to the maximum values of the Hole constant, Van-Flek paramagnetism, the apsolute thermoelectromotor forces and the minimum values of the concentration resistance coefficient and the parameter of position annihilation.

As the formation of compounds is generally the most probable in cases when the electronic equilibrium enables the formation of the most stable electronic configuratuons, then on this basis

is possible to prognosticate probabilities of compound formations.

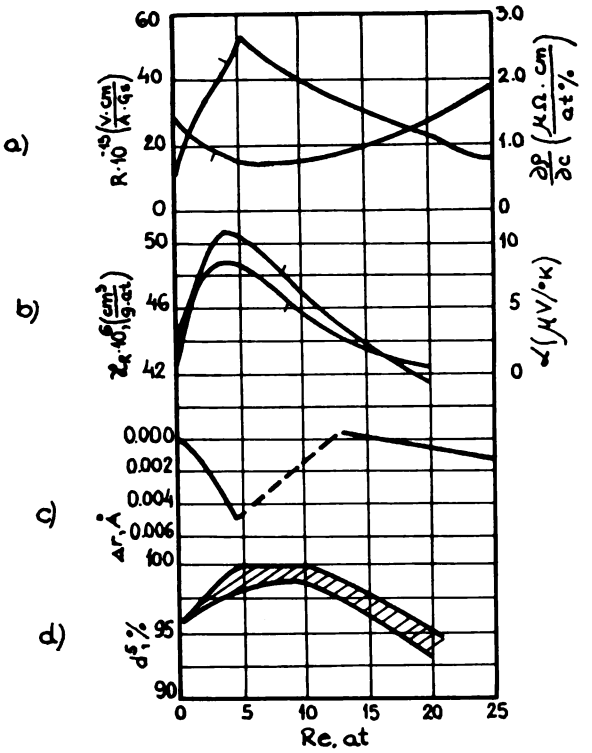

Fig. 3. Change in the localization degree in d^5configuration and alloy qualities in the W-Re system.

For example, in Fig. 4., according to Marhasev's data[15], is shown that the formation of compounds occurs, in most cases, when one of the components on d-orbit has less than 5 electrons, and the other one more; their combination offer the greatest possibility of d^5-localizations.

The localization in d^5-state causes the increase in the melting temperature of metals (Fig. 5) even more so if the principal

	IIIA d^0s^2	IVA d^1s^2	VA d^3s^2; d^4s^1	VIA d^5s^1; d^5s^2	VIIA d^5s^2; d^6s^1	VIIIA d^7s^2; d^7s^1	VIIIB d^8s^2; d^8s^1	VIIIC d^9s^2; $d^{10}s^1$; $d^{10}s^2$	IB $d^{10}s^1$
IIIA	no	no	no	no	9	14	12	24	22
IVA	no	no	2	6	13	10	10	31	31
VA	no	2	no	2	9	7	13	15	2
VIA	no	6	2	no	5	12	4	1	no
VIIA	9	13	9	5	no	2	2	no	2
VIIIA	14	10	7	12	2	no	no	no	no
VIIIB	12	10	13	4	2	no	no	no	no
VIIIC	24	31	15	1	no	no	no	no	no
IB	22	31	2	no	2	no	no	no	no

Fig. 4. Formation statistics of intermetallides in binary systems.

quantum number of valent electrons is bigger; with rare earth metals the approximation to stable f^7 and f^{14}-states causes the increase in the melting temperature, and the appearance of electrons above already formed stable states in Eu and Yb, causes the anti-binding effects, and they are manifested in the abrupt decreases in the melting temperature (Fig. 6).

The solution of the important task of the formation of solid materials, which are elastic at the same time, is connected with the formation of strong localizations which enable obtaining high strenght with unlocalized electrons that are responsible for plasticity. Certain plasticity of hard tungsten-carbide, based on this combination, conditions the use of it for more than fifty years, in fact obligatory, in hard alloys used for machining of metals; the substitution of tungsten carbides in hard alloys is

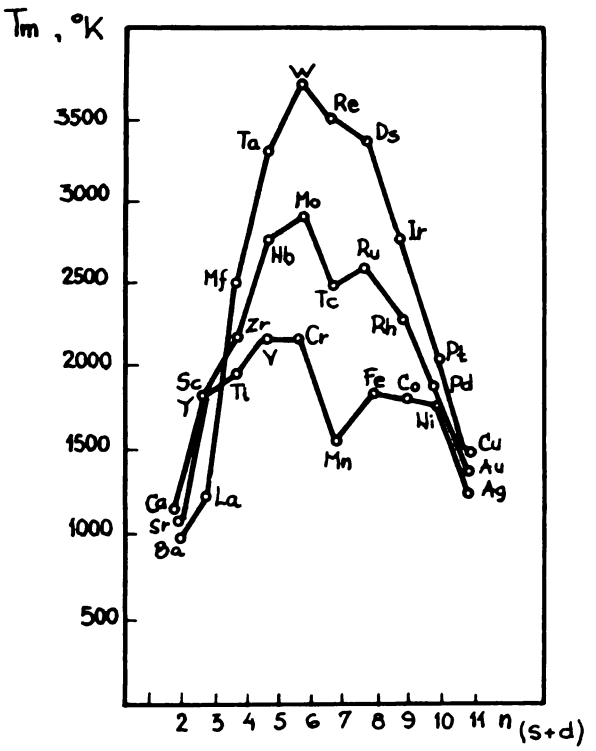

Fig. 5. Melting temperature of d-transient metals.

possible by means of alloying non-plastical titanium-carbides by nitrogen, whose atoms substitute a part of carbon atoms in carbide inserting over four valent electrons of carbon (wich form sp^3-hybride responsible for the high hardness) supplementary electron that makes the plastification of carbides possible. In exactly the same way certain plastification of diamond may be performed, which is necessary for the relaxation of the stresses formed in the surface layers, and which are treated by diamond material. In a cubic boron-nitride, which has diamond structure, the nitrogen atom, that is "superfluous" in relation to sp^3-hybride, migrates betwe-

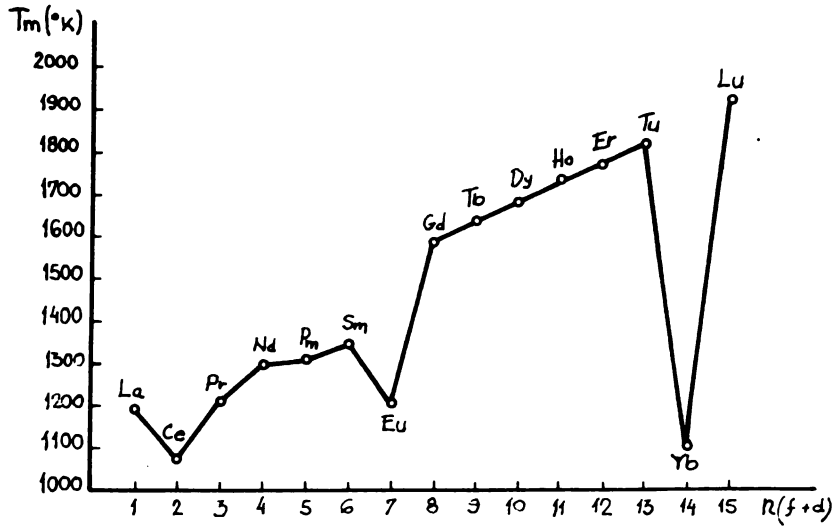

Fig. 6. Melting temperature of f-transient metals.

en atoms of nitrogen and boron, making for the boron to produce p^3-hybrides statistically possible and, in comparison with diamond, some plastification of nitride.

It is of interest to stress that for a milliard years Nature has not solved the problem of strength and plasticity bonding in one substance, so that this has caused formation of composite materials in which the plastic matrix bonds with the high-module strengthening[14]; a typical example of materials created by Nature is the wood mass, in which the soft, plastic lignin is strengthened by hard threads of cellulose.

Gradual development of theoretical approximations, which make construction of material with prognosticated properties possible, will undoubtedly lead to significant results, however, the level of the corresponding material properties will not be very high

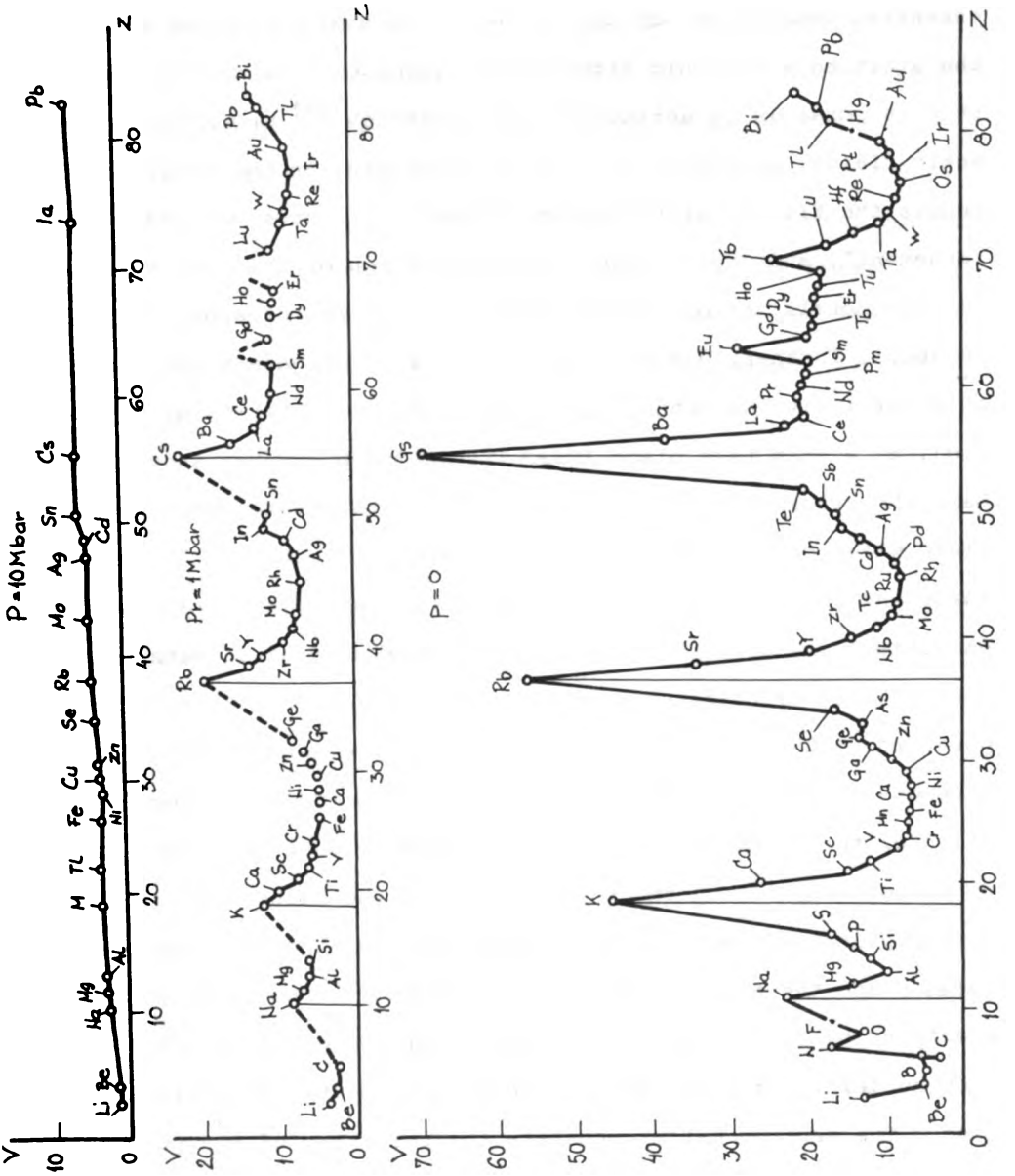

Fig. 7. Change in specific volumes of element with pressure.

because the possibilities are also limited by the usual picture of the electronic atom orbits existing in common conditions. For the essential improvement of properties of substances and materials, the starting electronic structure of atoms must be changed, and this is possible by acting of high pressures[18] and strong magnetic fields. During the increasing pressure, in the beginning, occurs the filling of the external electronic orbits, their "arrangement", and then follows the liquidation of this arrangement and the metallization of the matter (during the pressure up to 1 megabar); further, during pressures of 1.5-2 megabars the liquidation of individual chemical elements and degeneration of the periodical system take place (Fig. 7); during pressures above 10 megabars the transition into the superdense metal state occurs, the state which consists of the nucleus and the electronic "liquid". Hardening of the high pressure phases by the striking wave has been achieved, and in this way also the obtaining of a "metal diamond" whose strength ought to be up to 40 t/mm^2 and melting temperature 23000°C; supernitrogen ought to have density of 25 g/cm^2, strength of 280 t/mm^2, melting temperature of 80000°C. The formation of the superconductive hydrogen during such pressures is conditioned by the enormous importance of the magnet field of so a cold planet as Jupiter is. Under pressures above 10^{14} megabars takes place the neutronization of the matter - the grasp of the electrons by nuclei and transformation of protons into neutrons Such nuclei exist up to 10^{18} megabars having density up to 10^{11} g/cm^3. The neutron matter consists the periphery of the pulsars and is in the superfluid and superconductive state there.

Recently A.A. Abrikosov has experimentaly demonstrated

the transition of semi-conductors into metals and some other transitions of the matter under the influence of strong magnet fields. According to our data even in moderate magnet fields of the order of 30 kilo Oersted the melting temperature of gallium decreases for 7^{o} and that of tin for 0.6, due to the weakening of the localization of valent electrons[17].

In this way the application of strong excitations, reorganizations of the electronic orbit, change of the very chemical individuality of elements offer great possibilities for the formation of new materials with exceptionally good properties and for their combinations unreached for the time being.

(Translated by S.M.Radić and Lj.Popović).

References

1. E.M.Savickii, Vestnik AN SSSR, No.1, 33, 1975.
2. E.M.Savickii, V.B.Gribulya, in "Fiziko-himicheskie issledovaniya v metallurgii i materialovedenii s primeneniem EVM", "Nauka", Moskva 1974, p.71.
3. V.M.Vozdvizhenski, Prognoz dvoinyh diagramm sostoyaniya, "Metallurgiya", Moskva, 1975.
4. V.I.Kovpak, Problemy prochnosti, No.7, 88, 1971.
5. V.I.Kovpak, Problemy procznosty, No.2, 24, 1975.
6. V.V.Nalimov, Teoriya eksperimenta, "Nauka", Moskva, 1971.
7. E.V.Prihodko, Sistema nepolyarizovannyh ionnyh radiusov i ee ispolzovanie dlya elektronnogo stroeniya i svoistv veshchestv, "Naukova Dumka", Kiev, 1973.
8. A.K.Beskrovnyi, Chernaya metallurgiya, No.lo, 138, 1973.
9. V.M.Karashchuk, Trudy MIIZHT, Vyp. 165, Moskva, 1963, p.16.
lo. S.A.Kutolin, in "Polyprovodnikovye pribory", vyp. 4o4, Moskva, 1968.
11. N.I.Kobozov, ZJFH, 35. 2736, 1961.
12. G.V.Samsonov, I.F.Pryadko, L.F.Pryadko, Konfiguracionnaya model veshchestva, "Naukova Dumka", Kiev, 1971.
13. M.I.Korsunski, Ya.E.Genkin, Izv. AN SSSR, Ser. fiz., 28, 832, 1964.

14. M.I.Korsunski, Ya.E.Genkin, Izv. AN SSSR, Neorg. Materialy, 1, 17ol, 1965.
15. B.I.Marhasev, Izv. AN SSSR, Metally, No.5, 17o, 197o.
16. Sovremennye kompozicionnye materialy, ed. L.Brautman and P.Kroka, "Mir", Moskva, 197o.
17. G.V.Samsonov, I.M.Vinicki, B.M.Rud, Dopovidi AN USSR, seriya "A", No.11, 1o45, 1974.
18. P.Savić, Serbian Acad. Sci., Monographs, Vol. CCCLI, No.29(1962).

SYNTHESIS OF HEXAFERRITES: EFFECTS OF IMPURITY AND DEVIATIONS FROM STOICHIOMETRY

BY
A.L.STUIJTS AND G.S.KRIJTENBURG
Philips Research Laboratories
and Eindhoven University of Technology
and
ELCOMA, Ceramics Development Lab.
N.V.Philips'Gloeilampenfabrieken

Introduction

The permanent magnetic properties of ceramic hexaferrites are determined by three factors:

1. the degree of orientation (crystallographic texture), f, of the crystallites,
2. the apparent density, d, and
3. the grain size of the sintered magnet.

Variations in the saturation magnetization, $_{s}$, and the crystalline anisotropy, H^{A}, are in general small and will be neglected.

The remanence, B_r, can be expressed as

$$B_r = 4 \quad _s \times d \times f \qquad (1)$$

Maximum remanence is obtained for the highest apparent density, d, and at the highest value of the degree of orientation, f.For a perfect texture f equals 1. In isotropic specimens f equals 0.5.

The coercive force, $_{I}H_{C}$, is related to the grain size. In order to obtain high $_{I}H_{C}$-values a small grain size is required. The maximum value of the energy product $(BH)_{max}$ is only obtained if $_{I}H_{C}$ in Oersteds is larger than $B_r/2$ in Gauss. For many important applications even higher $_{I}H_{C}$ values are required.

Both requirements, a high sintered density and a small grain size, generally cannot be fulfilled in sintering pure compounds (1). Fundamental investigations on sintering seem to indicate the experimental fact that in pure powder systems shrinkage and grain growth are concurrent processes. A relation often observed is:

$$\bar{D}\ P^n = \text{constant} \qquad (2)$$

where $\bar{D}$ is the mean grain size, P the porosity and n some constant (1). Processing conditions, such as heating cycle, pressed density, etc., determine very much wheter the above relation is fulfilled or a less favourable combination of $\bar{D}$ and P is obtained.

Relatively few publications have appeared in literature which give an analysis of the main factors which determine the sintering behaviour of hexaferrites. It is common practice in the fabrication of hexaferrites to use an excess of earth alkali oxide. This also holds for Sr-hexaferrites although no systematic investigation on this subject has been published. The role of an excess earth alkali oxide has been attributed to a beneficial effect on the sintering properties either by the formation of an appropriate defect structure (2), or by the action of the liquid phase which is present above the eutectic temperature (3). Also it is applied sometimes to compensate pick-up of iron during milling or volatilization of earth alkali oxide (4).

The important place which ceramic permanent magnets have acquired in practice has primarily to be attributed to the low cost of the material compared to materials with much better magnetic properties. In the technical development, therefore, the introduction of cheap raw materials, even minerals, play an important role. It is very well possible in practice to eliminate variability caused by physical parameters of the raw materials (5). Also it is of great advantage for practice that many impurities do not substantially affect the magnetic properties of the sintered magnets.

The role of impurities in the sintering of hexaferrites can roughly be divided into three categories.

A. Impurities which do not affect the intrinsic magnetic properties, nor change the relation (2).

These impurities dilute the magnetic phase, However, it is very well possible that the impurity affects the sintering process in such a way that, for given process conditions, a better combination of $\bar{D}$ and P can be obtained. These impurities are called modifying agents. In general adjustment of the processing conditions will lead to a better result, but is not always possible in practice.

B. Impurities which change the intrinsic magnetic properties

$_s$ and H^A by entering into solid solution of the main magnetic phase. Well known examples are Al_2O_3 and Cr_2O_3, which increase H^A and decrease $_s$(6). These impurities have little or no effect on the sintering behaviour, but increase $_IH_c$ and decrease B_r.

C. Impurities which essentially change the relation (2) by suppressing grain growth during sintering and/or improving sintering rate. Suppressing grain groeth is very important for obtaining high values for $_IH_c$. The most effective means in practice appears to be the formation of a wetting liquid phase at the sintering temperature (4). Addition of SiO_2, or a silicate, is most widely used in practice, although other additions are possible.

In order to fabricate magnets in a reproducible way, it is necessary to understand and control the effect of impurities present in the raw materials. This is the more important as most impurities appear to be present in a variable quantity.

The role of anionic impurities in the raw materials has been little dealt with in literature. In the case of iron oxide usually some sulphate or up to one percent of chlorine can be present. The sulphate decomposes during prefiring, partly forming the more stable Sr- or Ba-sulphate, partly evaporating as SO_2 and O_2.

Sulphate forms a very common impurity in technical grade Sr-carbonate. The carbonate is generally synthesized from a natural sulphate (7) and, depending on the processing conditions, the sulphate content will be greater or smaller. It has been stated in literature that $SrSO_4$ present during sintering has a beneficial effect on the magnetic properties (8).

Although it is known that Fe_2O_3 lowers the decomposition temperature of $SrSO_4$ (7), we found degree of conversion depends very much on the experimental conditions, such as mixing degree and packed density. In the case of $BaSO_4$ hardly any reaction with Fe_2O_3 occurs.

In this paper a report is given of studies of the effects in strontium hexaferrite of:

1) excess SrO (Fe_2O_3/SrO mole ratio n 6),
2) substitution of part of the $SrCO_3$ by $SrSO_4$,

3) SiO_2.

Primary attention was given to eliminate experimental ambiguities by adequately normalizing the ceramic parameters (prefiring temperature, milling, etc.) on the one hand, and by chemical analyses at different stages of the process on the other.

Experimental

The main raw materials used were Fe_2O_3 C 201+50 from Société des Couleurs, with an SO_4 content 0.02 wt.%, and chemically pure $SrCO_3$ from Merck containing 0.01-0.02 wt.% BaO, 0.06 wt.% CaO, and 0.02 wt.% SO_4.

The raw materials were mixed in a ball mill under alcohol. Prefiring was done at a heating rate of about 100°C/Hr over the last 300°C, and keeping them for 15 minutes at top temperature. Pressed tablets were prefired at the temperature which gave about the same density for all compositions namely about 4 g/cm^3. As a result of this normalizing procedure a constant milling time could be applied of 16 hours, leading to about the same powder particle size for all compositions. This was verified by measuring with a Fisher sub-sieve sizer (1.1-1.2).

Milling was done in a steel ball mill under water, after dry precrushing the tablets to 200 /um. In several experiments some Na_2CO_3 and/or $NaHCO_3$ was added during the last 5 minutes of milling to precipitate dissolved Sr or to convert $SrSO_4$ into the less soluble $SrCo_3$.

Pressing of the tablets, 40 mm Ø, 15-18 mm high, from the sludge was done in a magnetic field parallel to the pressing direction, at a pressure of 150-200 kg/cm^2. Sintering was performed in a batch furnace, using the same time-temperature curve as in prefiring. The tablets were dried and ground flat after pressing. This allowed the calculation of the shrinkages and densities from the weight and the dimensions of the tablets.

Chemical compositions at different stages of the process were obtained from X-ray fluorescence analyses using standards. These standards were determined using quantitative wet-chemical analysis. Although this method suffers from some inaccuracy, it is sufficient to show the effects clearly. There are slight differences between different series of analyses. Thus, the values reported,

for instance of the ratio n = Fe_2O_3/SrO, will slightly differ from the actual values. The accuracy of the analyses sometimes suffered from the fact that samples were inhomogeneous where sulphates were present, due to a preferential decomposition in the surface region.

Magnetic measurements were carried out on all sintered specimens. Also, separate experiments were done to check the effect of milling time of the prefired materials on the sintering behaviour.

Results and Discussion

Two series of compositions, one in which the ratio n is changed by adding excess $SrCO_3$ over the stoichiometric ratio 6, and another one where this excess SrO was weighed in as $SrSO_4$, were investigated. It has been assumed that all SO_4 present in the sintered magnets was bound as $SrSO_4$, and the rest of the SrO found bound to Fe_2O_3. The main part of the SO_4 lost has been decomposed during prefiring. In the samples about half of the $SrSO_4$ added remains in the sintered magnets.

An excess of SrO with respect to Fe_2O_3 (n 6) drastically decreases the sintering temperature, allowing better magnetic properties to be attained at the same time. Sintering is very much retarded in compositions which contain part of the SrO as $SrSO_4$. A comparison of both series strongly suggests that the $SrSO_4$ present retards sintering with respect to the pure composition having the same value of n.

It was also found that the pure materials were very much dependent in their sintering reactivity on milling time, whereas the materials containing $SrSO_4$ were not.

The results of the experiments showing the drastic effect of the molar ratio n on sintering, explain the need for a normalizing procedure in order to be able to compare materials which are chemically different. It is a rather logical choice to normalize on the particle size of the milled powder, being the most relevant physical parameter determining the sintering reactivity. This makes it possible to clearly investigate chemical effects on the sintering behaviour. A constant density of 4 g/cm^3 after prefiring made it possible, with a constant milling time, to obtain powders with about equal particle size. A constant milling

time of the prefired blocks having about the same mechanical properties, also provides a rather constant shift in n resulting from milled-in Fe_2O_3.

The results of the experiments where the weighed-in mole ratio n is corrected by chemical analyses of the sintered magnets, point to an appropriate defect structure being of primary importance for explaining the sintering behaviour. Although the results are not completely comparable, this is analogous to the Ba-system (2). Other explanations for using an excess SrO (3,4) seem to b e invalid.

Neither with the pure materials, nor with the materials containing sulphate is grain growth sufficiently suppressed to obtain high values for $_IH_c$. In a separate series of experiments it could be shown that addition of 0.4 wt.% of SiO_2 to one ot compositions is very effective for obtaining materials with a combination of a high B_r and a high $_IH_c$. Over a large range of sintering temperatures the $_IH_c$ is about 1000 Oe higher, at the same values of B_r, compared to the materials with only $SrCO_3$ or $SrSO_4$ added. This is in agreement with previous results (9).

To further support the view that $SrSO_4$ has no beneficial effect on the magnetic properties, but as it partly decomposes only influences the sintering behaviour by changing n, several experiments were done. By adding carbonate ions during milling, $SrSO_4$ will react to form the less soluble $SrCO_3$ that shows the effect on the sintering behaviour. These results strongly support the view that the main effect to be considered is the ratio n.

Conclusion

The magnetic properties of Sr-hexaferrites depend very strongly on the sintering properties, which in turn are found to be primarily dependent on the ratio n = Fe_2O_3/SrO, where SrO is meant to be that part of the strontium which is bound to Fe_2O_3 is present in the raw materials it is necessary to take into account that the relatively stable $SrSO_4$ is formed. Depending on the processing conditions, more or less sulphate will decompose. The free SrO formed will the change the ratio n and thus strongly affect the sintering behaviour. To obtain a good combination of B_r and $_IH_c$ an additive like SiO_2 is needed to suppress grain growth.

References

(1) G.C. Kuczynski, Mat. Sci. Res., Vol. 6, 217 (1973).

(2) A.L. Stuijts, Trans. Brit.Ceram.Soc. 55, 57 (1956).

(3) J.S.Reed, R.M.Fulrath, J. Am. Ceram.Soc. 56, 207 (1973).

(4) R.H.Arendt, J. Appl. Phys. 44, 3300 (1973).

(5) C.A.M. van den Broek, Proc. 3rd Europ. Conf. Hard Magn.Mat., Amsterdam, 1974, H. Zijlstra, editor, p. 53.

(6) H.Kojima, Sci. Rep. RITU, A7, 507 (1955).

(7) Gmelins Handbuch der anorganischen Chemie, Nr. 29, Sr, Ergänzungsband (Verlag Chemie, GmbH, Weinheim, 1960) pp. 264-273.

(8) A.Cochardt, J.Appl. Phys. 34, 1273 (1963).

(9) G.S.Krijtenburg, 1st Europ. Conf. Hard Magn. Mat.(Vienna, 1965), papaer 2.13.

HOT PRESSED FERRITES: MAGNETIC-MECHANICAL-MICROSTRUCTURAL INTERACTIONS

BY

L.A.BRISSETTE, E.A.GROSSI, J.A.TITLAR AND R.M. SPRIGGS

National Micronetics, Inc., West Hurley, N.Y.
and Lehigh University, Bethlehem, Pennsylvania
U.S.A.

I. INTRODUCTION

Recent advances have been made with both NiZn and MnZn ferrites prepared by advanced ceramic hot pressing techniques. Utilizing unique processing technologies, it has been possible to prepare custom hot-pressed ferrite materials possessing superior magnetic and mechanical properties coupled with near theoretical densities and fine-grained-size microstructures. The interactions among magnetic and mechanical properties and microstructural features for hot-pressed NiZn and MnZn ceramic ferrite materials have been investigated. The following interactions will be presented:

A. Mechanical-Microstructural Interactions

B. Magnetic-Microstructural Interactions

C. Thermal-Magnetic Interactions

D. Thermal-Microstructural Interactions

E. Magnetic-Mechanical Interactions

The Table in SLIDE 1 shows some of the materials characteristics of the ferrites investigated.

The NiZn ferrite is designated LM-211 (next to last column) and has an Initial Permeability at 100KHZ of 1850 and a Saturation Flux Density of 3600.

TABLE 1

MATERIALS CHARACTERISTICS OF THE INVESTIGATED FERRITES

	LM5K	LM7	LM20	LM211	M211
Coercive Force - H_c	oersted < 0.15	oersted 0.35	oersted 0.62	oersted 0.19	oersted 0.15
Volume Resistivity - ρ	10 ohm-cm	$> 10^6$ ohm-cm	$> 10^6$ ohm-cm	$> 10^6$ ohm-cm	$> 10^6$ ohm-cm
Specific Density	5.50g/cc	5.30g/cc	5.30g/cc	5.30g/cc	5.30g/cc
Vickers Hardness - Hv	> 650	> 750	> 750	> 750	> 700
Thermal Coefficient of Expansion	11×10^{-6} in/in/°C	9.6×10^{-6} in/in/°C	9.6×10^{-6} in/in/°C	9.6×10^{-6} in/in/°C	9.6×10^{-6} in/in/°C
Average Grain Size	5 microns	4 microns	4 microns	4 microns	15 microns
Relative Density	99.8%	99.8%	99.8%	99.8%	$> 99\%$

The composition is quite familiar, being of the $Ni_{0.5}Zn_{0.5}Fe_2O_4$ - spinel type, with the Ni ranging near 0.35 and the Zn near 0.65.

Fig.1. shows a typical plot of Flux Density versus Drive Field for the NiZn ferrite, while

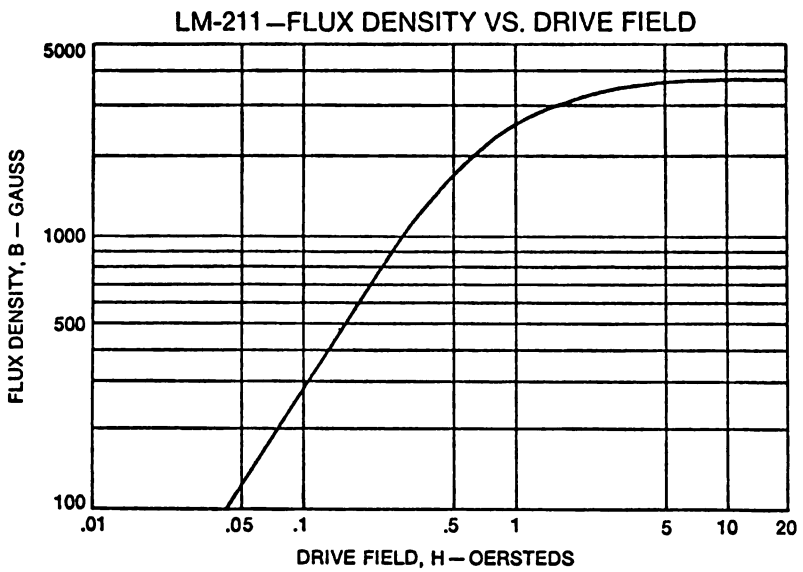

Fig.1. Typical Plot of Flux Density versus Drive Field for Ni Zn Ferrite

Fig.2. shows Permeability as a function of Frequency.

The MnZn ferrite is designated LM-5K (first column in Table in Slide 1). This has an Initial Permeability at 100KHZ of 5000 and a Saturation Flux Density of 5500.

The composition of the MnZn ferrite is also familiar, being of the 60-40 type, a manganese zinc ferrous ferrite with several mole per cent excess iron in the lattice as iron-two-plus and iron-three-plus.

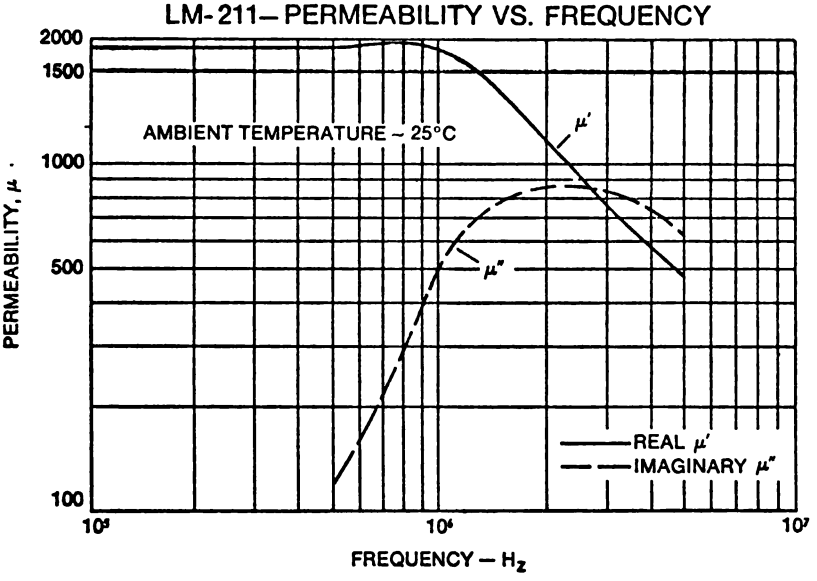

Fig.2. Permeability as a Function of Frequency for NiZn Ferrite

Fig.3. shows a typical plot of Flux Density versus Drive Field for the MnZn ferrite, while

Fig.4. shows Permeability as a function of Frequency.

Various thermal treatments were employed with the LM-211 NiZn ferrite and the LM-5K MnZn ferrite, especially to vary grain size.

Magnetic and mechanical strength measurements were made on the resulting samples, under a variety of experimental conditions, e.g., strength for polished surfaces versus "as machined" surfaces; initial

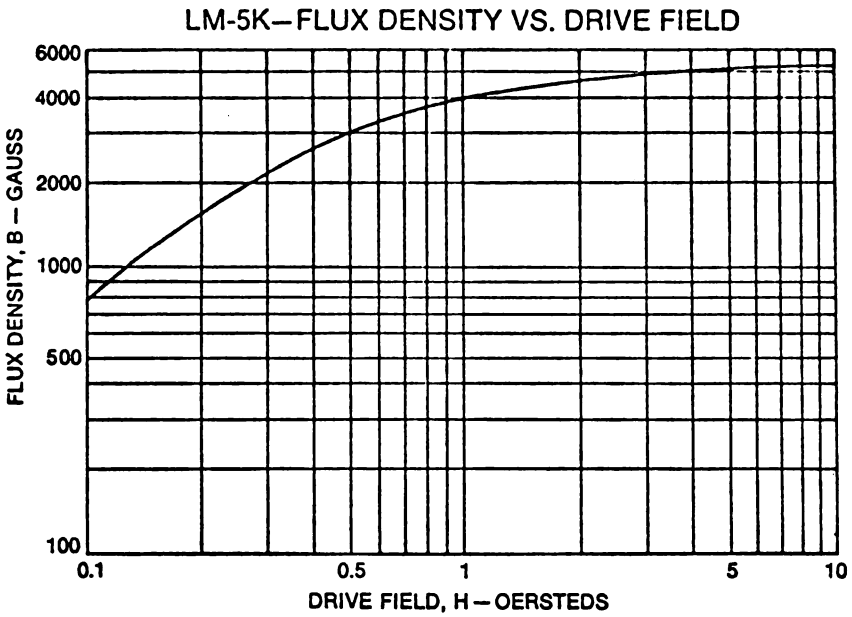

Fig.3. Typical Plot of Flux Density versus Drive Field for MnZn Ferrite

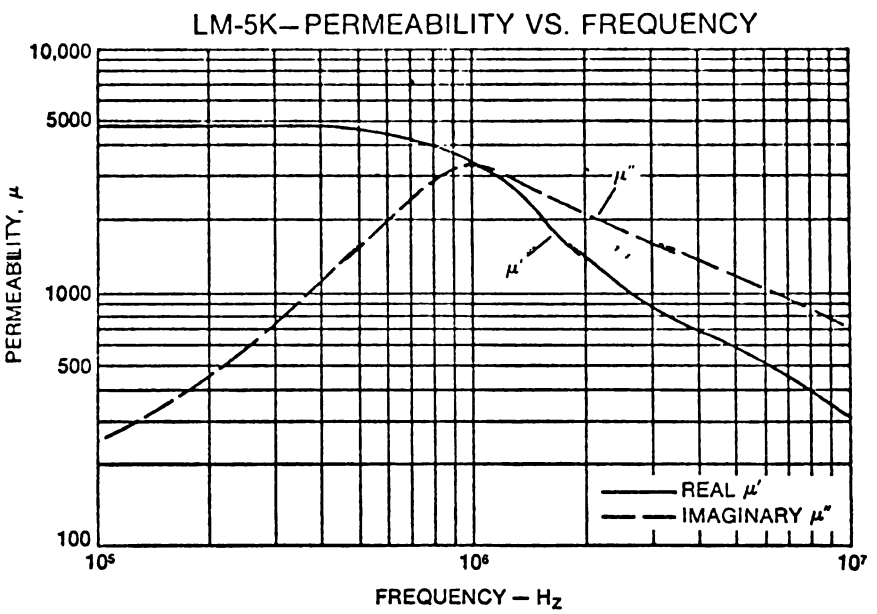

Fig.4. Permeabilyty as a Function of Frequency for MnZn Ferrite

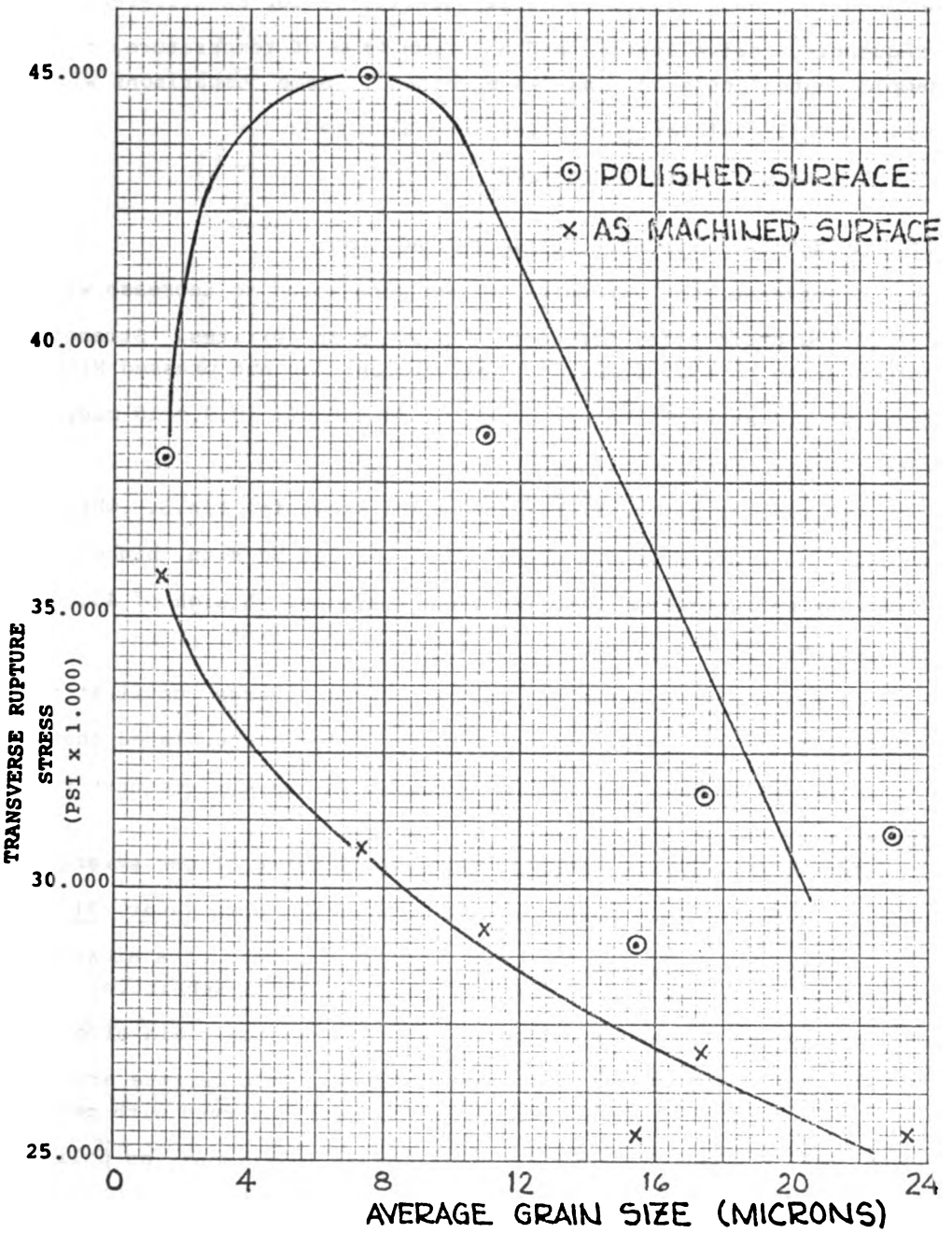

Fig.5. Transverse rupture stress versus grain size for hot pressed NiZn ferrite.

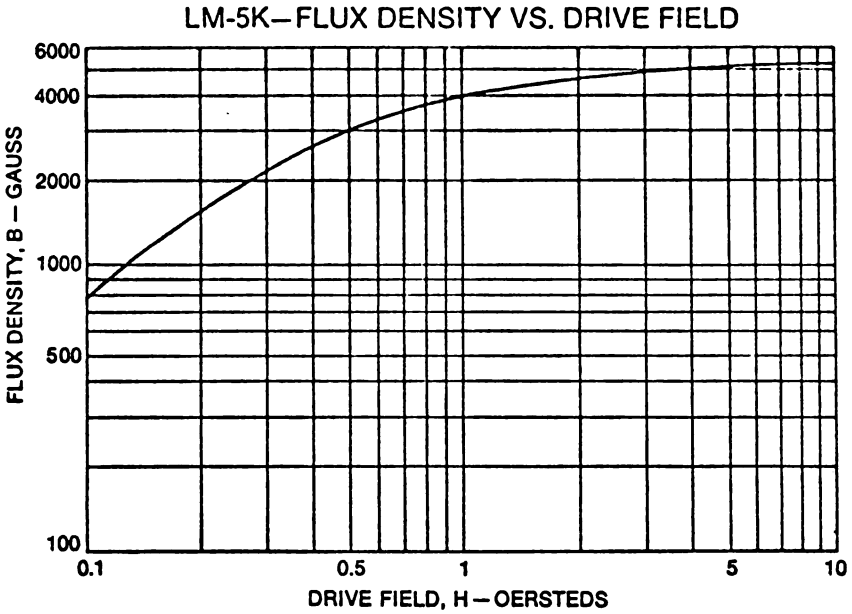

Fig.3. Typical Plot of Flux Density versus Drive Field for MnZn Ferrite

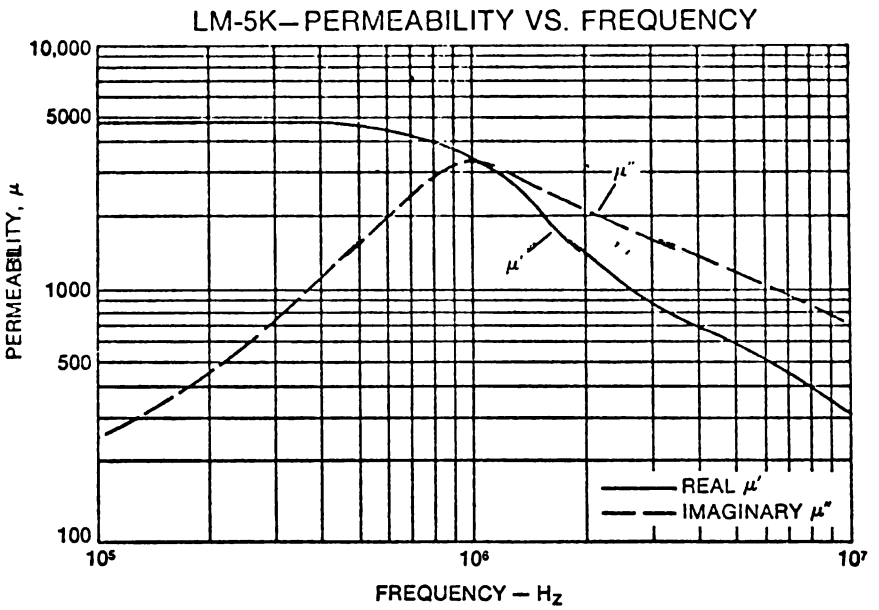

Fig.4. Permeabilyty as a Function of Frequency for MnZn Ferrite

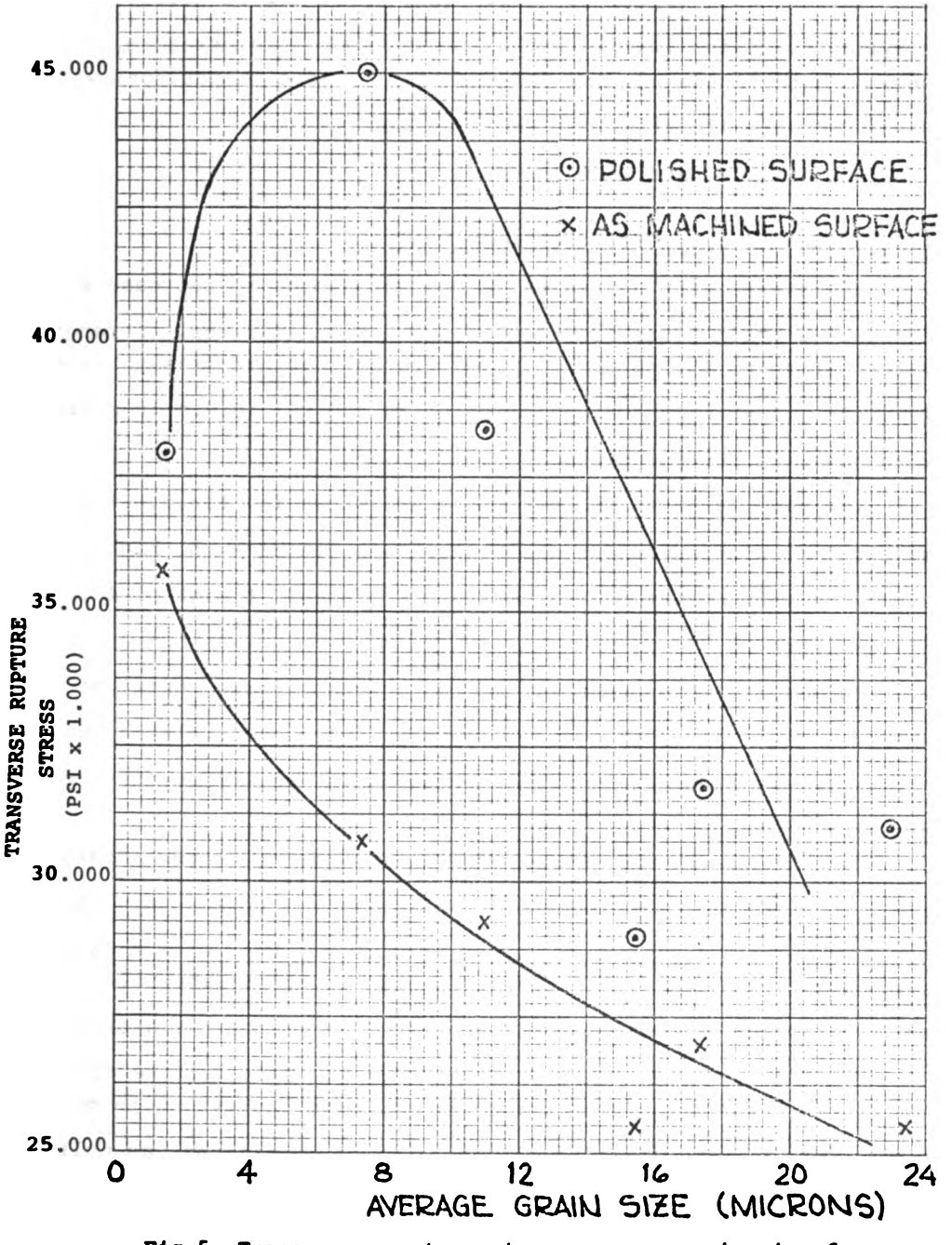

Fig.5. Transverse rupture stress versus grain size for hot pressed NiZn ferrite.

permeability and "figure of merit" quality factor at different frequencies, drive levels, and as a function of temperature, for samples both "annealed" and "as machined". Some comparisons with conventionally sintered ferrites were also made.

The results were as follows.

II. MECHANICAL-MICROSTRUCTURAL INTERACTIONS

Transverse bend strengths values were found to increase with decreasing grain sizes for both NiZn and MnZn ferrites. Strength values of up to 45,000 PSI (G.S.~7 micron) for hot pressed NiZn ferrites and strength values of up to 40,000 PSI (G.S.~10 micron) were observed for hot pressed MnZn ferrites.

The results of the NiZn ferrite are shown in Fig.5. where strength is plotted versus grain size. As can be seen, higher strengths were observed with polished surfaces. A high of 45,000 psi was seen at 7 microns.

As grain size decreases, the two curves diverge, until at the smallest grain size, the curves converge. It is speculated that machining may induce compressive stresses in the surface that the polishing removes.

As may be seen in Fig.6. the overall trend of our strength data is in general agreement with Kehr's recent work (Wear, 31 (1975 109-117) on the influence of grain size on the wear of a nickel-zinc ferrite by flexible media. However, his structure-sensitive magnetic properties did not improve with decreasing grain size.

Similar strength-grain size data for the MnZn ferrite are shown in Fig.7. Again, higher strengths were observed with polished surfaces. A high of 34,000 psi was seen at 10 microns, as polished, and individual values as high as 40,000 psi were recorded.

To our knowledge, such strength values for this system are unique and have never been reported before. There is also no indica

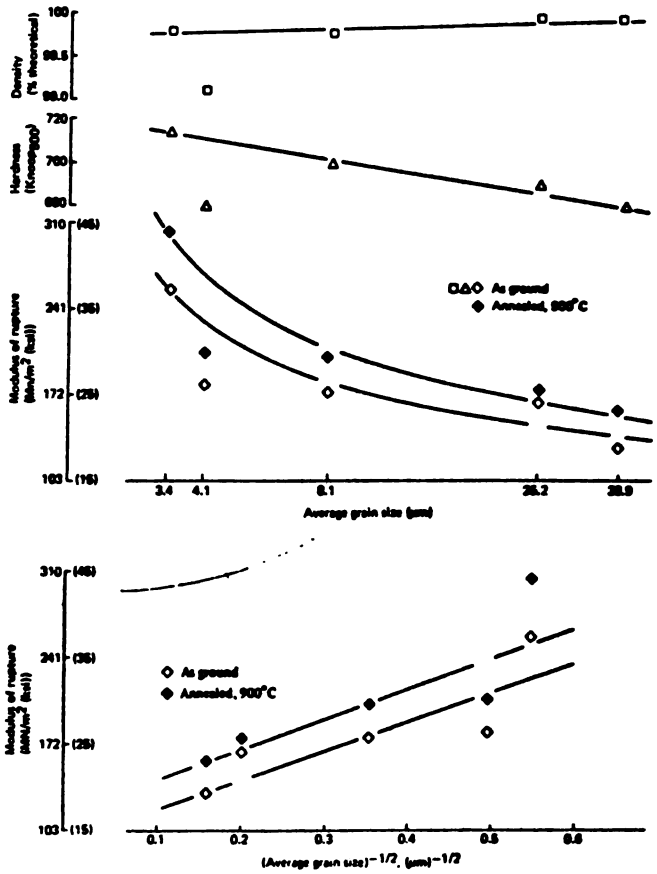

Fig.6. Density, hardness, and moduli of rupture as a function of grain size.

of a strength "drop-off" as one proceeds towards finer and finer grain sizes.

III. MAGNETIC-MICROSTRUCTURAL INTERACTIONS

The next two slides show the relationship between magnetic behavior and microstructure for both ferrites.

As shown in Fig.8. initial permeability (μ') and $\mu'Q$ values show a sharp decrease with increasing grain size at 1.3 MHZ for hot

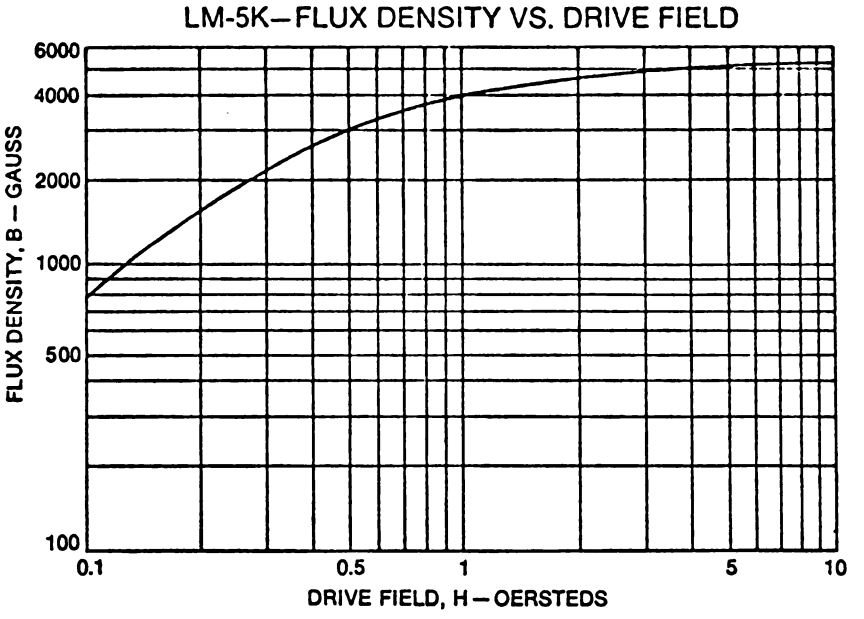

Fig.3. Typical Plot of Flux Density versus Drive Field for MnZn Ferrite

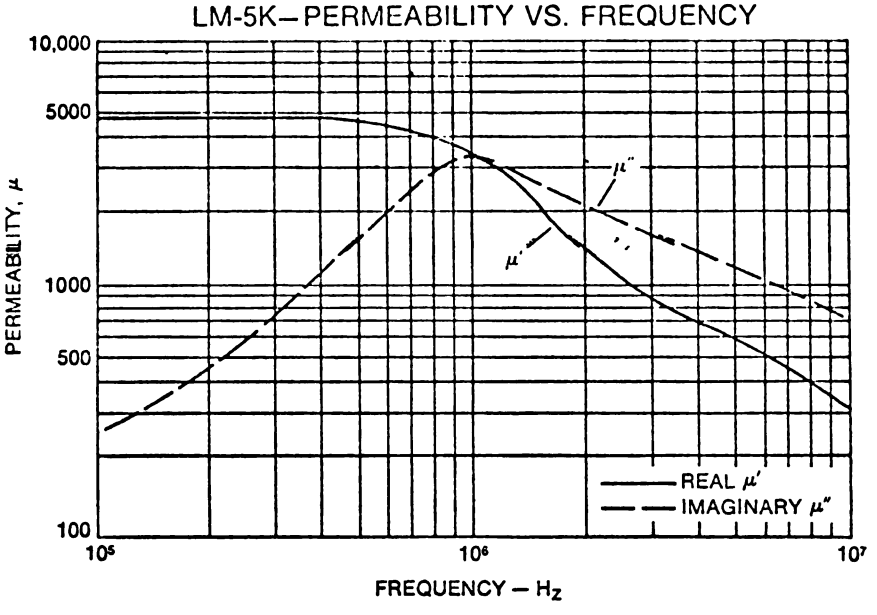

Fig.4. Permeabilyty as a Function of Frequency for MnZn Ferrite

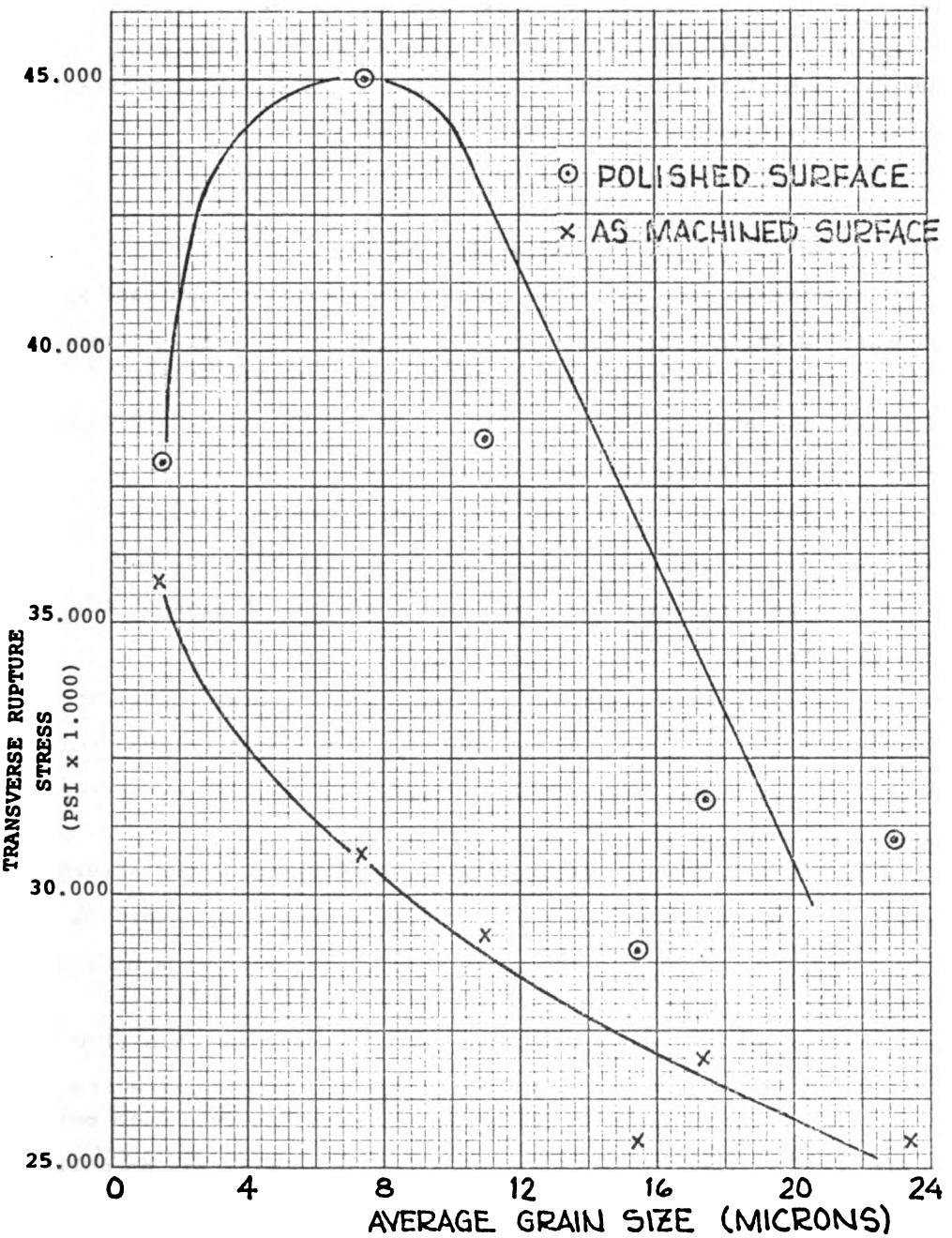

Fig.5. Transverse rupture stress versus grain size for hot pressed NiZn ferrite.

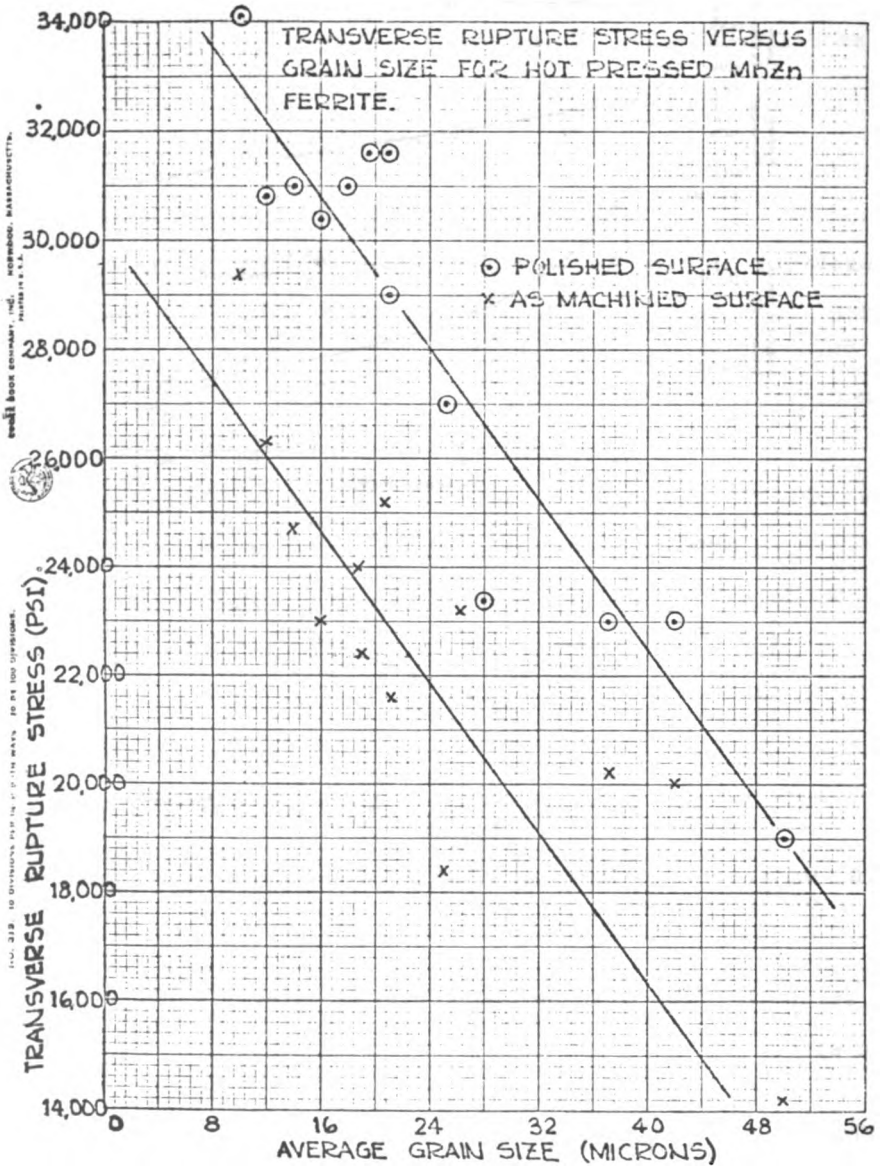

Fig.7. Transverse rupture stress versus grain size for hot pressed MnZn ferrite.

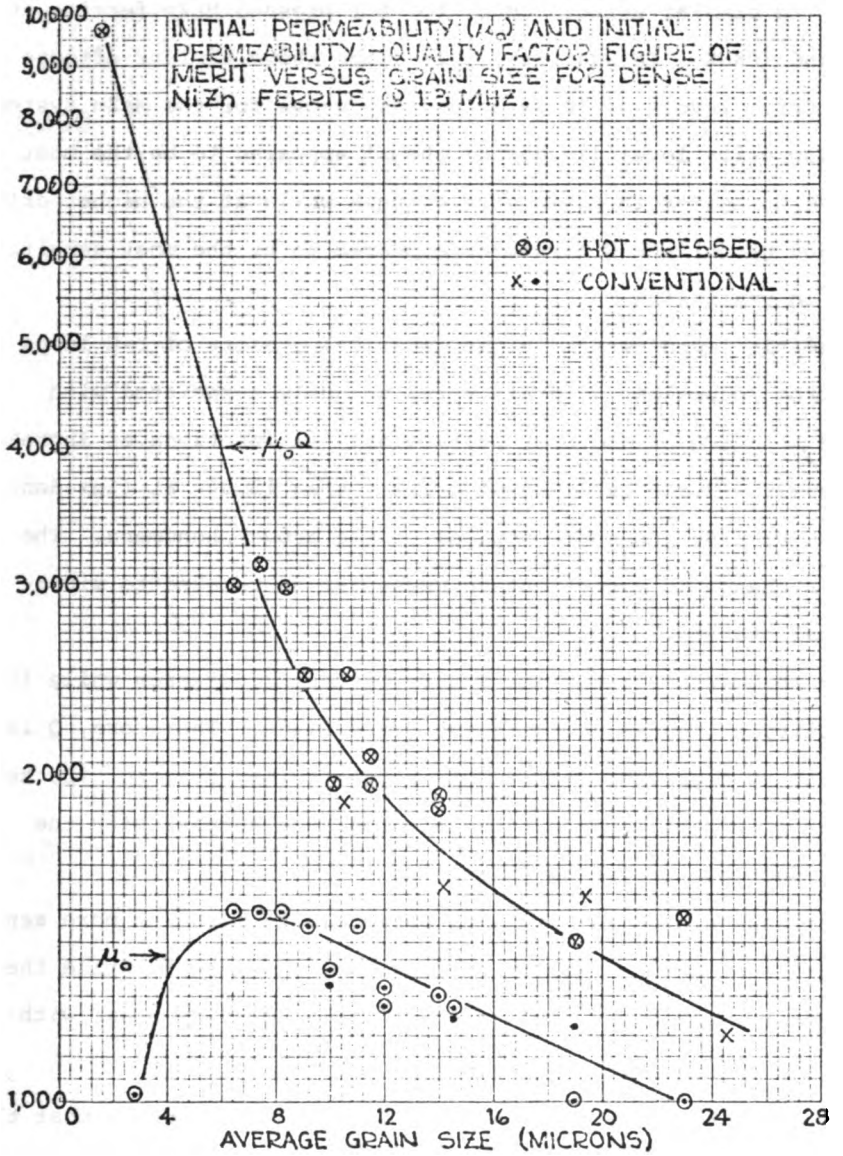

Fig.8. Initial permeability ( ) and initial permeability - quality factor figure of merit versus grain size for dense NiZn ferrite 1.3 MHZ.

pressed and isostatically pressed and fired NiZn ferrite. As seen in Fig.9. a similar effect occurs for hot pressed MnZn ferrite at 100KHZ and 10KHZ. In addition, this slide shows similar effects for two drive levels of 10 gauss and 500 gauss for the MnZn system. At the low drive level (10 gauss) the μ' appeared to be the most sensitive parameter to grain size changes while at the higher drive level (500 gauss) the Q parameter appeared to be the most sensitive to changes in grain size.

Dramatic improvements in the technical quality of B-H loops result from reductions in grain size, uniquely associated with enhanced μ' and Q parameters, particularly as functions of increasing drive levels. Permeabilities of greater than 15,000 at flux densities in excess of 1500 gauss are typical of the above phenomena. The data suggest a change in magnetization mechanism as related to micro-structural changes.

For the NiZn ferrite, the figure of merit increases while initial permeability decreases at the finest grain sizes. Therefore, Q is increasing at a greater rate. This suggests that Q is not the key to higher strengths because these are the same samples with the strength decrease (refer to SLIDE 6).

It is speculated that initial permeability might be more sensitive to crystal - or grain-to-grain bonding, as is strength, while the quality factor may be related to total grain boundary area, with strength as a complicated interaction.

For the MnZn ferrite (refer to SLIDE 10), it is clear that the quality factor greatly increases with decreasing grain size (with values exceeding 100,000).

At the low drive level (10 gauss), initial permeability appears to be the more sensitive parameter (values in excess of 10,000 have

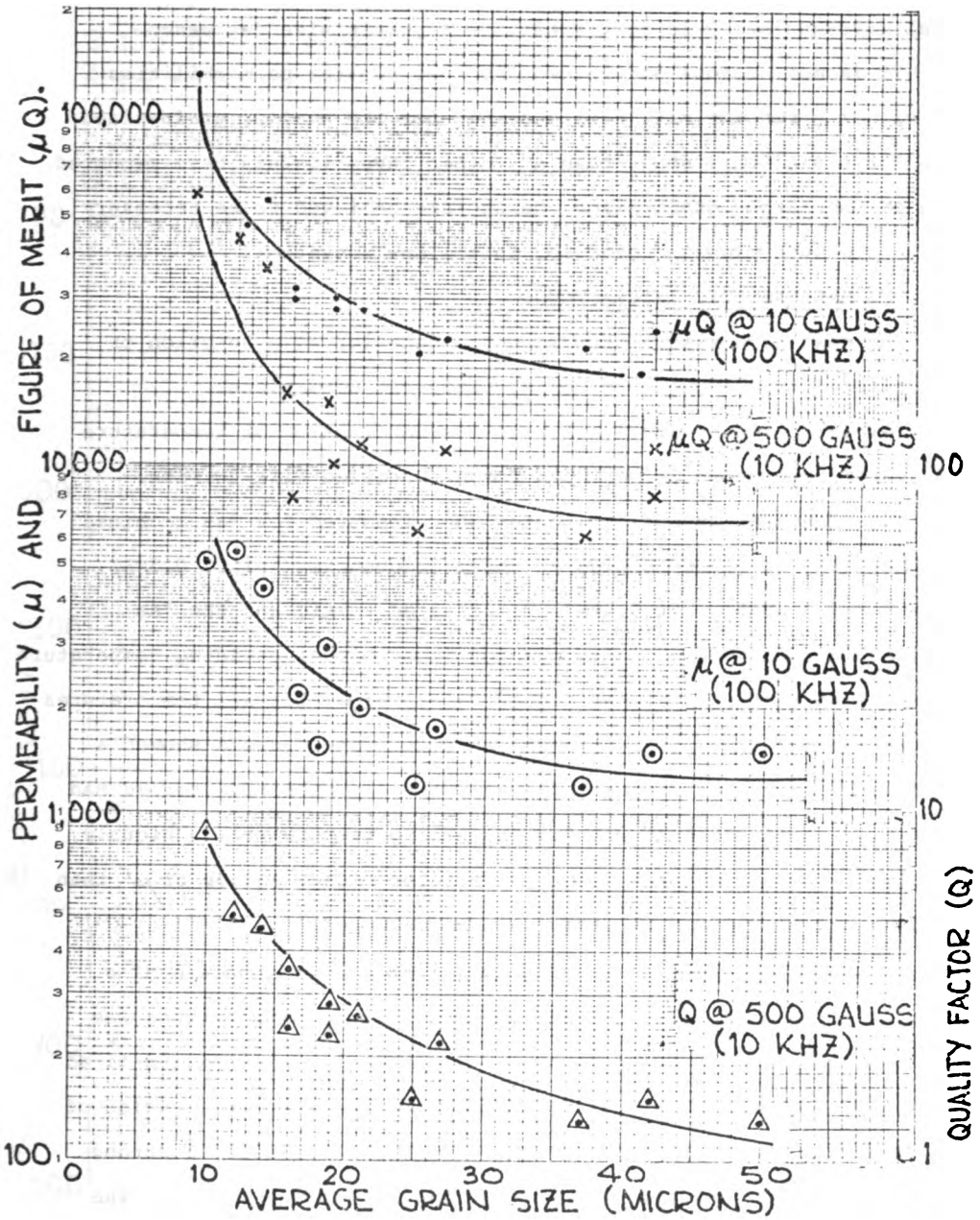

Fig.9. Interactions of magnetic permeability ( ) and quality factor (Q) versus grain size for hot pressed MnZn at two operating frequency and gauss values.

been observed at even finer grain sizes), while at the higher drive level (500 gauss), Q is more sensitive to grain size decreases.

It is most unique and noteworthy that greater permeabilities and higher strengths have been observed for the smaller grain-sized MnZn ferrite of this study than any other investigators have reported, even at the larger grain sizes, heretofore believed to be necessary to achieve such magnetic behavior in the Mn-Zn system.

IV. THERMAL-MAGNETIC INTERACTIONS

The next five slides show magnetic behavior as a function of temperature for the two ferrites at different conditions.

Initial permeability (μ') values as a function of temperature ($20^{o}C$-$80^{o}C$) are shown in Fig.10. for hot pressed NiZn ferrite. This shows several unusual responses when measured for "as machined" and thermally annealed toroids at three frequencies (viz., 0.5MHZ, 1.75MHZ and 3.5MHZ). At 0.5MHZ the annealed toroid and the "as machined" toroid show positive changes in μ' with increasing temperature. The annealed toroid again had higher values of μ' for all temperatures measured at 1.75MHZ. At 3.5MHZ the annealed toroid again showed a slightly negative coefficient of μ' and the "as machined" toroid had a positive coefficient of μ' with increasing temperature. Uniquely, at 3.5MHZ, the "as machined" toroid revealed higher values of μ' than the annealed toroid for all temperatures measured.

In a separate study, the μ' versus temperature response of a selected fine-grain-size (1.5 micron) hot-pressed NiZn ferrite was compared to a similar response of an isostatically pressed and fired version of the same formulation for the two operating frequencies of 0.5MHZ and 1.75MHZ. This is shown in Fig.11. Clearly, a strong interaction of μ' and temperature with microstructure exists. The hot pressed ferrite is obviously more temperature stable.

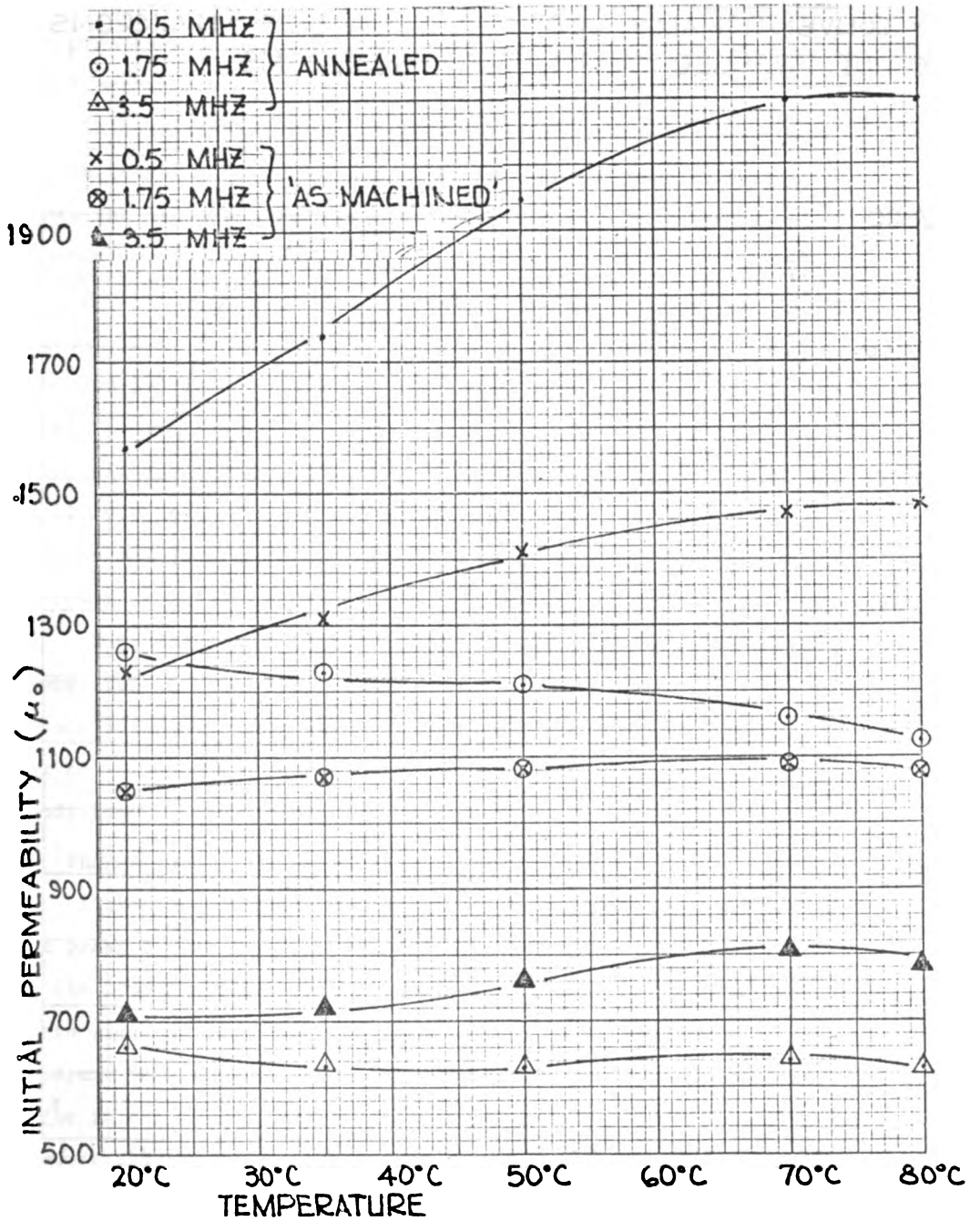

Fig.10. Initial permeability versus temperature for hot pressed NiZn ferrite for annealed and 'as machined toroids at three operating frequencies.

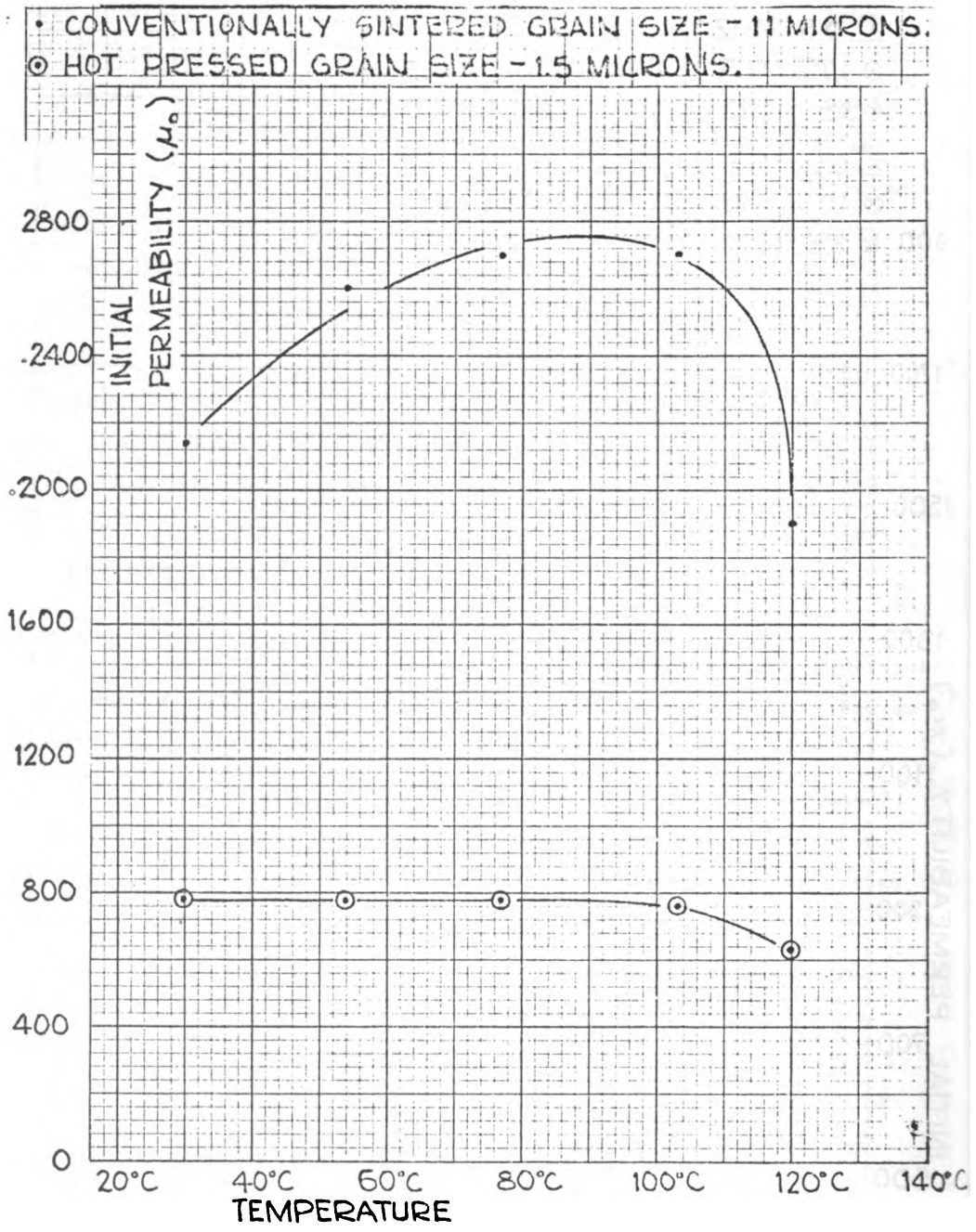

Fig.11. Initial permeability ( ) versus temperature at 0.5 MHZ for dense NiZn ferrites prepared by two varying ceramic processing techniques.

Fig.12. shows the figure of merit versus temperature for both hot pressed and isostatically pressed and sintered NiZn ferrite at two frequencies.

In each case, the hot pressed material is superior over the entire temperature range, and especially at the highest temperatures where the decrease in permeability and increase in losses are much greater for the conventionally sintered ferrite.

Initial permeability (μ') and $\mu'Q$ versus temperature ($20^{\circ}C$-$125^{\circ}C$) for selected grain sizes (10-50 microns) and for two flux density levels (100 and 500 gauss) are shown for hot pressed MnZn ferrite in Fig.13. In all cases, the μ' and the $\mu'Q$ parameters are highest for the smallest grain sizes. Specifically, at $20^{\circ}C$, $\mu'Q$ values (at 100 gauss and 10KHZ) of 110,000 and 8,000 were obtained for average grain sizes of 10 microns and 50 microns respectively. This factor of nearly 14 to 1 increase in the $\mu'Q$ "figure of merit" appears to be a unique interaction.

Fig.14. is a plot of permeability and quality factor versus temperature for the hot pressed MnZn ferrite at two drive levels for 10 and 50 micron grain sizes. Again, both μ and Q are higher for the finer grain size. Q is the more sensitive parameter at all conditions.

V. THERMAL-MICROSTRUCTURAL INTERACTIONS

Although not shown, the grain growth kinetics of fully dense hot pressed MnZn ferrites were also investigated for temperatures in the $1300^{\circ}C$ region and for times of 1 hour to 120 hours. Resultant grain sizes of from 5 micron to over 50 microns were achieved for apparent densities in excess of 99 percent of the X-ray limiting value in all cases. Subtle topographic features of the resulting microstructures were also observed. This study will be the topic of a separate future report.

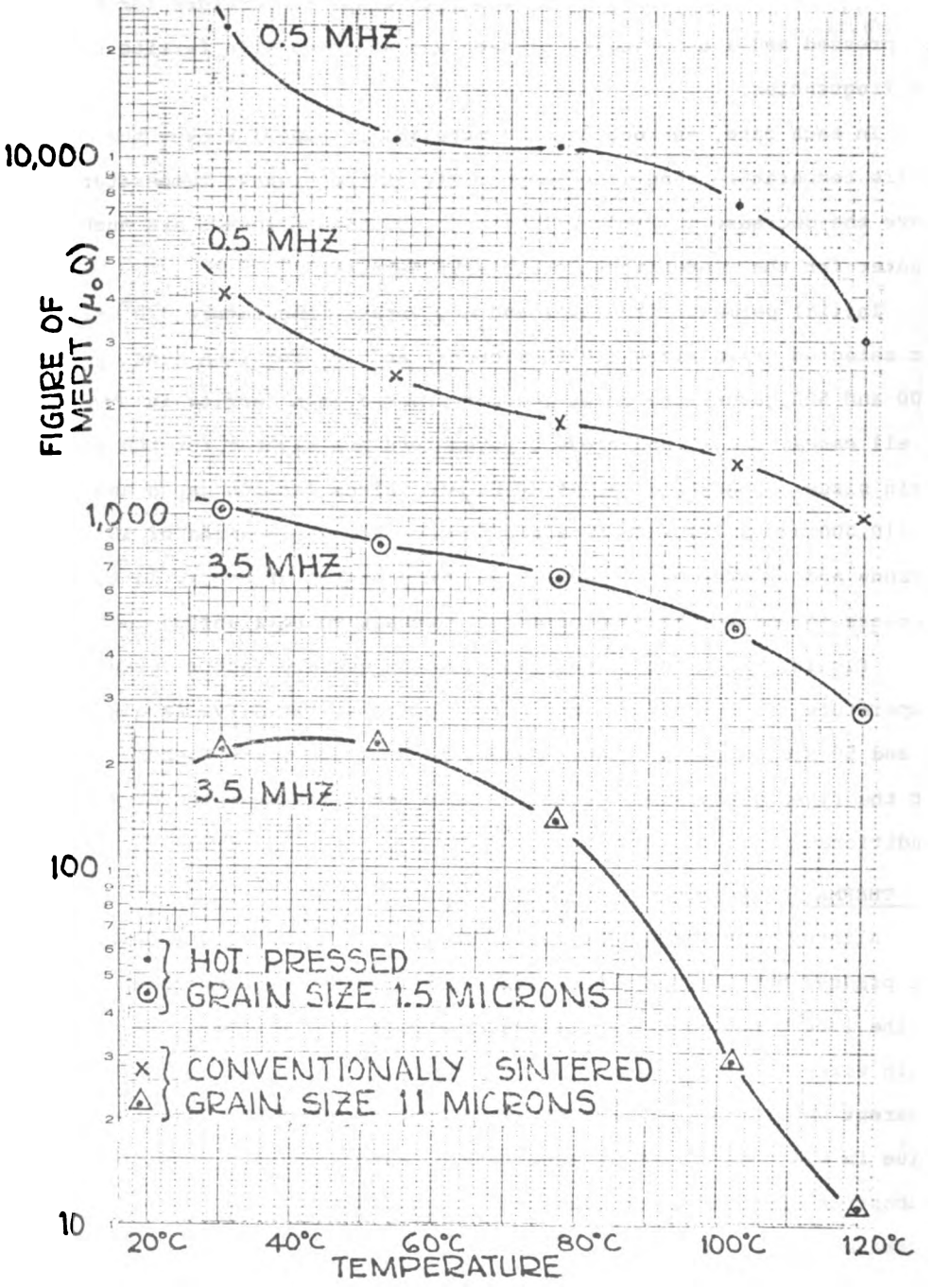

Fig.12. Figure of merit (Q) versus temperature for dense NiZn ferrites prepared by two varying ceramic processing techniques.

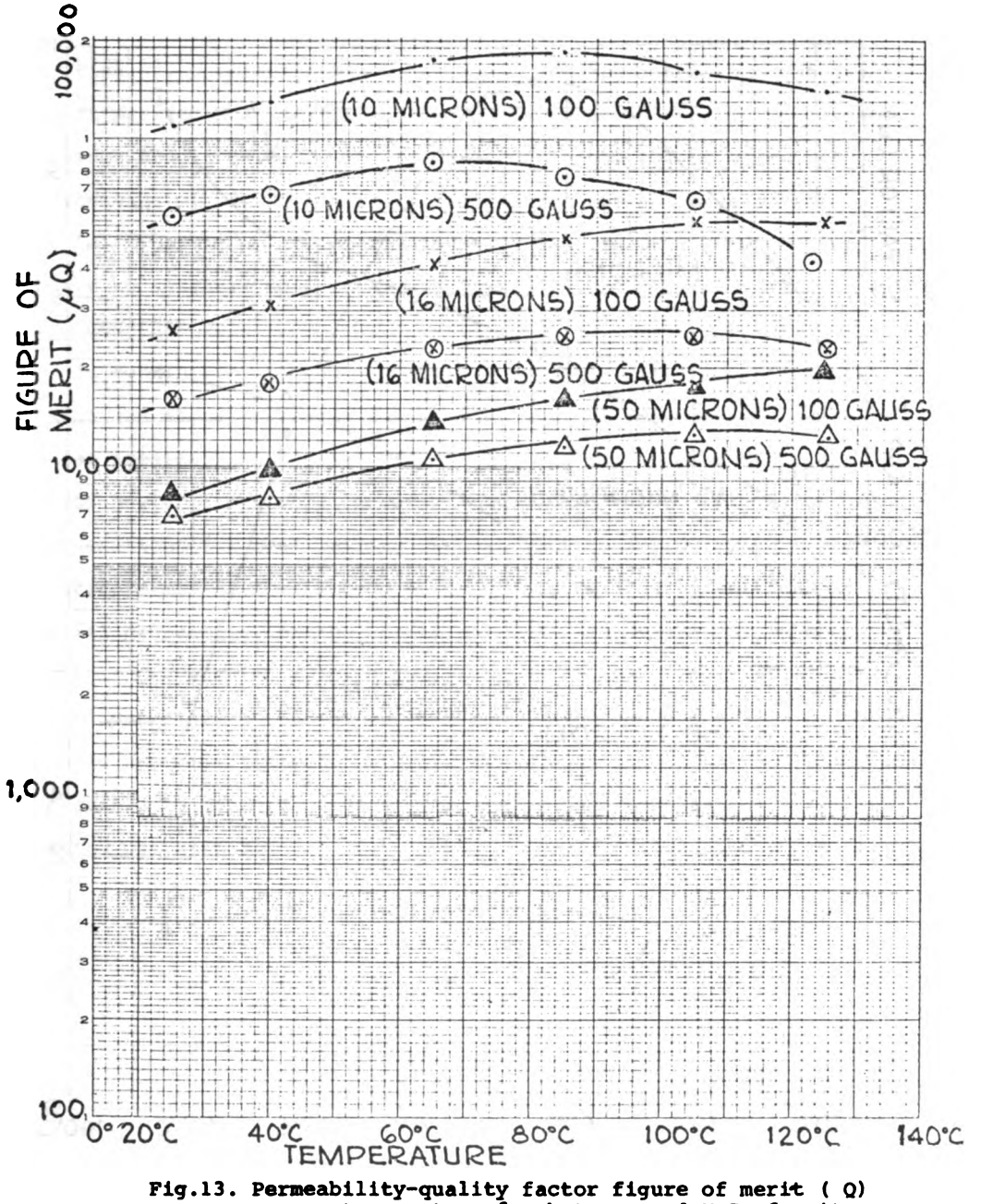

Fig.13. Permeability-quality factor figure of merit (Q) versus temperature for hot pressed MnZn ferrite for three grain sizes and two gauss levels.

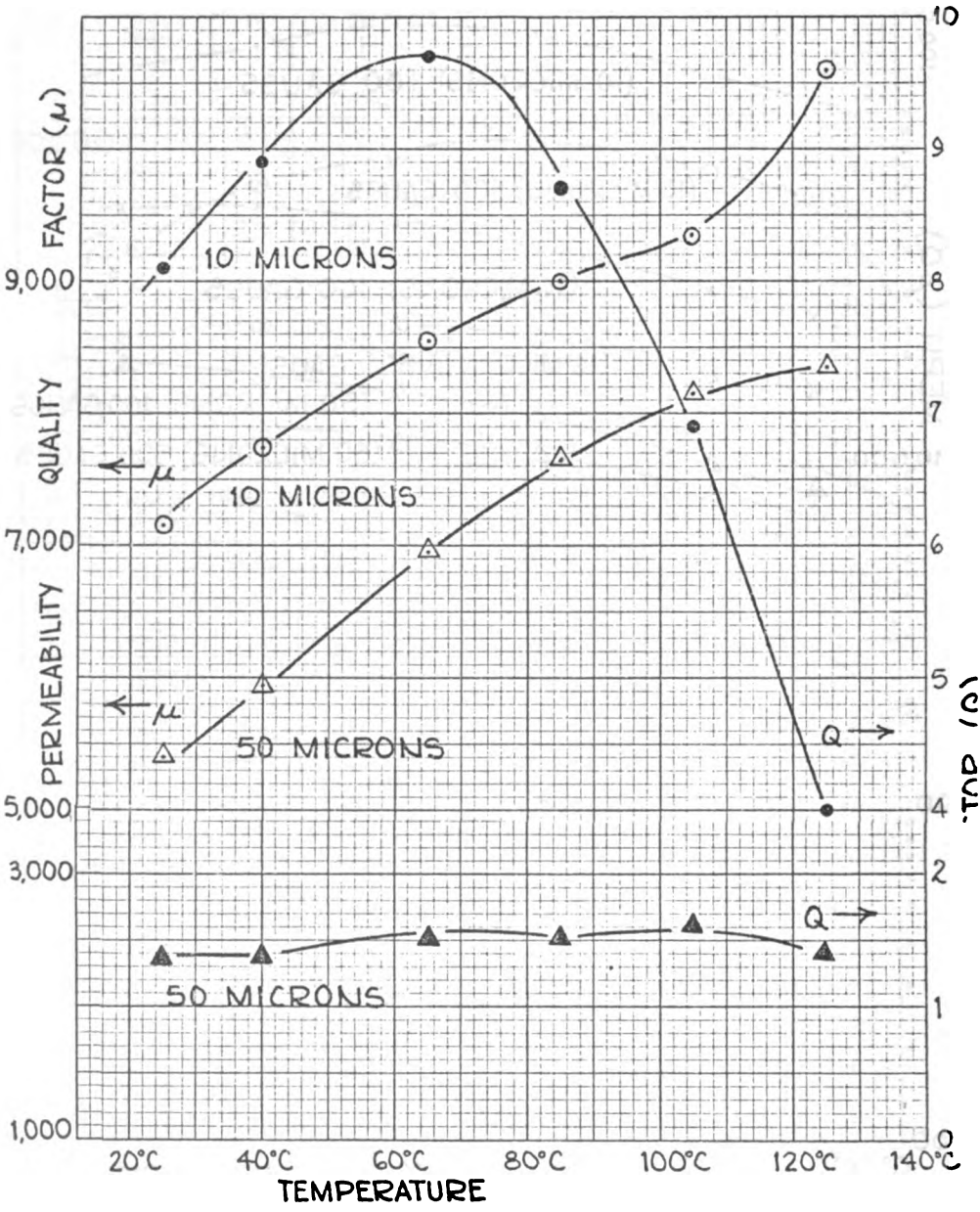

Fig.14. Permeability ( ) and quality factor (Q) versus temperature for hot pressed MnZn ferrite for two grain size values and at 10 KHZ and 500 gauss.

VI. MAGNETIC-MECHANICAL INTERACTIONS

Finally, a relationship between $\mu'Q$ and transverse bend strength for hot pressed MnZn ferrite at 100KHZ is shown in Fig.15. Average increases from $\mu'Q$=18,000 at strengths of 19,000 PSI to $\mu'Q$=45,000 at strengths of 32,000 PSI were obtained for the hot pressed MnZn ferrite. Therefore, the change is more than linear. Permeability appears to slightly more sensitive than Q to strength changes.

VII. CONCLUSIONS

In conclusion, it becomes obvious from the results of this work that unique magnetic-mechanical-microstructural interactions exist for hot pressed MnZn and NiZn ferrites. The way is opened for a host of new applications. However, the mechanical and magnetic design considerations for applications such as miniature high frequency inductor and transformer devices should be precisely related to the fundamental material properties for the conditions under which the device must operate. Conversely, precise manipulation of the properties of ferrite materials by custom ceramic processing techniques can produce uniquely superior thermal, magnetic and mechanical properties making it possible to optimize device performance over wide ranges of selected operations.

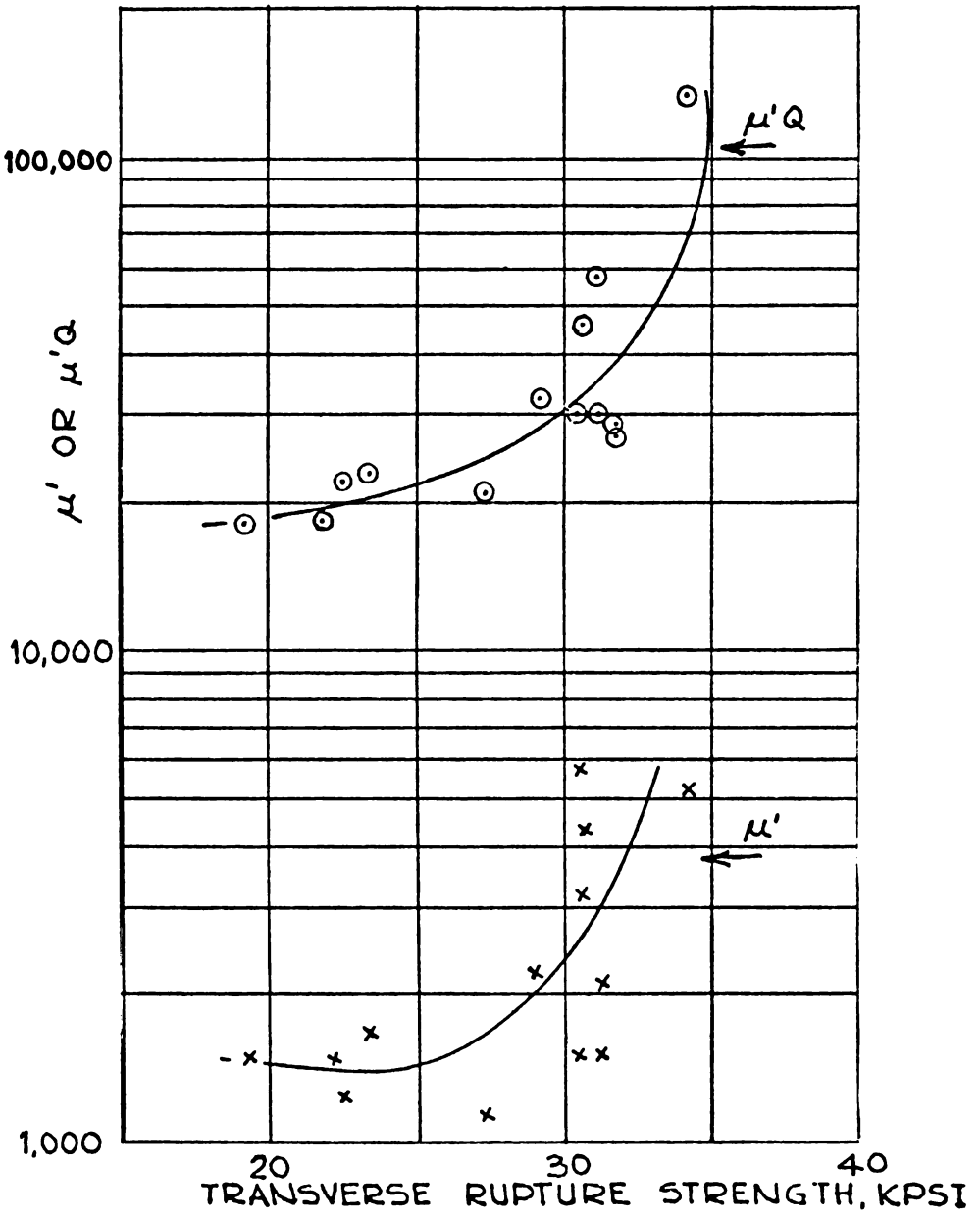

Fig.15. Initial permeability ( ) and initial permeability-quality factor figure of merit versus transverse rupture strength for hot pressed MnZn ferrite 0.1 MHZ.

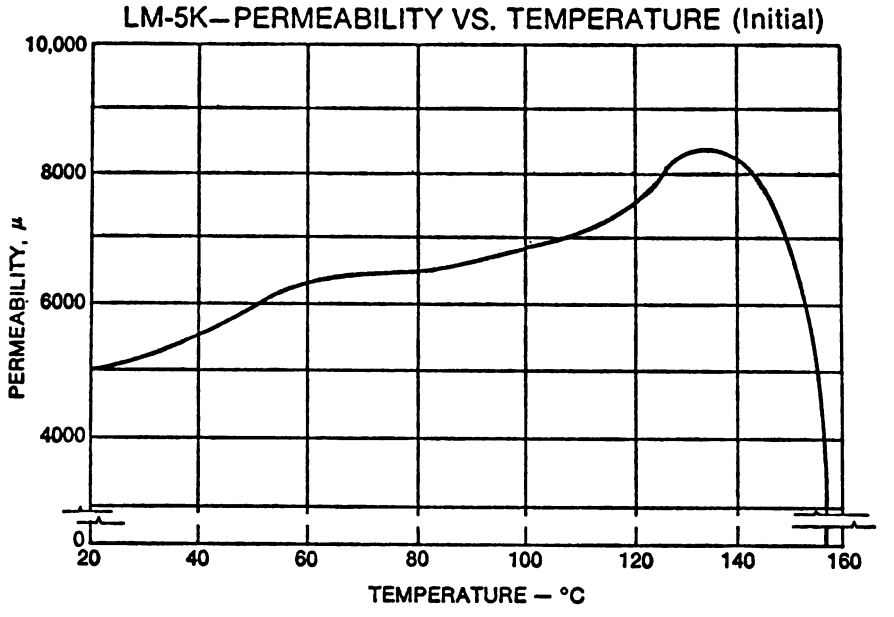

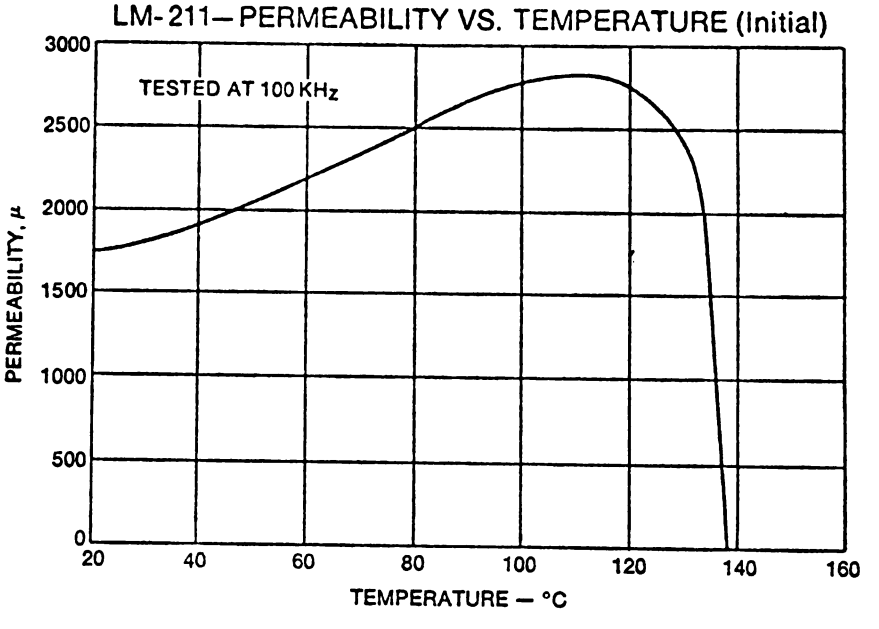

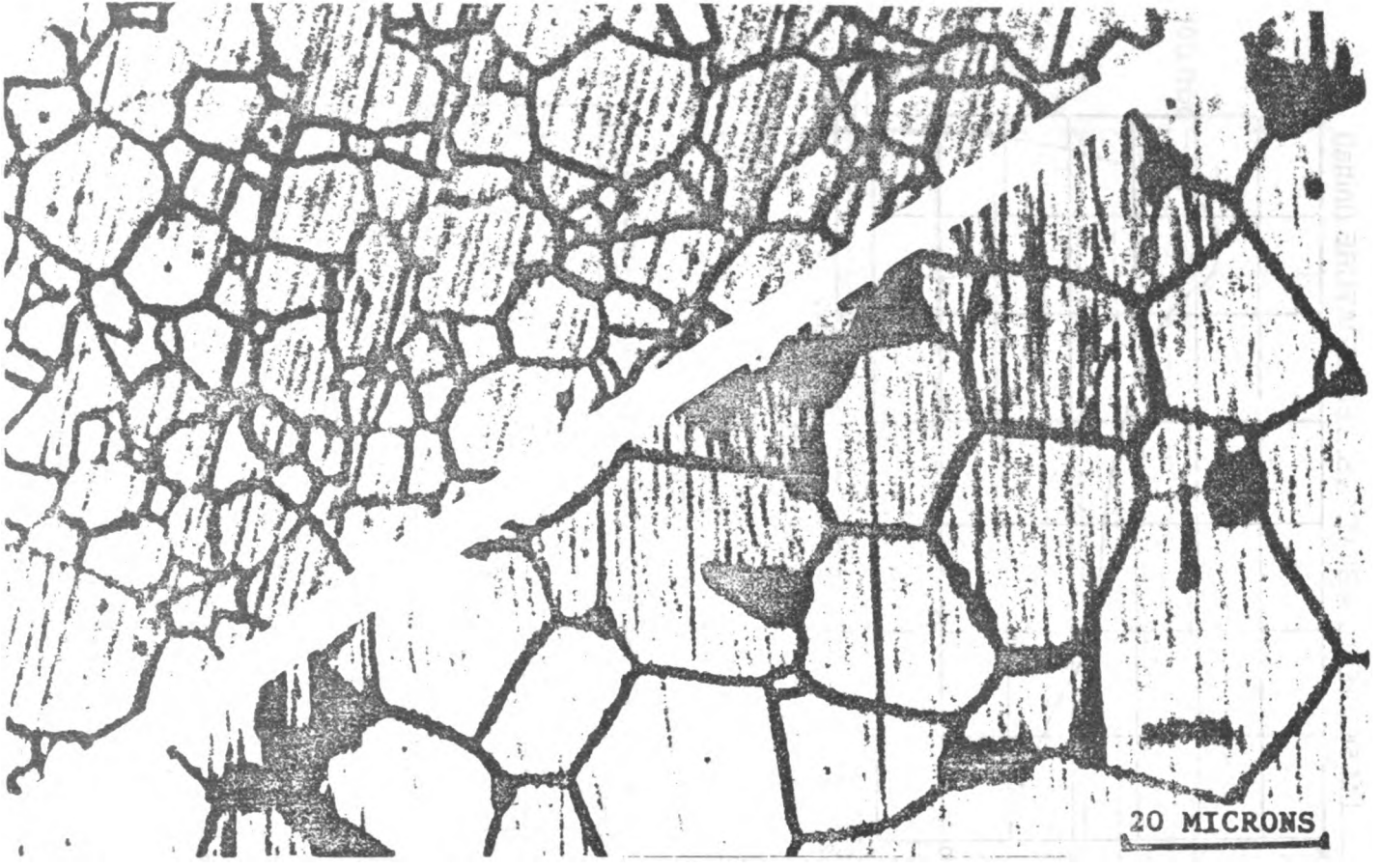

SPECIMEN OF NEW LM-5K MATERIAL, (upper left), CONTRASTED WITH CONVENTIONAL MATERIAL. BOTH ARE MnZn FERRITES POLISHED AND ETCHED. FINER GRAIN STRUCTURE AND HIGHER DENSITY OF LM-5K PROVIDE EXTREMELY SMALL GAP AREAS.

SINTERED MATERIALS FOR ELECTRIC CONTACTS IN POWER ENGINEERING AND THEIR PROPERTIES

BY

H. SCHREINER

Siemens AG, Zentrale Fertigungsaufgaben, Fertigungstechnische Entwicklung, Nürnberg, BRD

At first, let me give a general idea of the function and properties of electric contacts:
It is the task of electric contacts to make contact by closing a circuit with at least two contacts, the carrying of the current and circuit breaking by separating the junction.[1-3] We can distinguish contacts operating under no load as for example electrical connectors or plugs and contacts operating under load, for example switching contacts used in contactors and switch-gear, as well as sliding contacts in eletrical machines. The switching medium is of special importance with regard to arc quenching; generally, the operations are performed in air, sulfur-hexafluoride; in liquors such as oil or oil containing water (Expansin) and in vacuum.

The voltage of power engineering electrical circuits lies within a wide range from about 10 up to 10^5 Ampere the current includes a range of some Ampere up to 10^4 A. The contact materials used must have special properties for the contacts fit all possible requirements when operating under different loads.

As desirable physical properties we can mention a high electrical and thermal conductivity high melting and boiling temperature and specific heat, further a high melting and evaporation point.

As regards the mechanical properties electrical contacts should have a high Young modulus, high strength especially for sliding contacts high hardness and a low coefficient of friction are desirable. To avoid bad conducting surface layers by chemical

reaction the interaction of contacts and atmosphere should be minimum.

The technological properties require a low erosion rate when arcing occurs, further more a low weld strength when contact make is accompanied by bouncing and at last the contact resistance should be minimum, to insure a good current conduction. In the case of direct current material transfer should not perceed a certain rate and speaking of sliding contacts, the wear rate is required to be low as well.

The cited properties cannot be combined randomly because they are dependent on each other. The task of material development lies therefore in optimizing the desired properties. For electrical contact purposes heterogeneous materials are especially suited due to their favorable spectrum of properties.[4] The manufacture of these materials cannot be made by the methods of melting technique for the components are insoluble into each other. In this case we use the procedures of powder metallurgy. The PM-technique is often the only way for the economical production of these compound-materials.

In the following let us consider the structure of sintered contact materials.

We may divide the composite materials into three main groups:

1. the group of metal - metal
2. the group of metal - metal compound
3. and the group of metal - non-metal

The first system is characterized by the fact, that in a base metal a second metal is dispersed being insoluble in the first in the liquid phase. A very fine and regular dispersion of the components can be obtained using metal powders or precipitated powder mixtures. In special cases the dispersed metal may consist of directional or undirectional fibres (a so called fibre compound metal).

When a porous skeleton is sintered of a metal having a high melting temperature and when it is infiltrated by a metal with a lower melting point we obtain a so called infiltration-composite-metal, consisting of two metal skeletons penetrating each other.

The system of metal-metal-compound with favorable properties is manufactured from mixed powders of a metal and a metal compound by a pressing and sintering process. As metal compounds, oxides, hydrides, carbides, nitrides, silicides and others may be used.

As the representative for the system of metal-non-metal, carbon is used, most in form of graphite. Graphite has a good sliding behaviour and diminishes sliding friction; as solid lubricant it reduces the coefficient of friction and the wear. With regard to switching contacts metal-non-metal materials are of special interest due to their low weld strength.

As next I want to give some examples referring to the described material systems.

Systems	Base-Metal	Additive	Systems	Base-Metal	Additive
Me-Me	Ag	V, Nb, Ta, Cr, Mo, W, (Mn), Fe, Co, Ni, Ir	Me-Me-Me	Ag	2Me: V, Nb, Ta, Cr, Mo, W, (Mn), Fe, Co, Ni, Ir
	Cu	V, Cr, Mo, W		Cu	V, Cr, Mo, W
	W	Cu, Ag, Au, Ni, Pd, Pt		W	Cu, Ag, Cr, Mo, Fe, Co, Ni, Pd, Pt
	Mo	Cu, Ag, Au			
Me-Metal-Compound					
Me-MeO	Ag, Cu	CuO, MgO, CaO, ZnO, CdO, Al_2O_3, In_2O_3, La_2O_3, SiO_2, SnO_2, CeO_2, Sm_2O_3, PbO, TiO_2, ZrO_2, Sb_2O_3, Bi_2O_3, TaO_2, Cr_2O_3, MoO_3, MnO_2, Fe_2O_3, Fe_3O_4, CoO, NiO	Me-Me-MeO	Ag	Me: as column 3
			Me-MeO-MeO	Ag	2 Oxides: as above
Me-Me-Hydride	Ag, Cu	LiH, TiH_2, ZrH_2, CaH_2, BaH_2	Me-Me-MeC	Ag	Me: Ni
Me-Me-Carbide	Ag, Cu	SiC_4, TiC, Mo C, WC			MeC: TiC, WC
Me-Me-Boride	Ag, Cu	TiB_2, ZrB_2, VB_2			
Me-Me-Nitride	Ag, Cu	Si_3N_4, TiN, ZrN			
Me-Me-Silizide	Ag, Cu	$MoSi_2$			
Me-Metalloid MeC	Ag	C, Graphite Carbon	Me-Me-C	Ag	Me: Pb, Ni
				Cu	Me: Pb, Sn
	Cu	C	Me-MeO-C	Ag	MeO: as column 3

Fig. 1 System of composite metals for electric contacts.

Fig. 1 gives a general survey of the various composite metals and materials. On the left side you see the different systems, the base metals and the additives. On the right side we have some base metals and additives for three-component systems. Very often multi-component sintered materials are in use for

electrical contacts.
The picture shows very clearly the great number of material combinations; that means we can vary the material properties within wide limits.

The system of metal-metal includes the often used silver-nickel, tungsten silver and tungsten copper materials, the componants of which are practically insoluble into each other, even in the liquid state. By adding nickel and tungsten to silver the erosion resistance and therefore the life of the contacts is increased; further the contact properties are influenced by amount of additive, size and regularity of the metal particles dispersed in the base metal. Composite metals having a mean particle size of the dispersed component of some µm up to some ten µm can be manufactured from the powder mixture.[5)]

Electrical contacts of tungsten copper and tungsten silver are used for example as pre-contacts in high voltage-power switches due to their excellent resistance against arcing.

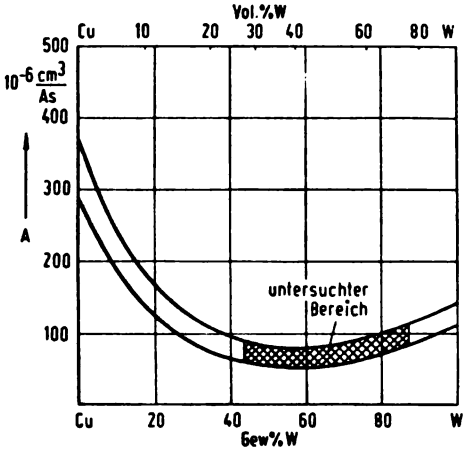

Fig. 2 Erosion of WCu-contacts in proportion to W-contents

Fig. 2 shows that we can expect the minimum erosion rate at about sixty weight percent tungsten.[6)] Besides the composition the erosion rate depends on the fineness of the micro structure. Tungsten silver as an infiltration composite metal is also used for the current carrying contacts in high power switches, the silver

contents being within 50 up to 90 weight percent.

In relation to low voltage switch gear, we have to consider the second system of a metal and a metal compound, especially silver-metal oxides with the oxides of Cd, Zn, Sn, Cu, sometimes Fe, Pb, Co, Ni, Sn, as well as the oxides of the rare earths metals. Additives of metal oxides with a decomposition temperature lying below the boiling temperature of silver as for example CdO, CuO, ZnO, SnO_2, PbO and NiO favour arc quenching; metal oxides in contrary, having a higher decomposition temperature favour the reignition of the arc; for example Al_2O_3, ZrO_2, MgO.[7)]

Structural parts, having an isotropic structure are obtained from the powder mixture, from precipitated mixed powders or from internally oxidized alloy powders, by means of the pressing-sintering-repressing technique.

Semi-finished products, having an anisotropic structure are formed by the pressing-sinter-extruding method.

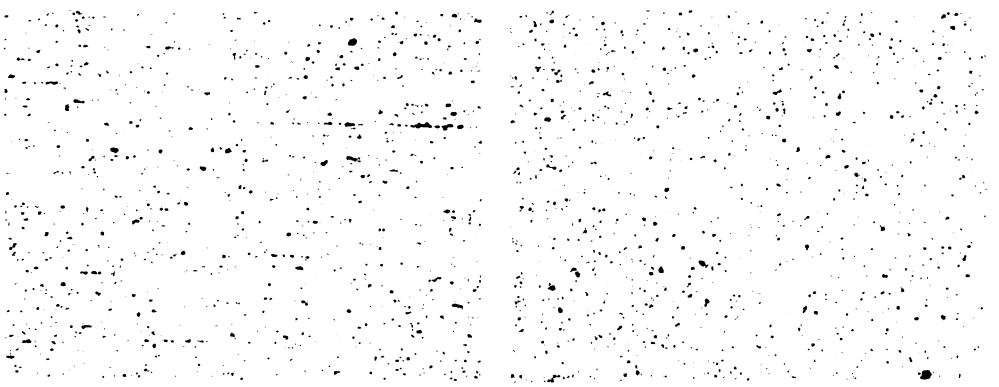

parallel section 100:1 vertical section 100:1

Fig. 3 Structure of an AgZnO 8 composite material prepared by pressing, sintering and extruding

The microstructure of a silver-zinc oxide (AgZnO 8) composite material which has been manufactured by this method is shown in Fig. 3.

In the left picture the section lies in parallel to the direction

of extruding, the right picture shows a vertical cross-section. Regarding the left picture we recognize the banded structure of the zinc oxide dispersions in the silber base metal, following the direction of extrusion.

The effect of dispersion-hardening is obtained when we have a fine and regular distribution of the oxide particles in the base metal; for example with an oxide particle size less than 1 µm and a mean particle distance less than 10 µm.[8] This phenomenon is already obtained with oxide additives less than 1 volume percent. As regards electrical contacts the oxide contents lies usually in the range of five and fifteen volume percent.

Silber-graphite, having a graphite contents up to 10 weight percent, that is forty Volume percent is a representative of the system of metal-non-metal The properties of this material can be influenced by adding nickel or tungsten, respectively. By sintering and extruding the powder mixture a compact with a banded structure is obtained, similar to that of the former cited example of silver zinc oxide. Compared with the silver metal oxide materials the weld strength of silber-graphite materials is considerably lower, however, with increasing graphite content the erosion rate by arcing is augmented.

In contactors and switches silver graphite contacts are often used in combination with silver nickel or silver metal oxide contact materials.

Another important point of view is that of the gas contents of electrical contacts, especially with regard to the development of vacuum switches and vacuum medium voltage contactors.[9] The contact materials are required to have a low gas contents or getter additives within the base metal. Besides copper based alloys, sintered and sintered infiltration materials have been used. The sintered skeletons may consist of Cr, Co, Ni ode Fe with copper or silver as infiltrating metal or of W, Mo, Ta, Re infiltrated by Cu, CuTi, CuZr and others.

The next important point in the field of electrical contacts I want to discuss is that of typical contact properties when making and breaking contact under specified test conditions. Very often we find descriptions of contact materials involving properties such as density, strength, hardness, electrical conductivity, further particle

size and distribution of the component dispersed in the base metal. These values are doubtlessly necessary, but not sufficient for an assessment of the contact material. Unsufficient informations about the material as well as about the test procedure and the different test conditions reduce the worth of information of the test results; in consequence a direct comparision of the test results of different authors seems to be unreasonable.

Confronted to this situation, we suggest to overcome these uncertainties by standardizing both test device and test conditions. In the case of low voltage switch gear, including contactors, we need, besides the physical data, information about weld strength, erosion rate and contact resistance. The test conditions should be as close to practice as possible. So the next point of my contribution is dedicated to thetesting device and the testing conditions as they have been developed in our laboratory. When projecting the test apparatus the priorities have been set to sensitivity and accuracy of measurement, reproduceability of the values, automatization of the whole procedure and last not least to the economical aspect of the measurements.

It is a well known phenomenon that the contact make process especially when we consider contactors, is accompanied by bouncing, that means the contact make is usually not finished at the first touch but as a consequence of bouncing the contact members make and break their contact several times before they reach a permanent state of contact. In the area of the arc spots the material is molten and the contacts may weld.[10] The force nessessary to separate the welded contacts must be available in the contactor other wise a failure occurs. So we understand by "weld strength" the tractive force required to separate two contacts welded under defined testing conditions.

The first three lines show the geometrical data of the contacts, followed by the mechanical switching conditions. As to duration of bouncing it is adjusted mechanically and means that three rebounces occur within five milliseconds under no-load conditions.

Contact making is performed close to current zero; contact break is initiated shortly before the current reaches its peak value, this results in well measurable erosion rates.

A summary of the mechanical and electrical testing conditions is shown in Fig. 4.

Contact area	$A = 10 \times 10\ mm^2$
Convex radius	$r = 80\ mm$
Contact gap	$a = 10\ mm$
Closing velocity	$v_c = 1\ m\ s^{-1}$
Contact force	$F = 60\ N$
Duration of bouncing	$t = 5\ ms$
Velocity at contact break	$v_b = 0{,}8\ ms^{-1}$
Voltage, frequency	$U = 220\ V,\ f = 50\ Hz$
Current at contact make	$\hat{I} = 1000\ A$
" " break	$\hat{I} = 1500\ A$
Power factor	$\cos\varphi = 0{,}36$
Operation 1 on / off	$\alpha_{on} = 0^0$ (0,1 after current zero) $\alpha_{off} = 80^0$
Operation 2 on / off	$\alpha_{on} = 180^0$ (0,1 ms after current zero) $\alpha_{off} = 260^0$
Magnetic flow	$\frac{B}{\hat{I}} = \frac{50 \times 10^{-4}\ T}{100\ A}$
Velocity at welding rupture	$v_r = 7{,}4 \cdot 10^{-3}\ ms^{-1}$
Number of operations	$n = 1000$

Fig. 4 Testing conditions

The magnetic induction has been measured near the current constriction in the closed state of contacts. As regards the number of operations we found out that one thousand values guarantee a reliable information about weld strength.

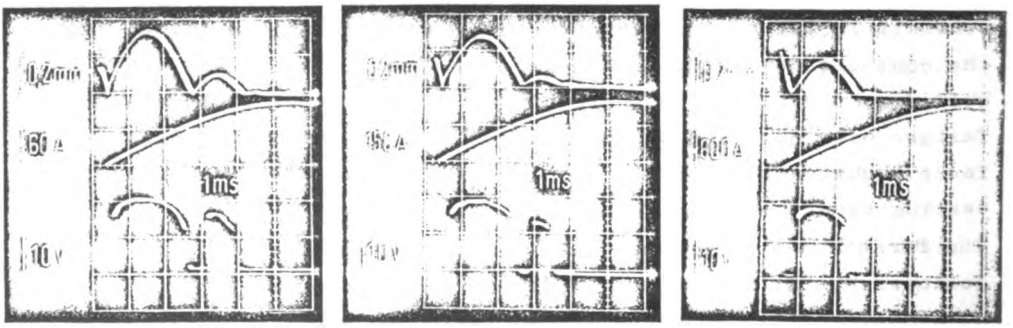

Fig. 5 Bouncing of contacts, current and arc voltage at different test currents, contact-material Ag1000

Fig. 5 reveals the dependence of bouncing behaviour on the value of the test current.

When the peak current value is one hundred Ampere the bounce diagram shows only little changes compared with mechanical bouncing. By increasing current rate however bouncing amplitudes and number of rebounces are reduced resulting in a reduction of the total duration of bouncing. The molten areas created by arcing provide a strong damping of the contact motion. The peak current values in the picture are one hundred, two hundred and fifty and one thousand ampere. Investigating the weld strength by means of a real contactor implies the disadvantage that we don't get the single values of the weld strength; this method leads only to the alternative conclusion whether a failure has occurred or not. With regard to a statistical treatment a sufficiently great number of single weld strength values must be available.

For this purpose a testing device has been developed fitting the cited requirements.

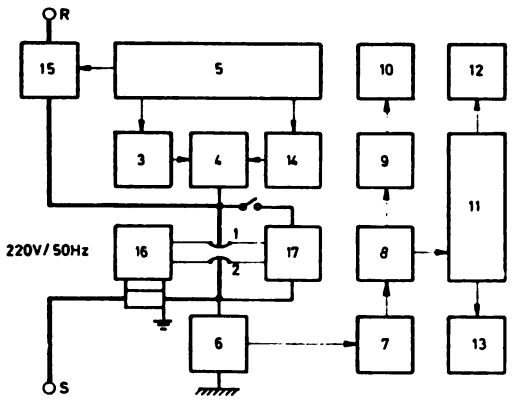

Fig. 6 Block diagram of test divice for measuring weld strength, erosion and contact resistance

Fig. 6 shows the block diagram of the testing equipment.[11] It consists of the movable contact (number 1) and the stationary contact (number 2). The contact make process, that means the closing of the contacts under defined bouncing conditions, is

initiated by a spring-system, number 3, and a magnet-system, number 4, by de-energizing the electro-magnet by means of a synchronizing unit (number 5) and excitation of the thyristors (number 15) at a certain phase of the voltage. Closing velocity, duration of bouncing and the contact force can be adjusted within wide ranges. The weld strength is measured as the tractive force by a pre-loaded quartz force transducer, number 6. The charge signal of the force link is transformed into a proportional output voltage in the charge amplifier, number 7, which is connected to an analog peak indicator, number 8 and a digital voltmeter, number 10. The output of data is performed by a printer (number 10).

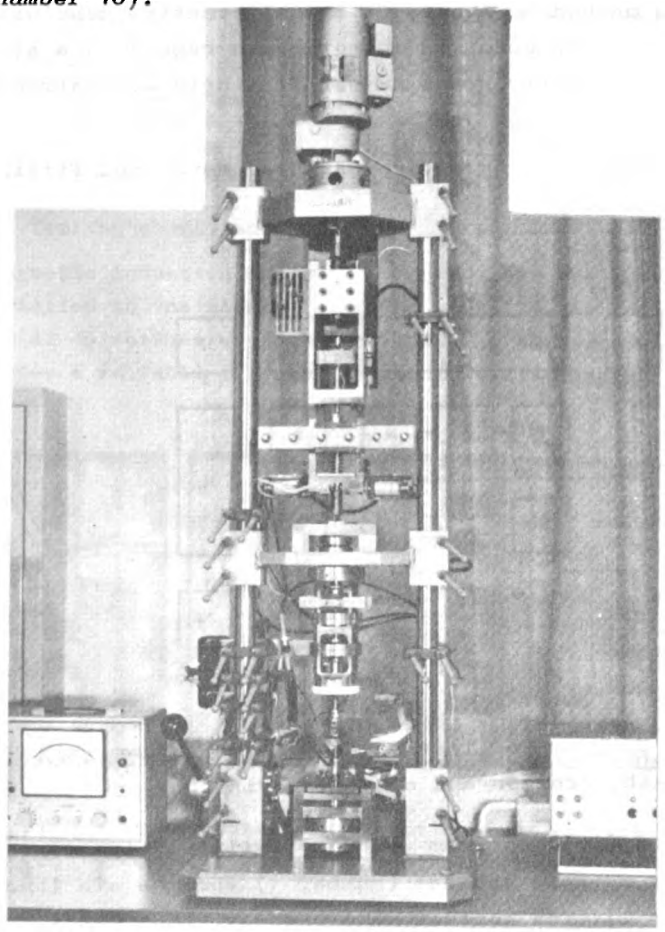

Fig. 7 Testing equipment for measuring weld strength, erosion and contact resistance

Fig. 7 shows a total view of the weld test apparatus. The switching elements are attached to a rigid frame to prevent oscillations and disturbances of the accurate contact make and break process.

The computer (number 11) is fed with the analog voltage signals of the weld strength.

A greater number of measured values, for example 1000, is stored in the computer for statistical evaluation.[12,13] The values are classified in accordance to their magnitude and written by a type writer (number 12). Finally the plotter (number 13) draws the cumulative frequency curve.

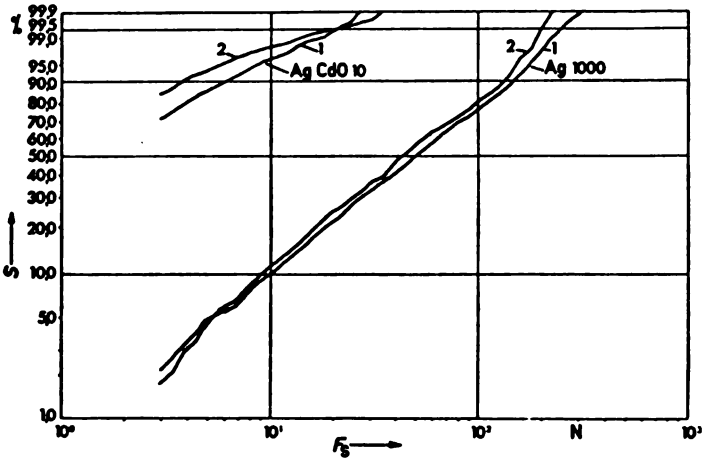

Fig. 8 Cumulative frequency of weld strength, contact material AgCdO10 und Ag1000

Fig. 8 shows cumulative frequency plottings of the weld strength of silver and silver-cadmiumoxide in a Weibull probability paper. The maximum values of AgCdO are one order of magnitude lower than those of silver.

The contact array is shown in Fig. 9. By means of a conductor winding (24, 25), similar to that of contact members of contactors, a Lorentz-force, proportional to current and magnetic induction, is generated. It forces the arc to move out of the contact gap on the arc runners (22, 23). Schröder und Schulz have used direct

current magnetic blow for propulsion of the arc when measuring erosion rates.

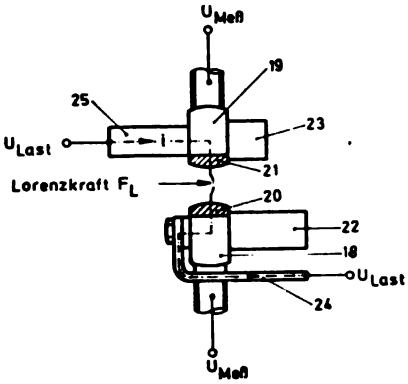

Fig. 9 Array of the stationary and movable contact with conductors

The same authors have also mentioned the influence of the moment of contact break on the erosion rate.[15)]

The arc runners are made of steel at the movable and of copper at the stationary contact. The contacts are hard soldered to the supports (18, 19). The erosion rate of both contacts is calculated from the weight difference before and after each test series.

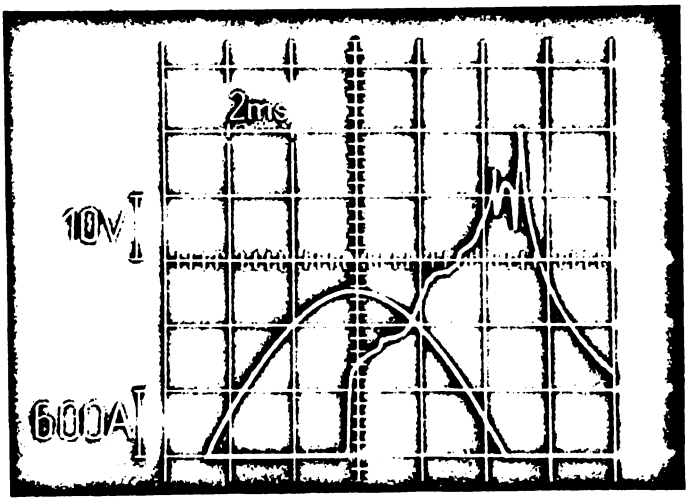

Fig. 10 Current and voltage at contact break

Contact break under current conditions is performed by an opening mechanism containing a mass-spring system.

The synchronizing unit (5) and the thyristor-controlling unit enable the contact members, by means of a magnetic system, to break contact at a pre-determined phase of voltage. Both current and arc voltage are recorded on a storage oscilloscope (Fig. 10).

The loss of weight caused by evaporation and splashing is specified as loss of volume in relation to current, fitting the following equation

$$V = c\left(\int i(t)\,dt\right)^n$$

c and n being material dependent constants.[14,15] For most contact materials the value of n lies between 1,5 and 2.

The rate of erosion is increased when the weld or soldered junction of contact and support metal is insufficient. Therefore junction technique and quality control are of particular importance. A second layer is often attached to the AgMeO and AgC contacts consisting of materials with good welding and soldering properties.[16,17]

	Erosion rates mg per 10^3 operations			Contact resistance R_K in mΩ		
	minimum	mean	maximum	1 %-	50 %-	99,5 %- value
Ag CdO 12	296	308,5	321	0,06	0,17	3,4
Ag 1000	4655	4817	4980	0,02	0,06	2,5

Fig. 11 Erosion rates and contact resistance of AgCdO12 and Ag1000

Fig. 11 gives a survey of erosion rates and contact resistance as have been measured for silver cadmium oxid and pure silver under the nominated test conditions. With regard to erosion there is a difference of the factor of sixteen between the erosion rates of both materials.

On the right side of the Fig. 11 we have noted the one - the fifty and the ninety-nine point 5 percent values of the cumulative frequency curve of contact resistance. Silber cadmium oxide has a maximum value that is approximately thirty-six percent higher

compared with silver. The contact resistance varies with kind and amount of oxide additives, however, the silver contents being about 90 %, it is of inferior importance. In a more general case we have to pay attention to oxid layers on the contact surface, for the contact resistance does not reach critical values.

Using the current-voltage method, contact resistance is measured; first after contact make second after rupture of the welding and third after contact break under current. The first two values being relatively low, we have found a considerable increase of contact resistance in the third case.

Summarizing our test results, we recommend, for the assessment of a contact material for power engineering purposes the specification of weld strength, erosion and contact resistance. These values have to be measured under defined test conditions, and should not exceed an upper limit.

The testing results show that the maximum weld strength or the position of the cumulative frequency curve, respectively, is in close relation to contact break current. Further, a reciprocal relation exists between weld strength and erosion rate. When the erosion rate is diminished as for example by alternation of composition, micro structure or manufacturing parameters, we find a simultaneous increase of the weld strength values.

As regards silver-cadmiumoxide with other additives of metal oxides, an evaporation of the metal-oxide component occurs due to arcing, resulting in a higher weld strength. This phenomenon is made evident by micro structure analysis.[18)]

A final testing of contact materials, however, has to be performed as usual in a real contactor or switch taken from the series production. Pre-selecting and testing of contact materials helps us to reduce both duration and costs of testing.

Literaturnachweis

1) Holm, R., Electric Contacts, Stockholm: Geber 1946 , Electric Contacts Handbook, 3.Aufl.,Springer Verlag,58, Bln.

2) Keil, A., Werkstoffe für elektrische Kontakte, Berlin Springer-Verlag 1960

3) Schreiner, H., Pulvermetallurgie elektrischer Kontakte, Springer-Verlag, Berlin 1964

4) Schreiner, H., Verbundwerkstoffe und ihre Anwendung für elektr. Kontakte, Z.f.Metallkunde 58 (1967) S.609-605

5) Stolarz, St., J.Golonka u. J. Kurzeja, Die Technologie der Herstellung von gesinterten ein- und mehrschichtigen WCuNi-Kontaktwerkstoffen, Planseeberichte für Pulvermetallurgie 17 (1969) S. 10-24

6) Haufe, W., W.Reichel u. H. Schreiner, Abbrand verschiedener WCu-Sintertränkwerkstoffe unter Öl bei hohen Strömen, Z. f. Metallkunde 62 (1971) S. 592-595

7) Vinaricky, E. u. U. Harnsen, Einfluß der Silber-Metalloxid-Kontaktwerkstoffe auf die Löschung kurzer Wechselstromlichtbögen, Metall 25 (1971) 749-754

8) Schreiner, H., Dispersionsgehärtete Kontaktwerkstoffe mit dem Grundmetall Silber IV.Int.Pulvermet.Tag. 23.-26.9.69 Dresden, S.18/0 - 18/20

9) Hässler, H. u. H.Schreiner, Sinterkontaktwerkstoffe mit kleinem Gasgehalt, Elektrische Kontakte (1970) 5. ITK Mch. VDE-Verlag, Berlin (1970) S. 71-74

10) Haufe, W., W.Reichel u. H.Schreiner, Ursachen der Schweißbrückenbildung und Einflüsse auf die Schweißkraft elektr. Kontaktstücke in der Energietechnik. ETZ-A 93 (1972) S. 305-306

11) Geldner, E., W.Haufe,W.Reichel u. H.Schreiner, Prüfschalter zur Messung der Schweißkraft von Kontaktwerkstoffen für die Starkstromtechnik, ETZ-A 92 (1971) S. 637-642

12) Haufe,W.,W.Reichel,H.Schreiner u. R.Tusche, Einfluß der Schaltzahl und Polarität des Prüfstromes auf die Statistik der Schweißkraftwerte von Reinsilber bei synchronem und unsynchronem Schließen der Kontaktstücke. Bull.SEV 63 (1972) S. 461-467

13) Haufe,W.,W.Reichel,H.Schreiner u. R.Tusche, Einfluß der Prelldauer und der Kontaktkraft auf die Statistik der Schweißkraftwerte von Ag1000 und AgCd010, Bull.SEV, 64 (1973) 8, S. 500-504

14) Erk, A. u. K.H.Schröder, Über den Materialverlust homogener und heterogener Kontaktwerkstoffe für Schaltgeräte mit magnetischer Lichtbogenbelastung. ETZ-A 89 (1968) S. 373-377

15) Schröder,K.H. u.E.D.Schulz, Einfluß des Trennaugenblickes auf den Lichtbogenabbrand öffnender Kontaktstücke beim Wechselstromschalter, Metall 28 (1974) S.463-468

16) Schreiner,H., Zweischichten-Sinterwerkstoffe 2.Europ.Symp.für Pulvermetallurgie,8./10.5.68 Stgt.Bd.II,6.8 S.1.18

17) Schreiner,H., Two-Layer Compact-Sinter-Infiltration Technique for Producing Contact Materials for Power Engineering Purposes, Powd.Met.Int. 7 (1975) 21-24

18) Kontaktwerkstoffe der Elektrotechnik mit Beispielen für die Energietechnik, DGM-Symposium, Werkstoffe der Elektrotechnik, 16.10.72 in Bad Nauheim

DISLOCATION MOBILITY IN SILICON

BY

A. VALČIĆ, R. ROKNIĆ AND M. TOŠIĆ

Tehnološko metalurški fakultet
Institut za hemiju, tehnologiju
i metalurgiju, i
Elektronska industrija
Beograd, Jugoslavija

During the Czochralsky growth of dislocation-free crystal of Si, after some time, that is at some length of the crystal, the appearance of dislocations may sometimes occur, i. e. the crystal ceases to be dislocation-free. During further growth the crystal will contain dislocations or even the occurance of polycrystals may take place. This occurance of polycrystals or dislocation during the proceeding crystal growth also leads to deformation of the crystal part which till that time was growing free of dislocations. Deformations formed in this way may be established at the length of 5-7 cm away from the place where the crystal ceased to be dislocation-free along the crystal axis.

In this papaer we wanted to examine the mobility of dislocations formed in this way, then to examine the possibility of changes in both their distributions and number in the crystal, and eventually their removal as well.

The method of measurement of dislocation velocity rate by means of the etch-pit technique has been developed by Johnston and Gilman[1] on LiF. The rate of dislocation motion has been measured on the alloy Si-Fe[2] in the same way, and then followed measurements on semiconductive materials [3,4]. Measurements of dislocation motion in Si have also been performed by the X-ray Topography [5,6,7]. What is common to most of these examination is the fact that crystals with few dislocations or without dislocations were used as samples. Dislocations were formed in the crystal immediately before measuring, and then their motion, in the function of the applied stress and temperature at which the experiments were carried out, was investigated.

As we wished to reduce the number of dislocations in the crystal of Si, or even to remove them completely, we did not venture to use external stress. In our experiments dislocations moved under the influence of stresses existing in the crystal due to the presence of dislocations.

Experiments

Samples for the examination were obtained by cutting crystal Si perpendicular on the axis of growth (111) above the place of dislocation appearance; in this way wafers 10-20 mm thick and 40 in diameter were obtained. The electrical resistivity of the crystals was 7-12 Ω cm, and they were doped with B.
The part of the crystal from which samples were cut off proceeded growing dislocation-free, but as it was near the place of dislocation appearance and at sufficiently high temperature, the temperature gradient, that exists while crystal was being pulled, made plastic deformations. Dislocations formed in this way lie on planes $\{111\}$ in direction $\langle 110\rangle$ and these are 60° dislocations. On the cross-section of the crystal, on plane (111), after etching, can be seen etch-pits arranged into slips along the direction $\langle 110\rangle$ (Fig.1) (Fig.2)

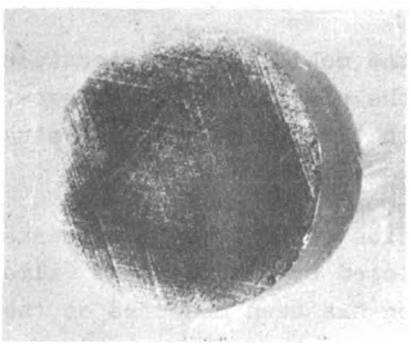

fig.1

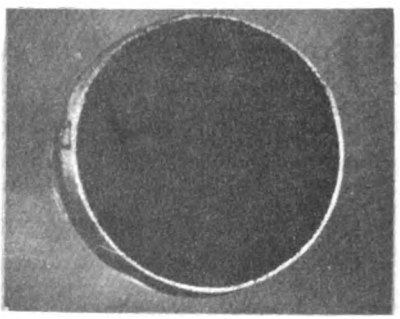

fig. 2

The measurements were carried out in this way: first the sample surfaces (111) were laped and chemically polished and then they were etched with Sirtle-etch in order to cause slips to appear. Then slips on plance (111) were selected and marked and their lengths were measured under the microscope. Thus prepared samples were heated in atmosphere Ar for a definite time (from 15 min.

10 h) at different temperatures. The temperature was maintained within limits of ± 5°C. When the samples were annealed, planes (111) were etched again in the same way as before heating, so that it was possible to measure the changed lengths of slips. The differences in slip lengths before and after heating, reduced to a time unit, represented the rates of dislocation motion. The shortening of the lines proceeded due to the fact that dislocations moved within planes of slipping {111} from the centre of the crystal towards the surface where they went out.

Results and Discussion

The measurements were carried out at temperatures of 700°C up to 1000°C. At 700°C the rate of dislocation motion was exceptionally low, so that we were not able to establish the shortening of slips in most number of cases. These shortenings were of value order of measurement error. At high temperatures, 950°C and 1000°C, the rates were very high so that the slips completely disappeared already after 15 min. For this reason it was impossible to determine the rates of dislocation motion at these temperatures. 1-1.5 h was necessary at 900°C for the complete disappearance of the slips, so it was possible for us to measure the motion rates at this temperature.

In Fig. 2 is shown the crystal after heating at 900°C 1 h. All slips had disappeared, and we were able to find out dislocations only in the narrow zone along the crystal circumference.

At lower temperatures, 700° and 800°C, was possible to establish the slips, the length of which was not shortened during heating. At 900°C all lines got shortened. Bessides this, it is of interest to mention that at lower temperatures we found out, although very rarely, even slips which got shortened very quickly. This was established for example on the sample which had only two parallel slips and which was heated at 750°C. The measured motion rates of these dislocations were $5{,}78 \times 10^{-5}$ cm/sec. and $5{,}15 \times 10^{-5}$ cm/sec these rates are about eight times higher than the average rate at 750°C. These rates agree with the rates that were measured [3,5] during the motion of individual dislocations under stress of about 1 kg/mm².

In table I are given the rates of dislocation motion in function of temperature. At each temperature about 20 measurements were performed, and in Table I are given only the mean values of dislocation motion rates.

Table I

Temperature dependence of dislocation velocity

T °C	750	800	850	900
$v_s \cdot 10^5$ cm/s	0.7	2.7	24.2	106.4

The diferences in dislocation motion rates that have been established by all authors who were engaged in this problems we have also established. These differences may be easily explained on the basis of the differences in the very nature of dislocations and their interactions with other dislocations and impurities.
Even the experiments carried out by Dash[8] showed that dislocation motion in Si leaves traces of vacancies and interstices.
With increasing temperature of measurement the differences between the minimum rates of dislocation motion decreases.
On the basis of the Table I, it is possible to establish the great influence of temperature on the rate of dislocation motion within slips, which indicates that this is a thermally activated process. In Fig.3. are presented the results from Table I in the system $\ln v_s - \frac{1}{kT}$. The activation energy of the dislocation motion process in slips is 3.5 e V. During the measurements of the rates of dislocation motion, great differences were established. The rates of dislocation motions can be accurately analised only if dislocations were defined. Jogs in screw dislocations, and even in edge ones, reduce the mobility in a very high degree. This effect depends on the jog density and the heights of jogs. For this reason nearly perfect crystals, most often dislocation-free crystals, were dealt with in earlier papers, no that the mechanism of dislocation intersection was not taken into account. Dislocations were formed in the samples immediately before measurement.

Hindrance in dislocation motion may be Peierls barrier or the interaction of dislocations with other defects. The rate of dislocation

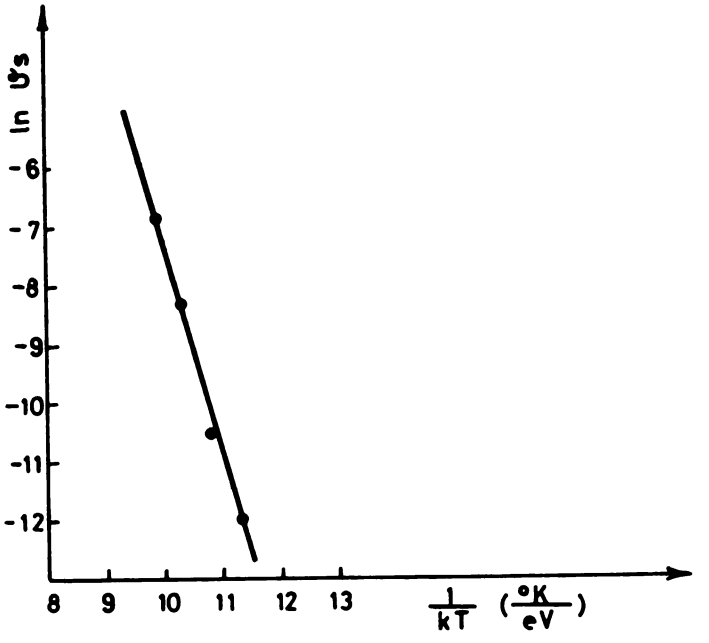

fig. 3

motion may be controlled by: 1/ nucleation and extension of kinks or 2/ nonconservative motion of jogs.

Dislocation mobility rapidly increases with temperature, which is in accordance with the assumption that dislocation motion is a thermal activated process.

When covalent crystals are concerned, the Peierls barrier is considered to play the main role in dislocation motion. Celli et al[9] gave the theory of dislocation motion in semi-conductors.

Numerous measurements of the rates of dislocation motion in semiconductive materials[3,4,5,6,7] in dependence on temperature and stress have been performed and the dependence between the rate of dislocation motion v and temperature T during constant stress was established:

$$v = C_1 \exp\left(-\frac{E}{kT}\right)$$

which is in accordance with the theory. The obtained values[3] for activation energy for dislocation motion in Si, Ge, GaSb and InSb show that they are approximately half less than the activation

energy for self-diffusion (E_{sD}) in these materials.
The value for the activation energy for dislocation motion in Si[3, 5,10], which have been obtained by different authors, are within limits of 2.2-2.4 eV, except the value 1.8 eV obtained by Kannan and Washburn[6]. The activation energy for self-diffusion in crystal of Si doped with B is 3.6 eV[11].

This value approaches the value that we obtained for the activation energy for dislocation motion of 3.5 eV.

In our experiments the samples contained quite a number of slips. The dislocations, that formed these slips, lay in planes $(\bar{1}11)$, $(1\bar{1}1)$ and $(11\bar{1})$. These were the slips whose rate-shortening we measured. Besides, in crystals there were slips whose dislocations lay in plane (111). In such distribution of dislocations, manifold cross-section takes place, and jogs have considerably bigger sizes.

On the basis of the obtained value for the activation energy for dislocation motion E=3.5 eV, one can assume that these big jogs, whose motion is non-conservative, determine the rate of dislocation motion in slips.

For dislocations moving in this way, for little values of the force and free of vacancy supersaturation, the rates of dislocation motion is given[12] by equation:

$$v = C_2 \exp\left(-\frac{E_{sD}}{kT}\right)$$

where C_2 is approximately a constant.

Conclusion

In this paper was examined the motion of dislocation at temperatures from 700° to 1000°C.

The activation energy for dislocation motion in slips was determined; it was E=3.5 eV. It was also established that all dislocations may be removed from the crystal, except those within the narrow ring of the crystal circumference, by heating the crystal at 900°C in the period of 1 h, but at 950°C and 1000°C even during a shorter time.

References

1. W.G. Johnston, J.J. Gilman, J. Appl. Phys. 30 /1959/ 129

2. D.F. Stein, J. Low, J. Appl. Phys. 31 /196o/ 362
3. A.R. Chaudhuri, J.R. Patel, L.G. Rubin, J. Appl. Phys. 33 /1962/ 2736
4. M.N. Kabler, Phys. Rev. 13o /1963/ 54
5. T. Suzuki, H. Kojima, Acta Metallurgica 14 /1966/ 913
6. V.C. Kannan, J. Washburn, J. Appl. Phys. 41 /197o/ 3589
7. S. Oki, K. Futagami, Japan. J. Appl. Phys. 13 /1974/ 6o5
8. W.C. Dash, J. Appl. Phys. 29 /1958/ 7o5
9. V. Celli, M.N. Kabler, T. Ninomiya, R. Tompson, Phys. Rev. 131 /1963/ 58
10. R. Haasen, Versetzungen und Plastzität von Germanium und InSB, Festkörperprobleme 3, Vieweg, Braunschweig /1964/
11. B. Henderson, "Defects in Crystalline Solids" /Arnold, London 1972/ p 113
12. J. Friedel, Dislocations Pergamon Press /1964/

SOME STRUCTURAL AND SYSTEMATIC PROBLEMS IN CERAMICS AND CERAMIC TO METAL SEALS

BY

R. JAKOWLEW, A. SZYMAŃSKI AND W. WŁOSIŃSKI

Ośrodek Naukowo-Produkcyjny Materiałów Półprzewodnikowych

Basic terms in Ceramography

The term "ceramography" was introduced into professional literature by E. Ryshkewitch (33) to isolate the science of internal structure of ceramic materials into separate discipline. Before this was done, the microscopic investigations were referred to as petrography, by an analogy to terms used in the studies of natural rocks. The introduction of the concept of ceramography for ceramic materials, analogous to metallography for metallic materials, allows for independent development of this discipline which, while employing research techniques similar to those used in petrography, greatly differs from the latter by the wealth of phases, the number of minerals in the materials under study, and their spatial arrangement.

Bielankin et al (5) proposed to relate the structure of ceramic materials to the analogous natural materials; it was found, however, that the principles of structural petrography classification adopted in petrography could not be transplanted, to ceramography. It seemed more justified to adopt the principles of systematics based on the structure of the given material and to arrange the materials according to the increasing size of the crystalline components for sintered and fused materials (Szymański, 37) (Fig. 1). In this way all the man-made products obtained from natural raw materials, i.e. the materials having equivalents in nature and the ones without such equivalents could be arranged into a fairly systematised whole.

What we call a rock is a natural aggregate of minerals

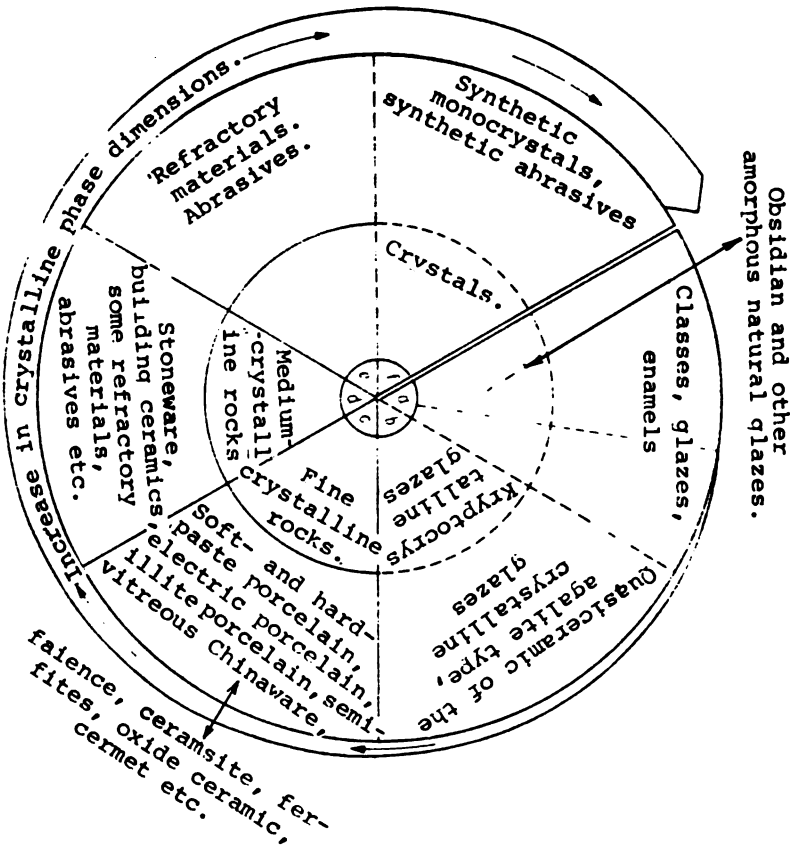

Fig. 1. Schematic comparison of natural crystals and rocks with their synthetic, fired analogues; a, b, f - there exist natural analogues to synthetic materials; c, d, e - ideal natural analogues to synthetic materials do not exist.

that can be simple, i.e. monomineral or complex - polymineral. Two terms are used to define its structure: texture - for the macroscopic structure, and structure - for the microscopic structure (Morozewicz, 27).

The structure of a rock comprises the features of its internal structure i.e. the degree of crystallinity, the size and shape of crystals, and the interrelations between the crystals.

The texture of a rock comprises these features of its internal structure which concern the spatial arrangement of

components and the degree of filling the rock space with these components.

The term "structure" was introduced into rock description terminology by Naumann, in 1824, as a synonym of a more general term of "Gefüge" used to characterize rock structure. In English terminology, the equivalent for "Gefüge" is "fabric" and for "structur" - "texture". This is why in the English literature the internal rock structure is defined as "texture", "structure" being used in crystal lattice investigations.

Nevertheless, some authors (Baumann, 4) use the term "structure" to define the degree of crystallinity and mutual phase component configuration in the material. Similar terminology has been adopted in Poland, the USSR and Czechoslovakia.

To avoid confusion, and following the practice adopted in petrography, the terms of "structure" and "texture" as given in this papaer should be used in the description of ceramic materials.

The basic operations in the synthetic materials production process include the preparation of the material, its moulding and appropriate physical or chemical treatment. Thus, according to Baumann (3), to understand the processes occurring during the synthesis, one should be able and know how to fully define the chemical and physical nature of the reagents in every production stage. Such investigations are, however, difficult to carry out, because the materials used in these processes are usually highly comminuted. The final products are characterized on the basis of their phase composition, phase structure and the spatial configuration of phases (that is by the "structure" of the material). These features usually depend on the composition, the physical and chemical nature of reagents and, also, on the reaction rate and conditions in which it takes place.

Most synthetic rocks (i.e. ceramic materials) may be regarded as the specific types of (igneous magmatic) rocks. Therefore, everybody carrying out research work on such materials, in addition to the knowledge of classical petrography and mineralogy, should be thoroughly acquainted with their production process in order to be able to provide a correct

interpretation of the stationary state in the final product or in any stage of the production process.

Modification of the production processes will often be possible on the basis of the results of examination of the mineral composition and structure of materials. To carry our such analyses one must posess appropriate qualifications. The analytical studies can be impeded by insufficient exchange of information between investigators and technologists. It would be advisable for the research workers to have at hand complete sets of theoretical (mineralogical and physicochemical) data for various industrial processes. Such analyses can be found e.g. for porcelain production in the works of Lundin 23; Bud-

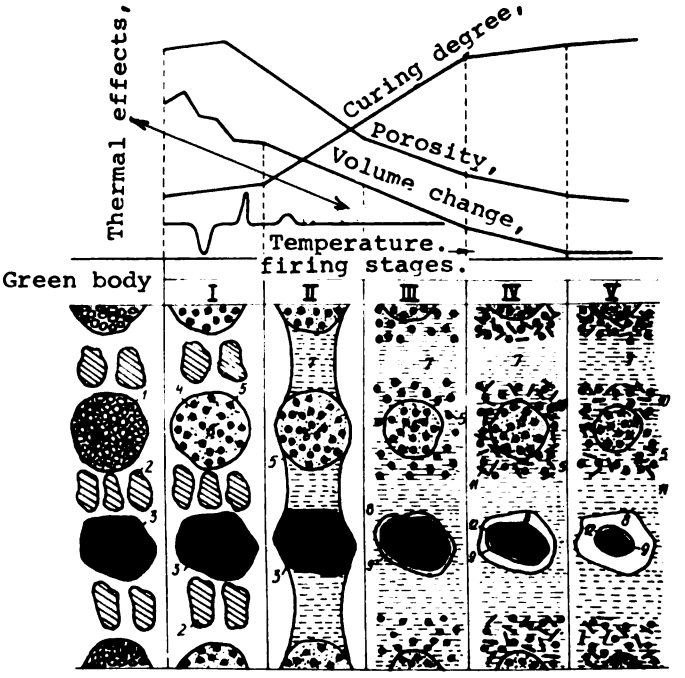

Fig. 2. Porcelain formation scheme, according tom H.O. Gieworkin (1037)
1 -kaolinite, 2 -feldspar, 3 -quartz, 4 -amorphous silica, 5 - primary mullite, 6 -kaolinite residue, 7 -fired feldspar, 8 -silicate-feldspar alloy envelope embracing quartz crystals, 9 -quartz residue, 10 -silicate-feldspar alloy near kaolinite residue, 11 -secondary mullite, 12 -metastable cristobalite.

nikow, and Gieworkin 6.

Mellord says that ceramics is the chemistry of detained processes. An excellent example to support his view and to illustrate the typical ceramic package moulding process is the diagram developed by Budnikow and Gieworkin (6) (Fig. 2). Analysing, for the sake of an example, the hard--paste (classical) porcelain firing process, the authors have shown the successive process stages which, if the process is stopped in any of the stages, give a series of silicate ceramic materials: green body faience semi:porcelain porcelain. A similar diagram has can be produced for any ceramic material.

2. Systematics of the Structure of Ceramic Materials

The properties of crystals (monocrystals) are vectorial; this means that they depend on the orientation of the crystals. All crystals except of those of the isometric system, are anisotropic.

The properties of the synthetic inorganic materials, consisting mostly of polycrystalline aggregates, depend not only on the internal bonds between individual crystalline components, but also - and perhaps above all - on forces bonding the crystals into aggregates. These forces are generally weaker than the intercrystalline forces, their value being closer to the molecular forces.

According to the structural type of a material, its bonding forces and properties of the material as a whole depend on the degree of sintering of the intercrystalline components (sintered carbides and oxides) or on the glassy phase appearing (in the case of porcelain) or purposely introduced (in the case of abrasives), whish binds together the individual material components. If the structure includes the glassy phase, the properties of the material would basically depend on the properties of this glassy phase which plays the role of the host for the crystalline components suspended in it. This is why the properties of ceramic bodies made from various disoriented components, are of the semi-anisotropic nature.

The structure of polycrystalline aggregates is de-

fined by their size, number, mutual spatial configuration of crystalline components and the presence of amorphous phases and pores. Similarly, and perhaps even more distinctly than in the natural rocks, the structure and the properties of inorganic materials will depend on their history (the pressure and heat treatment processes applied, etc.).

All the synthetically produced inorganic materials are - like natural rocks - the aggregates of minerals aggregates and crystalline or amorphous phases of a more or less constant composition. Their properties mainly depend on their mineral composition and macrostructure; structure and texture.

Under the term "structure" we understand the amorphous or crystalline structure of a material, the size and shape of its grains and the type of binding them into a material. In Table 1 the basic magmatic rock structure types adapted for ceramic materials are specified.

Fig. 3 presents diagrammatically several examples of ceramic materials structure (Glibowski, Swiecicki, 13). Further examples are given in Fig. 4 (Milligan, 26). Both figures are supplemented by structural description given in Table 1.

The presented examples indicate to the possibility of using, in ceramography, the elements of the magmatic rock classification system. Like in metalography, five basic structures are distinguished: monophasial and mixed polyhedral, shell matrix, oriented and isometric (Saltykow, 35).

The adoption of uniform systematics seems desirable because, under the conditions of a complete lack of relationships between the development of research work in industry and for practical applications, the own systematic patterns that are being adopted in industry and sience not always are justified from the point of view of the composition, structure and production of a given material. One can quote such examples as the division of ceramics into whiteware and red ceramics, the separation of glass from ceramics, the division of metallurgy into that of the ferrous and non-ferrous metals, and the like. The modern concept of ceramics comprises almost the whole applied solid state physics and this point of view seems to be most rational for the structural systematics of ceramic materials.

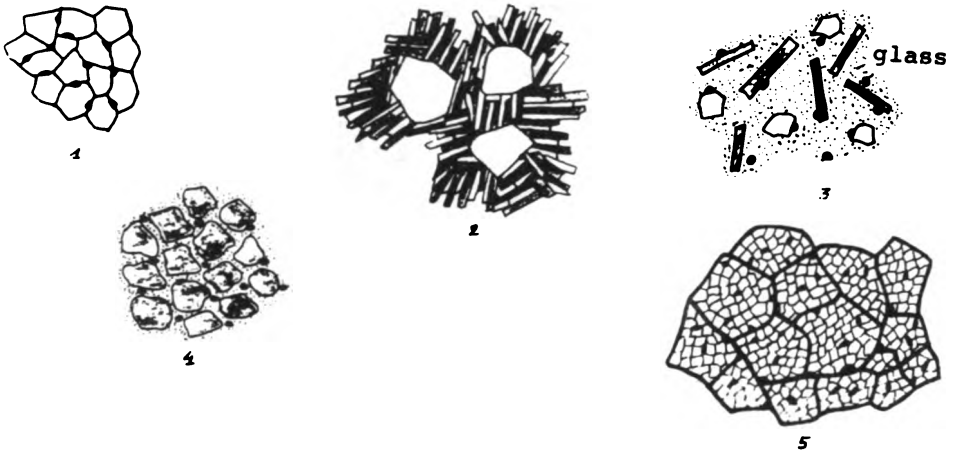

Fig. 3. Schematic example of typical ceramic material structure, after Glibowski and Swiecicki 91975.
1 -Monocrystalline material with pores on grain boundary.
2 -Material containing two crystalline phases, one composed of small and large crystals with pores on grain boundary.
3 -Material containing one crystalline phase, where grains are separated by glass and pores.
4 -Material containing two crystalline phases in glassy matrix and pores.
5 -Material containing polycrystalline grains and pores inside grains and on grain boundaries.

Structure description proposed after Table 1:

1. Holo-phenerocrystalline structure, coarse-, medium- or fine- crystals with hypoautomorphic grain formation.
2. Holo-phenerocrystalline structure, coarse-, medium- or fine- crystals with automorphic grain formation.
3. Holo-phenerocrystalline structure, medium- or fine- crystals with automorphic grain formation.
4. Hypophenerocrystalline structure, medium- crystals with xenomorphic grain formation.
5. Holo-phenerocrystalline structure, coarse crystals with xenomorphic grain formation.

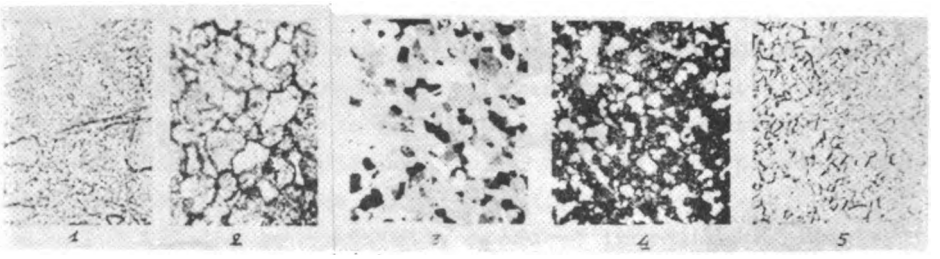

Fig. 4. Structure of some ceramic materials, after Milligan (1950)

1. Silicate porcelain, mullite, glassy-phase and remnants of quartz and feldspar; transmitted light x 500.

2. Oxide porcelain compoed of $3MgO\ 5BeO.8ZrO_3$; glass-free, intergrain mass bonds together the individual constituents; transmitted light x 500.

3. Carbide porcelain, composed of hot melted boron carbide. B_4C crystals; reflected polarized light x 500.

4. Oxide porcelain cermet. Alumina crystals of the oxide porcelain (dark) form the continous phase, with chromium metal (white) dispersed throughout; reflected light x 500.

5. Cemented tungsten carvide (not a porcelain) Crystals of tungsten carbide are cemented together by a cobalt metal continous phase. Surface etched after polishing; reflected light x 500.

Proposed structural description after Table 1:

1. Hypocrystalline structure, microaphanite with auto and hypoautomorphic grain formation.
2. Hypophenerodrystalline structure, fine- crystalline with xenomorphic grain formation.
3. Holophenerocrystalline structure, fine-crystalline with hypautomorphic grain formation.
4. Hypocrystalline structure, microaphanite with xenomorphic grain formation.
5. Hypophenerocrystalline structure with automorphic grain formation.

Table 1. Igneous Rock Structures Adjusted for Ceramic Materials Description

Basic structure	Structure sharpness	Grain size	Degree of grain regularity	Examples of ceramic materials
Holo-crystalline (fully crystalline)	fenerocrystalline (visibly cristalline	COARSE-grained ∅ 1-5 mm	Automorphis (or idiomorphic) - retaining their own shape ((regularly bordered)	refractory mat.
		medium-grained ∅0 1-1 mm		refractory mat. building ceram.
		fine-grained ∅ 0.1 mm		oxide porcelain sintered carbides
	afanite (invisibly crystalline)	microcrystalline/microlite/		
		kryptocrystalline/crystalite		
Hypo-crystalline (partly crystalline)		coarse grained	Hypautomorphic (or hypidiomorphic) - partly reatining their own shape (partly regularly bordered)	ceramic abrasive tools, stoneware
		medium grained		silicate porcelain, semivitreous Chinaware, faience, oxide porcelain
		fine grained		
		microctystalline	Xenomorphic (or allotriomorphic) not possessing their own shape) shape of crystals is determined by neighbouring crystals and not by their own natural form)	
		kryptocrystalline		
Glassy			Glasses and products where the glassy phase predominates	
Complex			Materials built from various structura components	composites, ceramsites

NOTE: Pores and their spatial distribution are to be treated as an independent phase.

The rising qualitative and quantitative requirements lead to an evolution of production processes, from the work--shop type to computer-programmed and operated technologies. Thus, there is a need for a schematic representation of the presently dispersed knowledge of ceramics so as to be able to describe quantitatively the ceramic production processes, from the raw materials to the final product.

Such attempts have been made by Glibowski and Swieciski (13), and Lach (21). Glibowski and Swieciski work systematically on the application of the graph theory for the quantitative description of substrates and the fired body structures of ceramic materials, where-as Lach makes attempts to schematically describe the dependence of the properties of ceramics on their structure, process parameters and conditions under which the ceramic materials are used. (Fig. 5).

To properly describe the structure of material, Lach adopts the "zero" phase concept for the pores, including them into phase composition. The diagram (Fig. 5) can be applied for the interpretation of properties of many ceramic materials, for development trends in technology, for substrate selection, and for the introduction of mechanization and automation of the process. In these investigations, the starting point is a proper and full characteristics of the structure of material.

Texture in ceramography is a special case of macrostructure, describing the predomint oriented arrangement of the microscopic body elements and determining its density. Like in the case of natural rocks, texture determines mutual arrangement of identical elements composing for the structure. The basic textures in ceramics are:

compact - with close particle packing, porosity below 1%, not oriented

medium-compact - close packing of particles, porosity 1-4%, not oriented

porous - porosity 4 - 16%

loose - porosity over 16%

lamellar - parallel arrangement of particles.

For ceramics it does not seem necessary, as in petrography, to distinguish more, sometimes very detailed structures and textures. The above mentioned structures and textu-

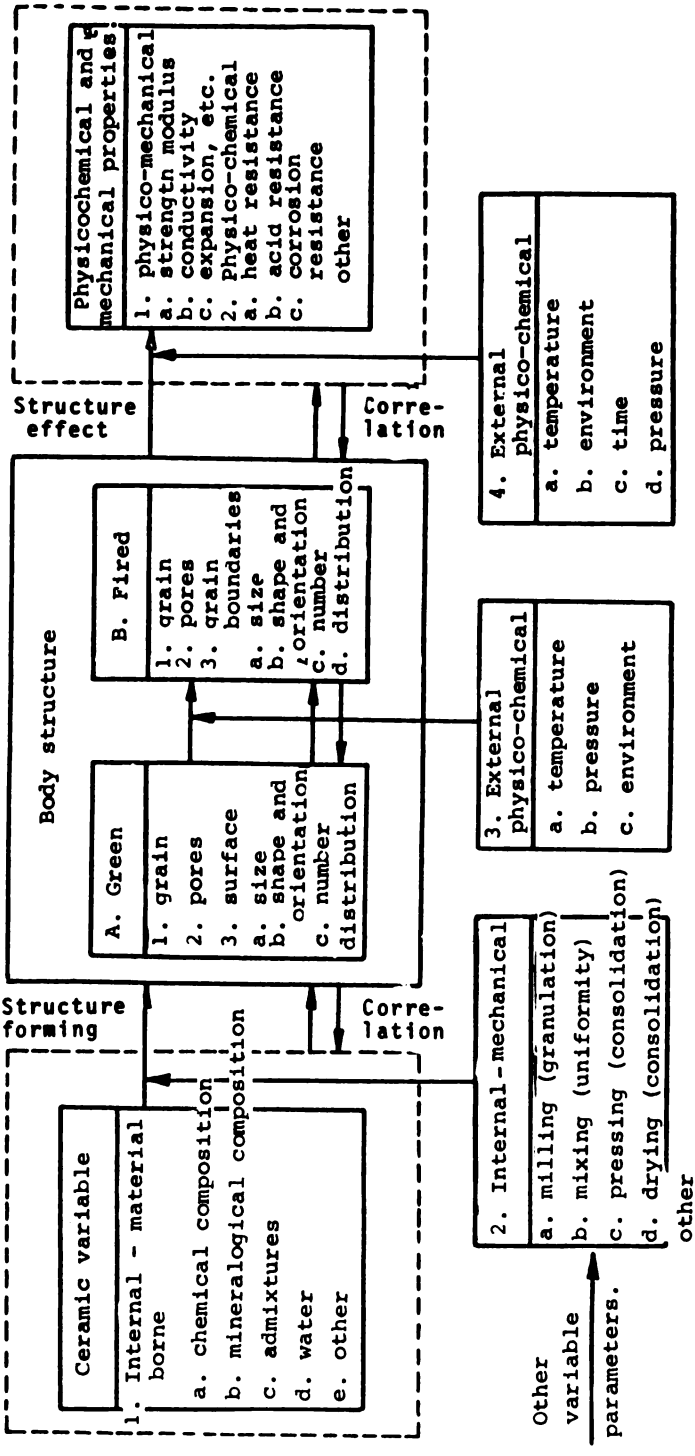

Fig. 5. Schematic representation of dependence of ceramic material properties on its structure, technological production process factors and use conditions (after Lach, 1971).

res adequately describe the technical properties of a material. As a precise classification of materials on the basis of the above systematics is often difficult, mineral and phase composition characteristics determined by other methods will be needed for a full description.

3. Ceramic Materials Systematics Based on their Structural Features

As was already said, ceramic material systematics and nomenclature take little account of structural description and often are controversial. The restrict ed frames of this paper make it harlly possible to fully decribe and discuss this problem. Therefore, we will limit ourselves to a detailed description of a single subgroup presented in Fig.6. We will analyse the nomenclature and structural features of sintered ceramics with a compact structure and porosity below 1%. This group comprises all types of porcelains, sintered oxides, ferrites, sintered carbides, sintered oxides and nitrides, as well as cermets, i.e., almost the whole of special ceramics. Nomenclature used for these materials is often controversial and does not reflect structural peculiarities.

The term porcelain, from the Latin word "porsella", (pearl shell) refers, generally, to sintered ceramic materials fired at temperatures corresponding to the maximum body density and featuring a uniform, compact structure (Salming 34, Bielankin et al 5). Singer and Singer (36) classify as porcelains only the compact-structure sintered materials that are more or less based on a similar alumina-silicate matrix. One could ask, however, the question why the alumina composed of 80,2% Al_2O_3, 16,5% SiO_2 and 3,3% BaO (ultraporcelain) fit the nomenclature, while pure alumina (99,7% Al_2O_3), also white and transparent (Lukalox), are not considered to be porcelains. These controversions have induced Maślankiewicz and Szymański (24) to the unification of their views and to treating as porcelains all the sintered materials of a compact structure, After Milligan (26), they have divided these materials into two main types:

- silicate porcelain

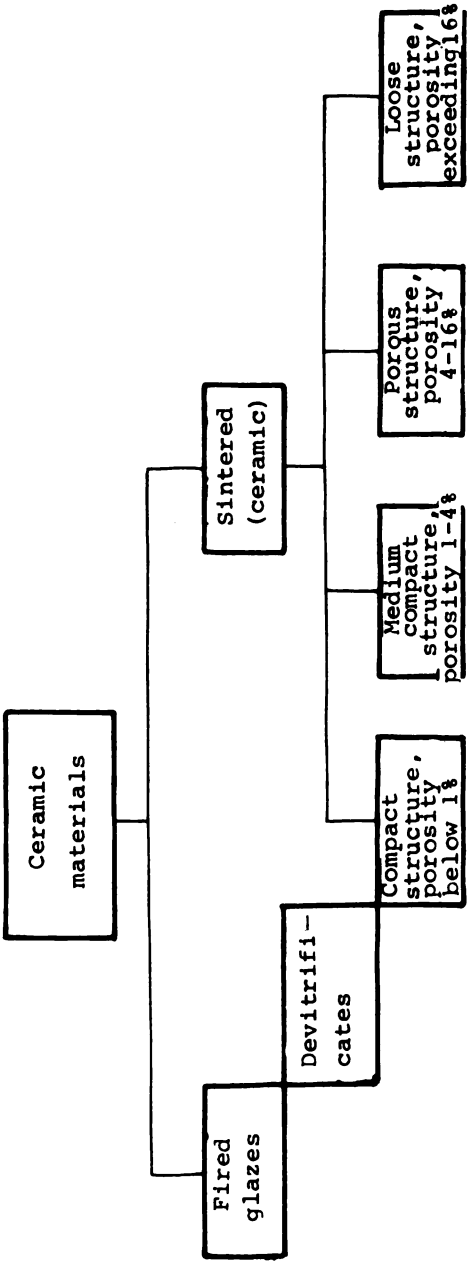

Fig. 6. Schematic division of ceramic materials.

- glass-free porcelain

Milligan's approach assumes that the general term "porcelain" covers any fine-crystalline, compact and strong material, not necessarily containing silicates. He thinks that sintering of some oxides gives materials of similar properties to these of porcelain, free of feld-spar, clay and quartz. He calls them "oxide porcelains" and says, that generally they should be included into the second, glass-free group of porcelains.

According to Miligan, the second group, comprises "oxide porcelain" (provided that their inorganic refractory components are fine-grain crystals of compact and glass-free structure), and, also, the "oxide porcelain cermets", when the cermet consists of oxide porcelain in the continous phase and metal is distributed in a discontinuos manner. Thus, according to Milligan, a subgroup should be isolated and this sub-group should comprise oxide porcelain cermets, carbide porcelain cermets, nitride porcelain cermets, etc. The sub-group should include all the compact, heat-matured ceramic materials made from the inorganic solid phases, if their properties such as hardness, modulus of elasticity, nonductibility, etc. are dominated by the porcelain phase with a crystalline structure. From this statement it results, of course, that cermets can be divided into two groups: porcelain cermets and those having a discontinous ceramic phase, not dominant in determinating material properties. These are the ceramic type materials (metamic - as Milligan calls them) and not the porcelain type ones.

According to Milligan the Cermet porcelain products should not be confused with "sintered" compositions, such as e.g. sintered carbides, where the fine-grained material is cemented by a metal phase or some other phase that disturbs the continuity of ceramic particles. Such an approach permits for the presence of minor amounts of metal (10-15% by volume) both in cermet porcelain and in sintered carbides; but in spite of the identical amount of this phase, its distribution in the structure is different. In the porcelain cermet the ceramic phase is a continous matrix and the metal phase has the form of discontinous particles, whereas in sintered carbide and in other "sintered" materials the ceramic phase particles form a discontinuous element of the structure, the metal phase being a continous matrix.

To conclude these comments, a typical definition of

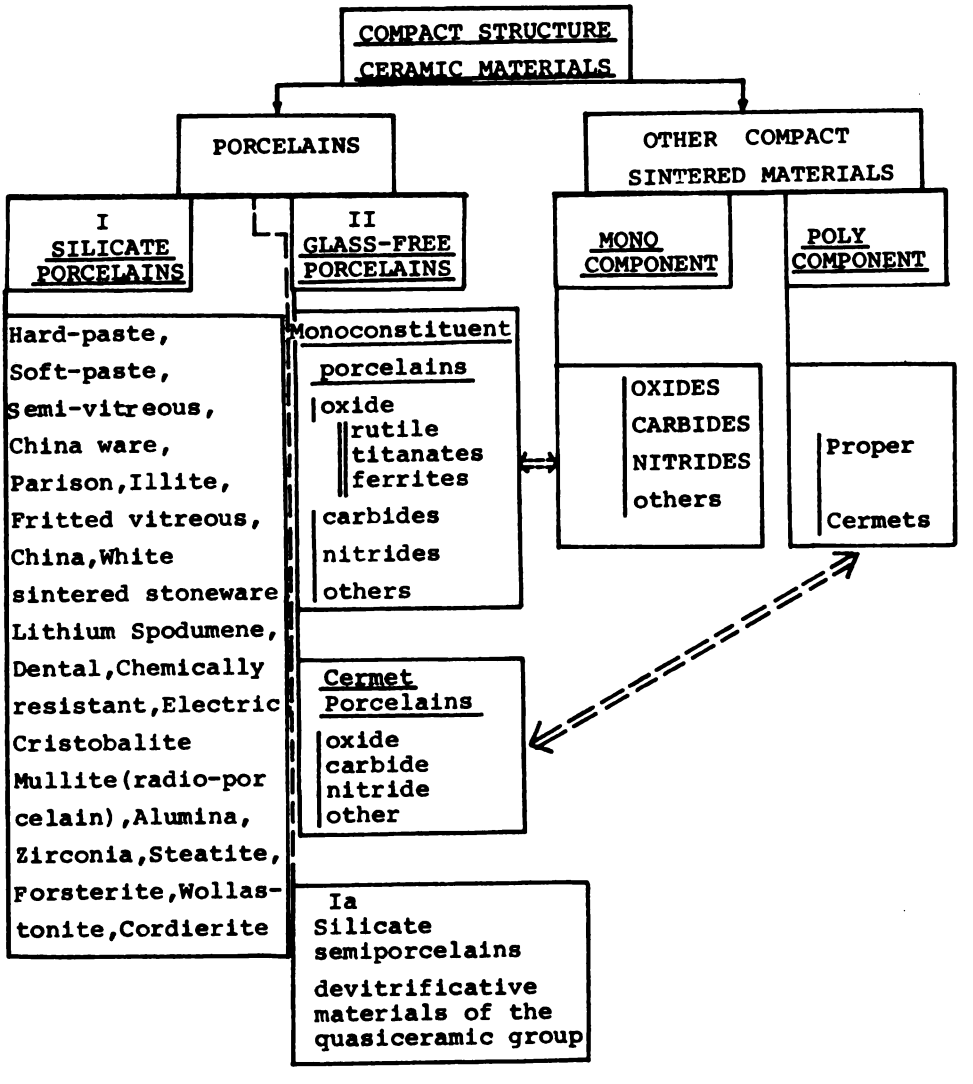

Fig. 7. Schematic division of compact structure ceramic materials according to Milligan (1950).

alumina porcelain cermet (Fig.4) would read as follows: "Crystalline alumina in a material forms the continous phase containing uniformly distributed spherical pores of an average diameter of about 20 and the equally uniformly distributed, irregularly shaped particles of chromium metal of about 10 on the average, spredd in a discontinous way in the porcelain matrix". Referring to Table 1 and Fig. 4, this material should be defined as "alumina porcelain cermet of a hypocrystalline, microaphanite structure, having a xenomorphic shape of its grains".

Fig. 7 shows (after Milligan) the classification of the compact structure ceramic materials.

4. Structural Aspects of Ceramic to Metal Contact Layers

The time and temperature of sintering a metal film layer onto a ceramic base have not only a decisive effect on the quality of the seal, but they also directly affect the depth and the mechanism of diffusion of the metal paste components to the ceramic base.

The mechanism of the metal-to-ceramic sealing has been the subject of many studies and concepts. One of the most sommonly known has been devlloped by Pincus (30), who says that the adherence of metal to the ceramic base is attained through chemical reactions. As an effect of the reaction, managanese metal oxidizes in the water-laden hydrogen atmospheres;

$$Mn + H_2O = MnO + H_2$$

Managanese oxide formed in this way reacts with Al_2O_3 to produce a manganese-aluminate spinel ($MnOAl_2O_3$). Manganese oxide can also react with SiO_2. The low-melting compounds resulting from these reactions wetten the molybdenum grains forming a strong band between metal and the ceramic base.

The chemical reaction concept has been supported by Rawson and Denton (10), who have furthermore stated, that grain size is of a great importance in interface layer formation,with best results obtained for the fine-grain structures.

Cole and Sommer (8) offer a different concept of seal sormation, i.e. one based on the penetration of the ceramic glassy phase to the metal film. The low-melting glassy

phase surrounds and integrates the molybdenum grains of the metal phase, bonding it with the base. The cited authors support their concepts with the results of experimentation showing that seals formed from ceramic containing more glassy-phase (94% Al_2O_3) have a higher strenghh than the ones made of ceramics containing less glassy-phase (99% Al_2O_3). The weakness of this cone cept lies, however, in the simultaneous forming of selas between metal films and ceramics poor in the glassy-phase (e.g. monocrystalline Al_2O3), which indicates to the existence of yet another sealing mechanism.

Floyd (12) investigated the effect of glassy-phase composition and grain size in the ceramic on metal film adherence. Experiments were carried out on 94% Al_2O_3 alumina ceramics. Floyd concludes.that the larger the grain size, the higher the seal strength; thus, for example, for an average grain size of 6 μm, the strength was 4.55 kG/mm^2 and for an average grain size of 25 μm 8.75 kG/mm^2. Also, increasing SiO_2 content in the glassy plase considerably affects the quality of the seal. Thus, Eloyd rather supports Cole and Sommer's concepts. Similar results were obtained by Twentyman (41) - Fig. 8.

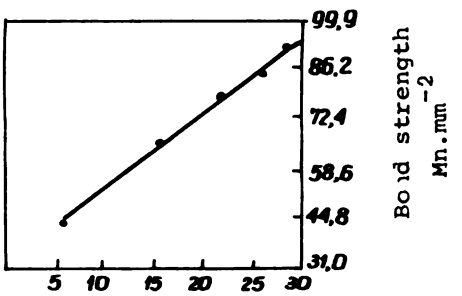

Fig. 8. Dependence of seal strength on grain size in alumina ceramic structure (after Twentyman).

Meyer (25) seeks a seal that would provide a compromise between the chemical reaction approach and the glassy-phase penetration concepts;

- manganese at temperatures below 850°C oxidizes to MnO,
- above 950°C manganese oxide (MnO)reacts with Al_2O_3 and with the glassy phase, forming spinels,
- in the presence of MnO the glassy phase dissolves the spinel,

simultaneously penetrating into the metal film.

Clark, Hench and Bates (7), fully adopting the coexistence between chemical reaction and the glassy phase penetration concepts, state that microfractures in the interface layer constitute additional metal film components transport sources. According to them, microfractures arise from the thermal stress due to differential linear thermal expansion coefficients of metal and ceramic. The stress can be calculated from formula:

$$S_x = \frac{E \cdot \varepsilon_x}{1 - v} + \frac{u \cdot S_z}{1 - v}$$

where

S_x - stress in interface

S_z - stress perpendicular to interface

E_x - strain in interface

E - Young's modulus, equal to $2.5. 10^4$ kG/mm^2

v - Poisson's ratio, equal to 0.25

Cooling of a beryllium ceramic sample from 1475°C and 1650°C produces interfacial stress of 18.977 kG/mm^2 and 13.50 kG/mm^2, respectively.

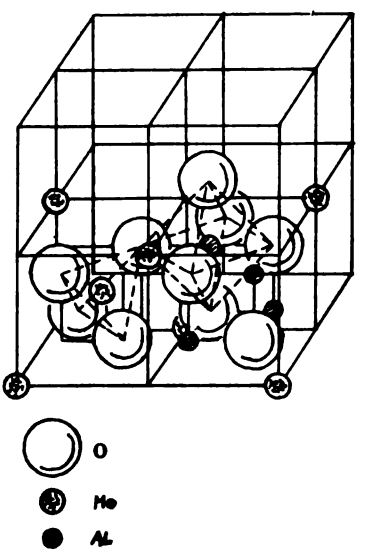

Fig. 9. Elementary $MnAl_2O_4$ spinel cell.

Extensive X-ray investigations of the MoMn and alumina ceramic interface layer, carried out by Hirota (17), show that the aluminate-manganese spinel is formed in the initial sintering stages. An increase in temperature and sintering time reduces its content until it disappears completely at 1450°C Hirota states that with an increase in the temperature and duration of sintering, the spinel lattice constant (Fig. 9) falls due to Mn diffusion from the interface layer, mostly to the glassy phase of the ceramic and, partly, to the metal film. He also states that in the initial sintering stage the manganese-sluminate spinel ($MnAl_2O_4$) is a product of reaction between Mn and Al_2O_3, and not only the glassy phase. However, with the increase in temperature, the spinel dissolves in the glassy phase. Fig.10 shows changes in $MnAl_2O_4$ concentration relative to Al_2O_3 as a function of sintering time. Fig. 11 explains the cause of the

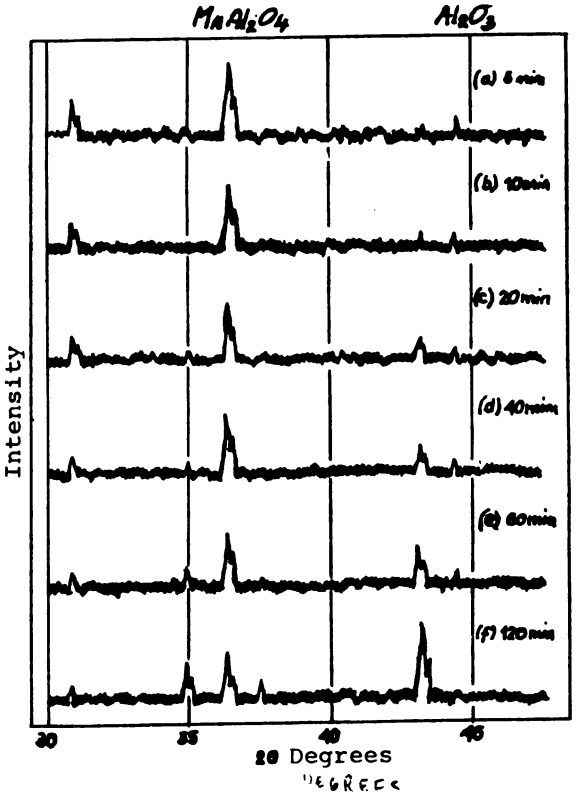

Fig. 10. Changes of Al_2O_3 and $MnAl_2O_4$ concentration in various sintering conditions.

occurence of the $MnAl_2O_4$ spinel in large quantities only at shorer sintering times and temperatures below 1450°C. This results

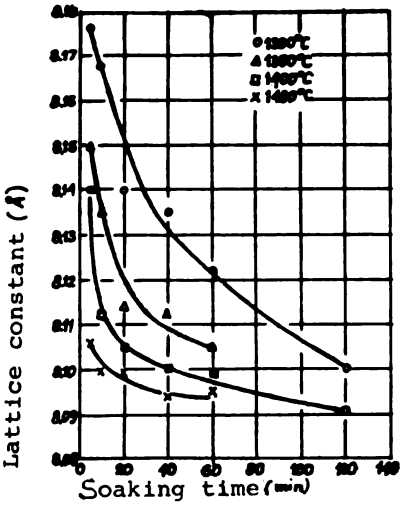

Fig. 11. Lattice constant changes for the $MnAl_2O_4$ spinel as a function of temperature and annealing time.

from Mn ions leaving tetrahedral lattice nodes and diffusing deep into the ceramic, or from the substitution of the manganese ion (Mn^{+2} r = 0.80 Å) by magnesium ions (Mg^{+2} r = 0.65 Å).

Helesson (16) in his numerous studies also points to the formation of the $MnAl_2O_4$ spinel during the MoMn bond-forming process. He annealed, i.a., for two hours a mixture of 28.5% (by weight) of Mn metallic powder with 71.5% (by weight) of Al_2O_3 at 1400°C in a water-laden hydrogen atmosphere. Under these conditions, 100% of the investigated powder were converted into the manganese-aluminate spinel.

Attention of all the cited authors is concentrated on the metal-to-ceramic seal forming processes. Studies carried out at ONPMP (Poland) into the diffusion phenomena in the near-to-surface layers will probably lead to a more precise interpretation of metal to ceramic bonding and to the utilization of diffusion processes in ceramics for other needs. It may seem strange that these diffusion phenomena have not yet been seriously investigated and that the data available e.g. for manganese to ceramic seals can be regarded only as approximate.

It seems that such structural properties as grain size, the distribution of glassy components and the percentage sha-

re (fraction) of grain boundaries highly depend on the kind of substrate materials and on the pressing and sintering of ceramic bodies. Experimental results will thus be scattered over a defined interval.

One of the significatn factors affecting the concentration gradients of the diffusing substrance is its grain size (percenage share of grain boundaries and defects). Thus, for fine-crystalline materials, the share of the boundaries in penetration is higher, which increases the concetrantion of the diffusing elements. The results obtained will therefore refer to definite ceramic materials and their extrapolation to ceramics produced by other techniques will introduce some errors.

Helesson for instance, reveals a deeper MnO penetration in the polycrystalline ceramic material (up to 15 μm after annealing for 10 hours at 1400°C) than in monocrystalline Al_2O_3/6 μm under the same conditions). Different diffusion mechanisms in various materials may be responsible for different penetrations. Helesson's results (Fig. 12) seem, however, be too low compared

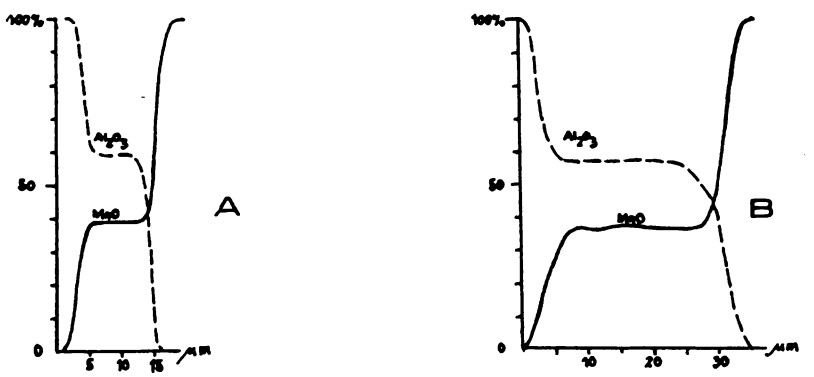

Fig. 12. Depth of Mn diffusion into the ceramic a - for sapphire, b - for alumina ceramic.

to the results obtained by the authors of this paper.

On the basis of own experiments and data available from literature (especially from the contributions by Pincus; Cole, Rawson; Helesson; Meyer; Floyd; and Hirata op. cit.) one can establish the mechanism of forming a stable seal between metal and ceramic as a result of diffusion processes (Włosiński,30).

Managanese and iron diffusion to the ceramic during

the metal sintering stage and at an appropriate concentration, manganese-ferrous-aluminate spinel $Mn_{0,9}Fe_{0,1}Al_2O_4$ is formed. This is accompanied by the diffusion of ceramic components, especially of the glassy type, to the metallic film. The direction of silicon diffusion depends on its percentage content in ceramic and in the mtal film.

As a result of this complex diffusion process, an interfacial layer (proved by X-ray spectroscopy) (50) and consisting of 25% manganese-aluminate spinel phase and 75% amorphous phase, with the predomination of silica, is formed. This interfacial layer is responsible for the strength of the metal to ceramic seal. At the same time, these diffusion processes occurring at h high temperatures and in appropriate protective atmospheres, cause sintering between metallic grains and oxides or the glassy phase. The formation of the interfacial layer takes place during a relatively short period of time (about 15 minutes). A further diffusion during prolonged high-temperature tratment is harmful as it causes lattice constant changes and, eventually also the decomposition of the spinel, a reduction of the seal strenthh, a loss of the metal surface wetting properties by diffusion of glassy components to its furface, and the deterioration of electroinsulation properties of the ceramic due to intensive surface diffusion. The negative effects of prolonged diffusion in seal formation can be positively made use of in the solid state reactions, e.g. while obtaining β-Al_2O_3 from α-Al_2O_3.

5. Review of Metal to Ceramic Sealing Techniques

The vacuum-tight metal to ceramic seals can be produced by one of the following methods:

- powder metallization,
- active soldering,
- diffusion welding,
- glaze bonding,
- simultaneous sintering of metal films and Al_2O_3.

The powder metallization technique is most widely known in practice. Recently, gaining popularity is also the simultaneous metal film and Al_2O_3 sintering process, especially in the production of packages for the monolithic integrated circuits.

Powder metallization technique

The ceramic element is covered with a paste consisting of tungesten and manganese, molybdenum and manganese of ferro-silicon (15) by silk-screening or brushing on, forming a layer 10-35 μm thick. The methods of applying the paste, and its composition have been extensively studied, but even today the paste additives are kept secret by almost all the ceramic to metal seals producers. Some of the more known and published metallization paste compositions are given in Tbble 2.

Most widely used is the paste consisting of 80% Mo and 20% Mn, developed in 1950 by Nolte and Spruek (29). The existence of a great veriety of pastes can be attributed to the need of metallization of alumina ceramics, significantly differing from each other by chemical composition (Al_2O_3 content 90-99%) and sintering temperature (1450-1850°C). Substitution of elements (t (tungsten, titanium) by their carbides (WC, TiC) invreases the strength of the seal. Still, according to the opinion of one of the authors (47) of this paper, chemical composition has a minor effect on seal strength, which depends, first of all, on stress distribution in the ceramic, and on the strength of the interface layer.

Paste coating is sintered after drying in a water--laden hydrogen atmosphere (dew point +15°C) for 5-30 minutes at 1200-1650°C, depending on the chemical composition of the paste and the type of the ceramic. The effect of sintering conditions (type of protective atmosphere, time, temperature, type of ceramic) on interface layer formation was studied in detail, and will be discussed below (48, 49, 39, 15).

To improve the solder wetting properties, the metal film is additionally covered by a second layer often consisting of iron and nickel. This second layer is about 6-12 μm thick (1/3 thickness of the first layer). The iron paste is sintered at 1070°C in dry hydrogen (dew point - 20°C). Fig. 13 shows the structure of such metal to ceramic seal, obtained by metallization with a paste consisting of 69,8% W, 15% Mn, 0.2% Ni and 15% lithium glass).

Active solder technique

The active solder techniques utilize Zr, Ti and Mn

Table 2

Chemical composition of pastes for ceramic metallization

No	Chemical composition, % by weight																
	W	Mo	Mn	FeSi	WC	TiC	Co	Ni	Fe	TiO_2	SiO_2	MnO_2	MoO_3	Y_2O_3	WO_3	MnO	lithium glass
1.	69,8		15					0,2									15
2.		80	14	6													
3.					78	16	6										
4.		80	20														
5.		95								5							
6.		80									20						
7.		64	10									4	15				
8.	90													10			
9.										5					90	5	
10.		78	20							2							
11.	99									0,5				0,5			
12.		80	15					3								2	

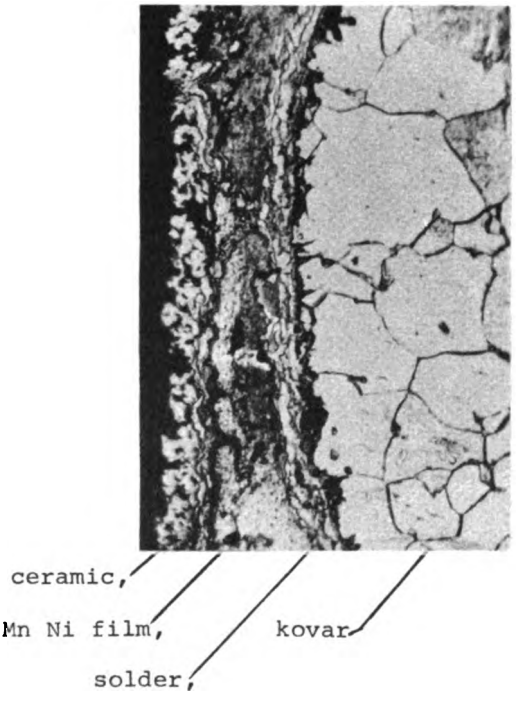

Fig. 13. Structure of a seal obtained by the powder metallization technique.

as conventional solders. At high temperatures the metals actively diffuse into the ceramic. Soldering takes place in a c vacuum, jin very pure hydrogen or argon.

There are many methods of introducing active metals. The one most often used is the Bandley (2) TiH_2 hydride method developed in the fifties. It is based on spreading a 10-20 μm TiH_2 film on the ceramic. After bringing together the ceramic and metal with the use of appropriate solder, it is soaked in a vacuum furnace. Active seals are received at pressures of 1.10^{-5} Tr and at temperatures up to 1100^0C. During heating, titanium hydrogen, which partly reduces Al_2O_3 and improves the composition of residual gases in the vacuum space. Reduced aluminium with titanium forms a high-strength interface alloy. The photomicrograph (Fig. 14) illustrates the interface layer structures obtained by this method.

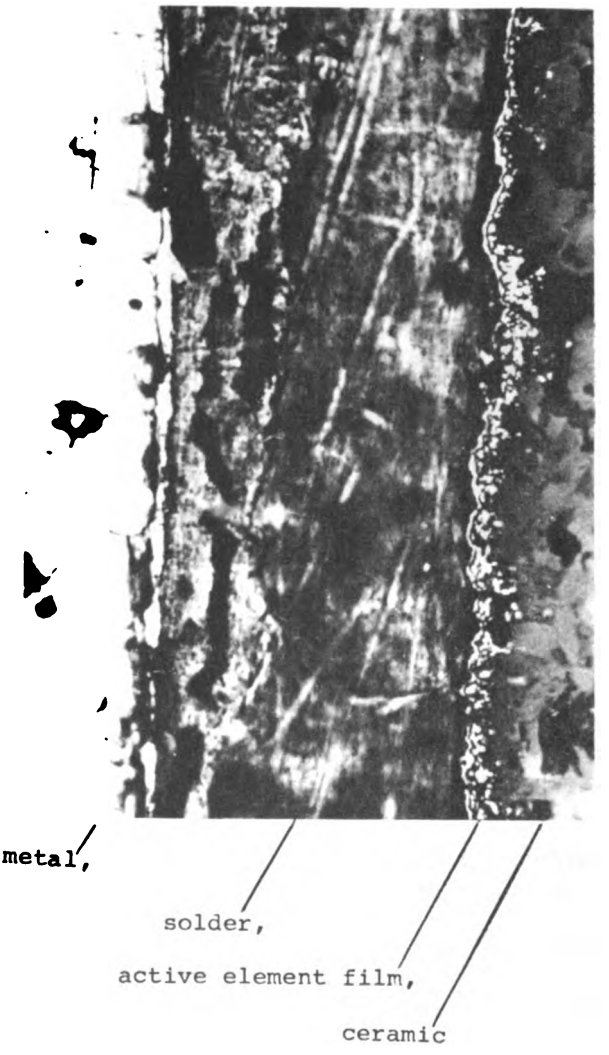

Fig. 14. Structure of a seal obtained by active soldering technique.

Diffusion welding technique

Seals are obtained through simultaneous action of pressure and temperature, where the load can be applied in vacuum furnaces, under prot ective gas atmospheres and, even, in the quenching salts. According to Jaroszew (19), optimum ceramic to copper seal process parameters in a hydrogen atmosphere are: pressure - 1,6 kG/mm^2; temperature - 1000 - 1030^{o}C welding time - 10-15 min; hydrogen dew point - +5 to +15^{o}C.

Process parameters for the method developed at ONPMP (38) for the diffusion vacuum welding of alumina ceramics containing 97.5% Al_2O_3 with copper are: pressure - 0.1 kG/mm^2; temprerature - 900^{o}C; vacuum - 3.10^{-5} Tr; welding time - 15 min. These process conditions give vacuum-tighz (leakage 1.10^{-8} Tr(s), te thermal-shock resistant (within the range from - 60 to +200^{o}C) and mechanically strong seals. Fig. 15 shows an alumina ceramic to copper seal obtained by the diffusion welding technique.

The interface layer formation mechanism has been

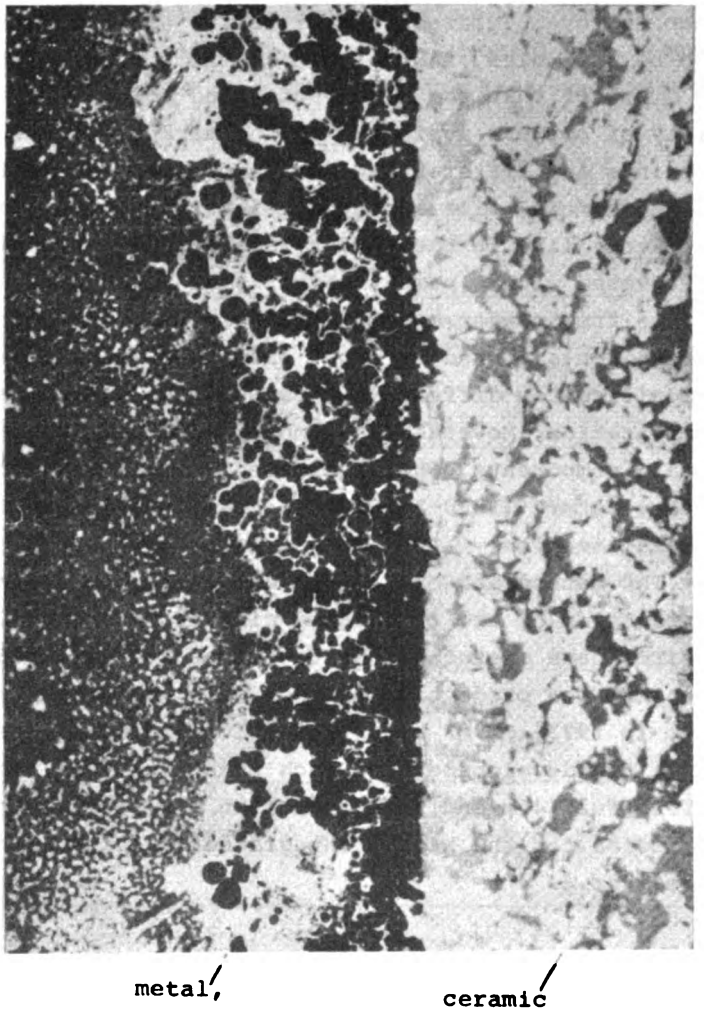

Fig. 15. Ceramic to metal seal structure obtained by the diffusive welding method.

studied by many authors (18, 20). Nevertheless, up to now there is no evidence clearly favouring the diffusive character of the bonding. The authors´opinion is that the problem could be solved by applying more precise investigation methods (e.g. the isotopic method).

Glaze bonding technique

This technique was applied recently in the production of microelectronic element housings. The glaze film (glaze solder) is sprayed on the metal and ceramic elements to be connected: the film is then sintered (glazed) and, finally, after mounting the housings to be assembled, they are bonded at a temperature which is some 40°C higher than the glaze softening point. There is a great variety of solders available on the market, with various softening points and different thermal expansion coefficients.
The simultaneous metal film and Al_2O_3 sintering technique

Here, like in the powder metallization technique, the ceramic is covered with a paste, which is sintered afterwards.The method differs from powder metallization in that the paste is applied on green non-sintered ceramic. Also, the paste chemical composition significantly differs from that of the pastes used for powder metallization. Nevertheless, molybdenum and tungsten remain to be its main components. The simultaneous metal and ceramic sintering temperature (1550-1750°C) is considerably higher than in powder metallization.

The method has been found especially valuable for the mass production of the integrated circuit packages. Only a few world firms have mastered this technique and employed it in mass production. The production process belongs to the best-guarded secrets. In 1973, ONPMP begun intensive collective research work aimed at the developement of such technique. The research s stage was fruitful (46) and the production - by this method - of the cermet bodies for the highly integrated circuits is being started this year.

Basic Requirements for Cermet Bonds

Cermet seals and bushings must fulfil many stringent requirements: they must be vacuum - tight, weather-resistant (high

and changing humidity, saline fog, temperature fluctuations) and must feature adequate insulation resistivity.

One of the most important properties for the housings and bushings is a high strength of the seals (resistance to abrupt temperature changes, tensile and torsional strength). Some of the technical requieements for seals are specified in Table 3. The problems of seal tightness and reliability have been studied by Taczanowski (40).

The strength of a housing or bushing is not only a basic feature of a good product, but also a measure of the correctness of the technological process. Mechanical strength of the housings is tested in almost all checking measurements.

Table 3

Some Requirements for Cermet Housings

Requirement	Housings for			
	Power diodes and SCRs	microwave semiconductor elements	integrated circuits	opto-electronic elements
Insulation resistance	1.10^{12} ohm	1.10^{9} ohm	1.10^{11} ohm	1.10^{11} ohm
Thermal shock resistance	from - 60°C to + 200°C	from - 50°C to + 150°C	from - 65°C to + 155°C	-
Bending strength	2 kGm	2.5 kg bending force	-	-
Tensile strength	200 kG	-	0.5 kG per terminal	0.5 kG per terminal
Tightness	10^{-8} Tr/s	10^{-8} Tr/s	10^{-8} Tr/s	-
Materials used	97.5% Al_2O_3 Cu kovar, steel	97.5% Al_2O_3 Cu kovar	97.5% Al_2O_3 kovar	95% Al_2O_3 kovar

Most cermet housings and bushings operate under dynamic heat loads or carry external mechanical loads. In one of the papers (43), the effect of heating and colling on stress was investigated, with an assumption that the physical properties of material are constant and the heat expansion coefficients of constructional materials are identical. Temperature distribution was investigated and the stress on the power diode packages was calculated under stnndard temperature fluctuation within -60°C and +200°C.

Temperature distribution within the seal was measured by the Cu-Ni microthermo-couples mounted inside the package walls (Fig. 16). Temperature measurements for a single heating and cooling cycle are presented in Fig. 17. From temperature differences, assuming that E and v are constant the thermal stress during a single cycle was calculated for the cermet bond. Calculations were based on the following formula:

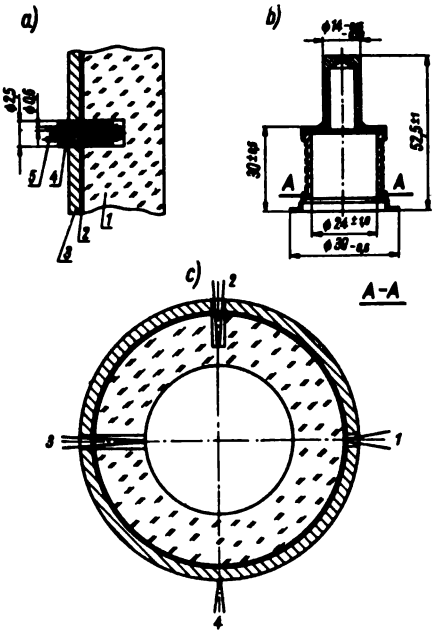

Fig. 16. The tested diode body and arrangement of thermocouples a) thermocouple mounting, 1 - aluminium block, 2 - hard metallization folm, 3 - kovar ring, 4 - insulation tube, 5 - thermocouple; b) thermocouple arrangement scheme, 1, 2, 3, 4 - microthermocouples.

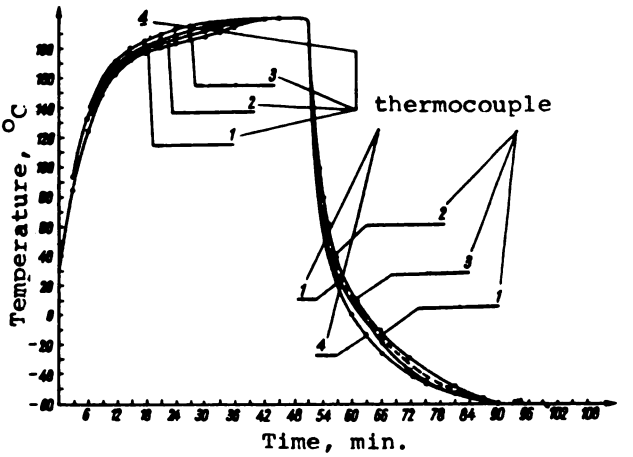

Fig. 17. Temperature changes during a single cooling and heating cycle for a cermet body.

$$\zeta_\theta = \frac{\alpha E}{1 - v}\left(\frac{1}{r^2}\right)\left(\frac{r^2 - a^2}{b^2 - a^2}\right)\int_a^b t.r.dr +$$

$$+ \frac{\alpha E}{1 - v}\left(\frac{1}{r^2}\right)\int_a^r t.rdr - \frac{E}{1 - v}\left(\frac{1}{r^2}\right) t.r^2$$

where:

α - thermal expansion coefficient ($\alpha_{ceramic} = \alpha_{kovar}$), $1/^oC$

E - Young's modulus = 235344 MN/m^2

v - Poisson's ratio = 0.25

a - package internal radius = 11.5 mm

b - package external radius = 15.5 mm

r - radius of interface bonding = 15,2 mm

t - temperature, ^oC.

Integrals have been calculated planimetrically. Calculation results are given in Table 4 and in Fig. 18.

The knowledge of the thermal stress values simplify the designing of the development of technological processes and the determination of critical working conditions.

After numerous investigations and experiments, Arthur (1) has stated, that most favourable technological parameters for sintering a paste containing 90% Mo and 10% Mn, are: temperature - 1540^oC; sintering time - 12 min; protective gas atmosphere -

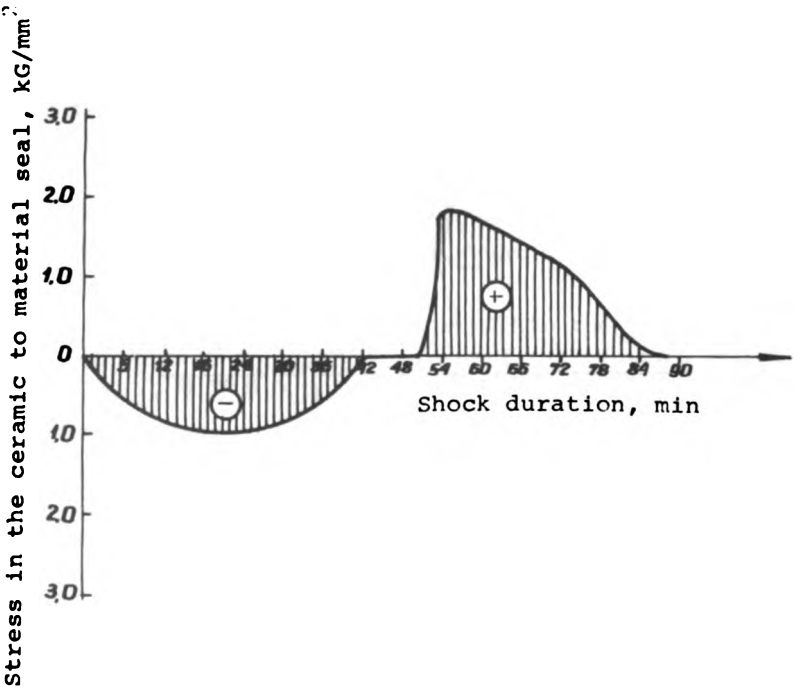

Fig. 18. Stress changes in the bond during a thermal shock.

25% H_2 + 75% N_2. The bonds obtained in this way have a strength of about 14,70 kG/mm^2.

7. Some Own Technological and Structural Investigation on Cermet Bonds

C

The main subjects of research work in this field cover: modern bond forming techniques, structure of bonding materials and bonding mechanisms.

Micrescopic investigation of ceramic materials in use in Poland

Mosti videly used in Poland is

Alumina ceramics, Al19, containing 97.2% Al_2O_3; 1.6% SiO; 0.8% Fe_2O_3 and 0.4% of TiO_2 + BaO + MgO + NaO is the ceramic material commonly used in Poland. Its properties are the following: bulk density 3.75 g/cm^3; water absorbability 0%; compressive strength 2000 kG/cm^2; dielectric constant at 20^{o}C and

3MHz 9.0; linear expansion coefficient $\alpha_{20}^{200} = 68.10^{-7}$ 1/°C, $\alpha_{20}^{800} = 83.10^{-7}$ 1/°C, $\alpha_{20}^{500} = 81.10^{-7}$ 1/°C; lateral resistivity 10^{14} ohm/cm at 20°C, 5^{11} ohm/cm at 300°C, 5^{10} ohm/cm at 500°C, 5^{7} ohm/cm at 800°C; dielectric strength 40 kV/mm; specific heat

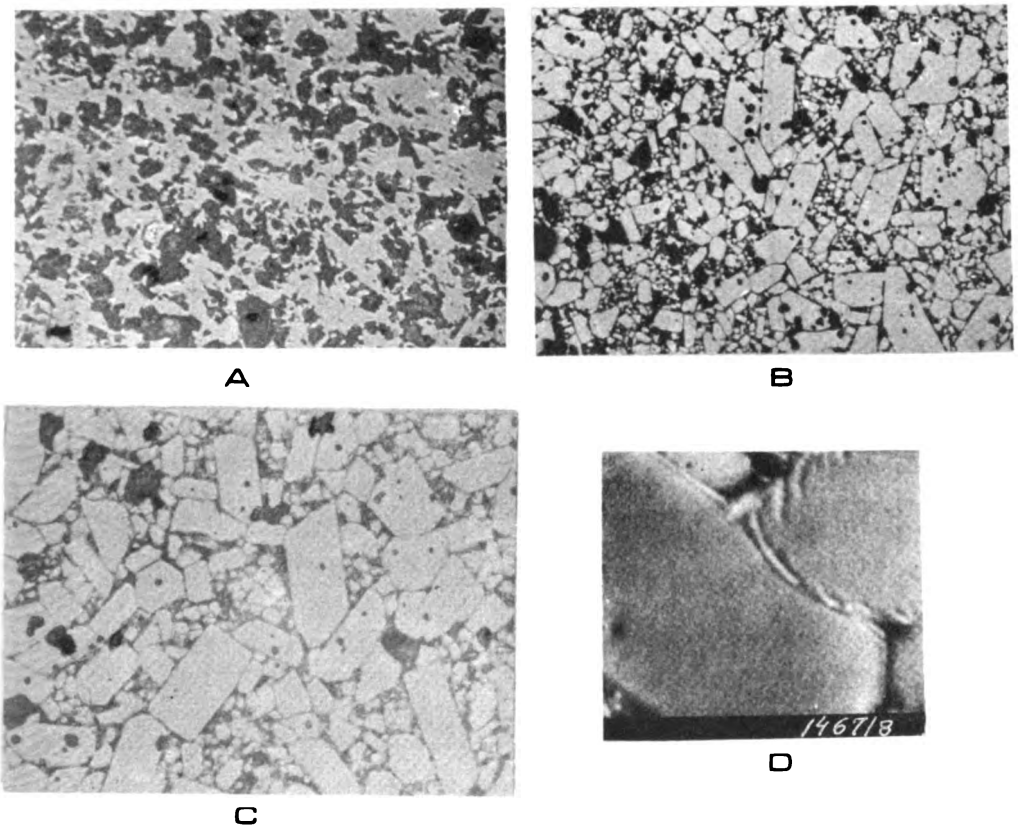

Fig. 19. Structure of alumina ceramic: a - unetched alumina ceramic. b - the same alumina ceramic etched thermally for 1 hour under vacuum 5.10^{-5} Tr at 1450°C, magnification x 250; automorphic and fine-grained fenerocrystalline structure can be seen. c - As above, magnification x 500; among automorphic grains the hypautomorphic alumina and the glassy phase can be seen. d. - the same alumina ceramic, thermally etched (1450°C, 1hour, 5.10^{-5} Tr) seen under a scanning microscope, magnif. x 1000; alumina grain boundaries can be seen.

0.21 cal/g.°C; Young's modulus $3.3.10^4$ kG/mm^2.

The optimum sintering temperaturs for this ceramic is 1750°C. The structure of Al19 alumina ceramic is shown in Fig.19. The percent fraction of grain boundaries and glassy phase (50) is 13.67%; fraction of pores 0.14%. The glassy phase in Al19 ceramic is discontinous.

The second ceramic material used in the research work is polycrystalline aluminium oxide - lukalox, containing 99.98% Al_2O_3; 0.003% MgO; 0.003% CaO; 0.003% SiO_2; 0.003% Na_2O; 0.001% TiO_2; 0.1% Y_2O_3 and 0.2% MgO additionally introduced into the mass. This material is sintered and recrystallized at 1850°C. The basic properties of this material are bulk density 3.98 g/cm^3; bending strength 2500 kG/cm^2; Young's modulus 3.3 - 4.4 . 10^4kG/mm^2.

The polycrystalline structure of Al_2O_3 is shown in Fig. 20. The percent fraction of grain boundaries is 2.78%; the amount of pores is equal to zero (50).

The third material, used in diffusion investigations in the boundary layer, is monocrystalline Al_2O_3 - leukosapphire. Its

Table 4 Calculated Stress as a Function of Time in a Single Colling and Heating Cycle (32)

Time min	Stress kG/mm^2
0	0.00
9	-0.736
24	-1.036
54	+1.814
60	+1.520
72	+1.200
78	+0.700
90	0.00

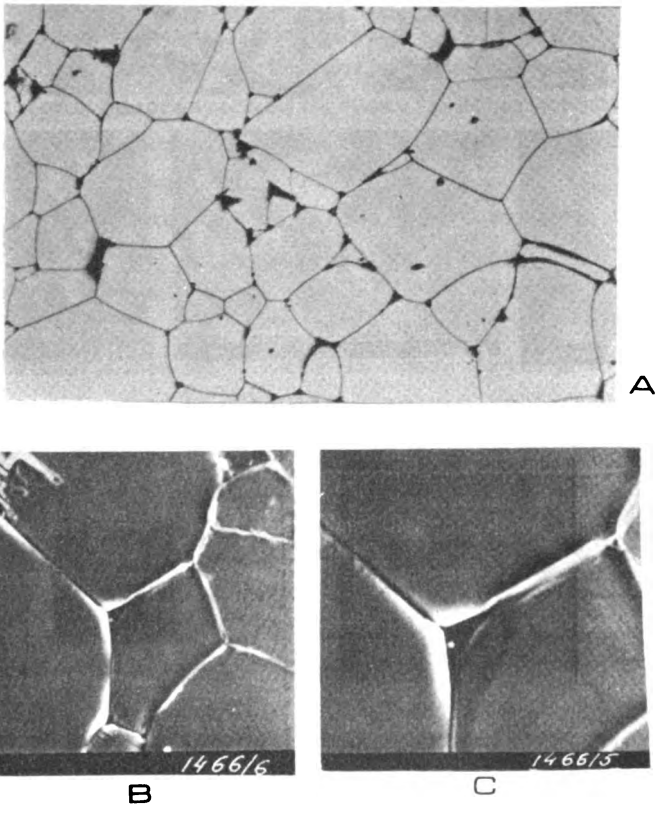

Fig. 20. Thermally etched Al_2O_3 polycrystalline structure (1450°C, 1 hour, 5.10^{-5} Tr). a - metallographic microscope (x200), b and c - scanning microscope (x500 and x 1000).

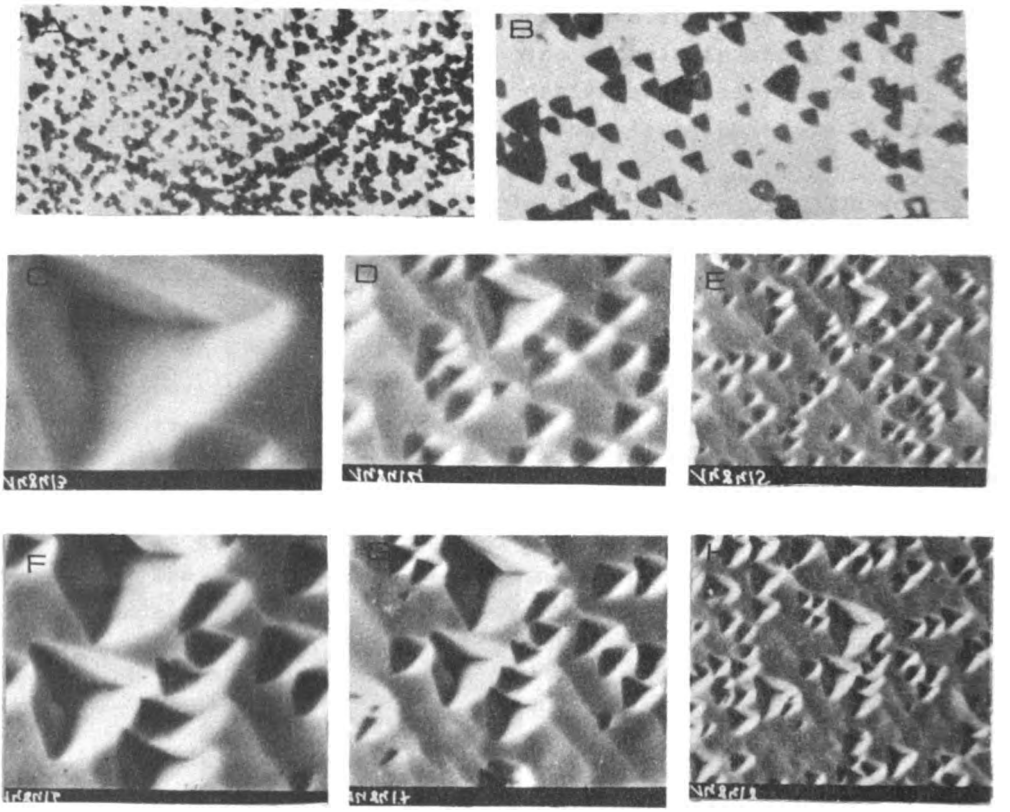

Fig. 21. Monocrystalline Al_2O_3 - leucosapphire thermally (1h, 1700°C) and chemically (concentrated H_3PO_4, 25 min., 420°C) etched. Dislocation cavities on the 0001 surface can besseen. a - Density 5.06 cm^{-2} (except the central band) scanning microscope photomicrograph (x200)
Small cavities $\bar{A} = 274.10^{-7}$ mm^2; $N = 404893$ $1/cm^2$.
Large cavities $\bar{A} = 1150.10^{-7}$ mm^2; $N = 73195$ $1/cm^2$;
in all $4,8.10^{-5}$
cm^{-2} metallographic microscope photomicrograph (x450)
c. scanning microscope x 500
d. scanning microscope x 1000
e. scanning microscope x 500
f. scanning microscope x 3000
g. scanning microscope x 1000
h. scanning microscope x 5000

basic properties are as follows: bulk density 3.98 - 4.01 g/cm^3; heat conductivity 0.004 cal/cm.s. ^oC/at 20^oC/; compressive strength 4060 kG/cm^2; dielectric constant 11 /at 10 GHz/; lateral resistivity 10^9 ohm/cm /at 900^oC/; defect density $4.8.10^5$ - $5.06.10^5$ 1/cm^2, with the number of defects of an average area of 274.10^{-7} mm^2 was 404893 per sq. cm. and of an average area of 115. 10^{-7} mm^2 was 73105 per sq. cm. Leucosapphire structure after thermochemical etching is shown in Fig. 21, with the dislocation lines entering the area under investigation, 0001.

Fig. 22 illustrates the results of ceramic and metal interface for MoMnFeSi (50). Several additional methods were utilized for verification purposes. Microscopic investigation of microstructure gives the linear distributions of Mn, Mo, Fe and Si with a visible shift of Mn and Si concentration maximums in the interface (results obtained by the electron probe method). Manganese additionally exhibits non-uniform distribution in the ceramic, which testifies to its diffusion along grain boundaries and glassy regions. Results obtained by two methods are, however, not sufficinet for a precise determination of boundary diffusion coefficients, and for the investigation of the interface structure.

A proof of maximum Mn concentration in the interface is given by the photometric analysis of a radiograph shown in Fig. 22. ^{54}Mn radioisotope investigations give more precise results than those obtainable by the electron probe method, due to the elemination of the linear distribution errora caused by accidental grain boundary arrangements, defects and grain sizes. Owing to this, the radioisotope investigation results enable the exact calculation of diffusion coefficients for various diffusion mechanisms including boundary diffusion. For the pairs of materials under study, i.e. leucosapphire; and MoMnFeSi; alumina ceramic Al 19 and MoMnSi, the following results were obtained:

For leucosapphire annealed for 50 h at 1280^oC

$$D = 2.2.10^{-13} \text{ cm}^2/\text{s}$$

for alumina ceramic annealed for 50h at 1180^oC

$$D_I = 4.86.10^{-9} \text{ cm}^2/\text{s}$$

(intergrain diffusion)

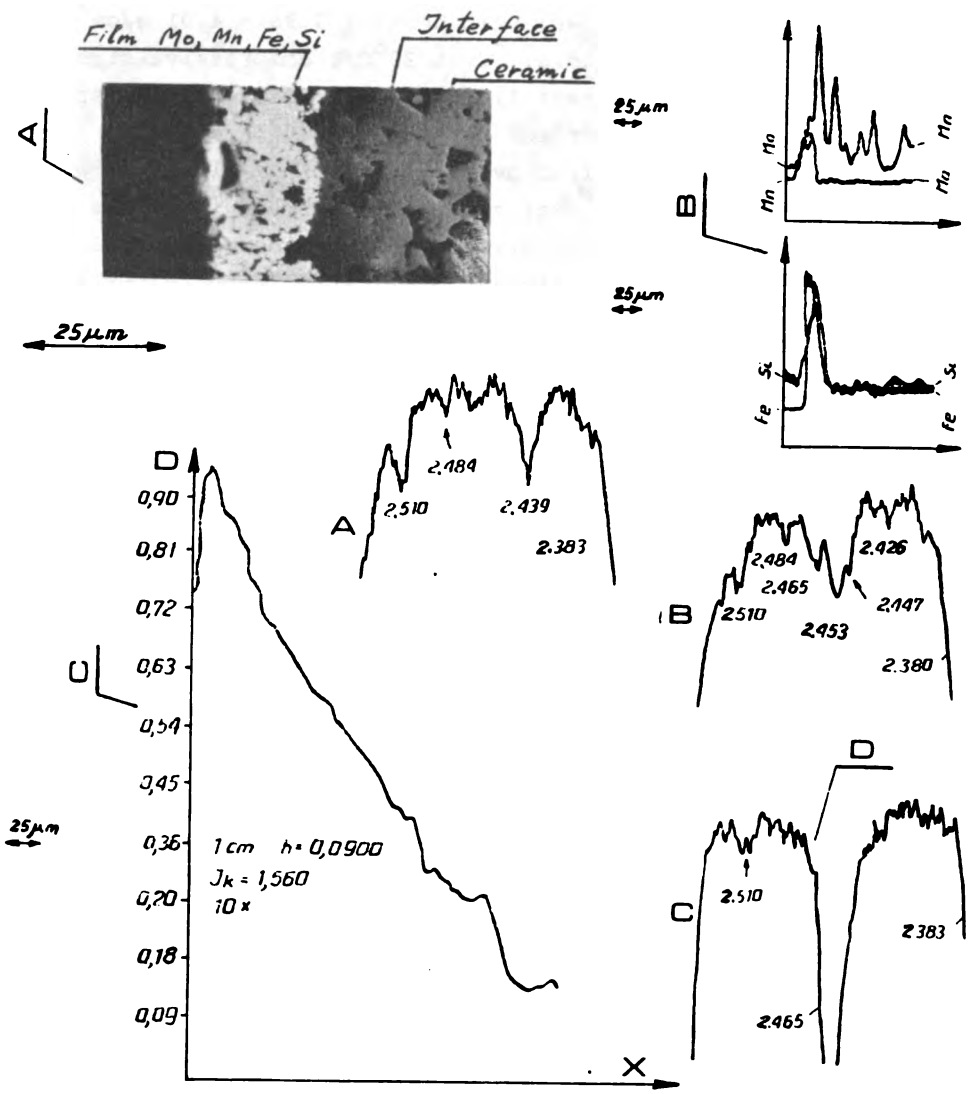

Fig. 32. Interface investigation results.

a - Ceramic to metal seal microstructure received from microscopic studies.

b - Linear Mo, Mn, Fe and Si distributions received from electron probe studies.

c - Autoradiograph fotometric curve of the ceramic to metal seal.

d - X-ray diffraction micrograph (A - ceramic, B - interface, C - Mo, Mn, Fe, Si film).

$D_{II} = 3.10.10^{-10}$ cm^2/s

(valume diffusion)

for alumina ceramic annealed for 50h at 1280°C

$D_I = 3.5.10^{-8}$ cm^2/s

$D_{II} = 6.8.10^{-10}$ cm^2/s

$D_p = 2.0.10^{-7}$ cm^2/s

(surface diffusion)

The results of autoradiographic investigations show maximum Mn concentrations at the interface, testifying to the existence of reactive diffusion in that region.

The X-ray structure investigations confirm the existence of differences between ceramic, metal and interface structures (Fig. 22). X-ray structurography and X-ray spectroscopy enable the investigation of the interface structure which has been found to be a manganese-iron-aluminate spinel $Mn_{0.9}$ $Fe_{0,1}$ Al_2O_4. Determined was also the composition of lthis layer (25% spinel and 75% of amorphous substance). Determination of composition by other methods was not possible.

All of the above mentioned methods can be applied successfully for the investigation of the alumina ceramic to metal seals, the information obtained in this way being, however, fragmentary and not sufficient for a full description of the interface layer and for drawing conclusions be concerning the optimization of technological processes on the basis of these results. Optic microscopy and electron probe methods give only a merely qualitative description of microstructure and of the linear or surface distribution of elements. A detailed investigation of diffusion mechanisms, structure and chemical composition of the interface will only be possible using the more elaborate radioisotope, X-ray structurography and X-ray spectroscopy methods.

References

1. Arthur M.E., Fussel L.E.: Cer. Bull. 50, 12, (1971)
2. Bandley R.J.: Ceramic Age 58(1), 15(1951).

3. Baumann H.N.(1956) Am Cer. Soc. Bull. 35(9), 358-360.
4. Baumann H.N.: (1958), Am. Cer. Soc. Bull. Vol.37(4),171-84.
5. Bielankin D.S., Iwanow B.W., Lapin W.W.: (1957). Petrografia kamieni sztucznych, Wyd.Geol. Warszawa.
6. Budnikow P.P., Gieworkin H.O.(1973) Obzig farfora. Moskwa.
7. Clark D.E., Hench L.L., Bates S.R.: Cer.Bull.vol.53,6(1974).
8. Cole Sommer G.: J.Am.Cer.Soc., 44(6) (1961).
9. Dennis J.G. (1967)International Tectonic Dictionary. Pub. by Committee on Structural Nomenclature. Tulsa, Oklahoma.
10. Denton E.P., Rawson H., Trans. Brit.Ceram.Soc., 59(2) (1960)
11. Drzewiecki P., Jakowlew B., Osuch Z., Piela E., Włosiński W., zgłoszenie patentowe nr UP-0-172, 175, 15.04.1974 (patant application).
12. Floyd J.R., Am Ceram Soc.Bull., 42, 2 (1970).
13. Glibowski E., Swiecicki Z. (1975) Ceramika, Politechnika Wrocłaeska, Wrocław.
14. Gołajewski Z., Materiały Elektroniczne 7 (1974).
15. Grudzinski J., Drozdz T., Badania strukturalne polaczen ceramika-metal. Sprawozdanie z prac ONPMP (1975).
16. Helesson C., Investigation of the bonding mechanism between metals ceramics. Trous. Chelmers, Univ. Techn. Gotenburg, Sveden 1966.
17. Hirota M., Trans. JIM, vol. 9 (1968).
18. Izycki B., Ph. D.Dissertation, Politechnika Warszawska (1974).
19. Jaroszew W.K., Mietalokieramiczeskoje wakumnoplytnyje konstrukcje, Energia, Moskwa 1970.
20. Kazakow N.F., Diffuzjonnoje spajanije w wakumie mietalow, splawow i niemetaliczenkich materialow. Moskwa 1970.
21. Lach V., (1971), Sklar e keramik, 21(12) 314-317.
22. Levin E.M., Robbins C.R., McMuridie H.F., Phase diagrams for ceramic, Amer.Cer.Soc. Columbus, Ohio 1964.
23. Lundin S., (1958), Triaxial porcelain, Stockholm.
24. Maslankiewicz K., Szymanski A., (1976) Mineralogia stosowana. Wyd. Geol. Warszawa.
25. Meyer A., Ber.Deut.Keram Ges. 42, 11(1965).
26. Milligan L.H., (1950) Bull.Am.Cer.Soc., 29(4) 154-157.
27. Morozewicz J., (1925), Mineralogia i petrografia T.V s. 119. Warszawa.

28. Muszkat W., Metalizacje wysokotemperaturowe ceramiki alundowej. Sprawozdanie nr 15 z prac ONPMP (1974).(research report)
29. Nolte H.J., Spurek R.F., Television Eng., 1, 14, 11(1950).
30. Pincus A.G., J.Am.Ceram. Soc. 36(5)(1953).
31. Presnow W., Kieramika i jejo spoi s mietalom w tiechnikie. Atomizdat, Moskwa 1969.
32. Radziszewska E., Sprawodzanie nr 13 z prac ONPMP (1973). (research report)
33. Ryshkewitch E., (1960) Oxide Ceramics. Academic Press, New York.
34. Salmang H., Die physikalischen und Chemischen Grundlagen der Keramik. Berlin (1954).
35. Saltykow S.A., (1970) Stereometriczeskaja mietallografia, Moskwa.
36. Singer F., Singer S.S. (1963) Industrial Ceramics, London.
37. Szymanski A., (1972), Post. Nauk. Geol. z. 4 Wyd. Geol. Warszawa.
38. Taczanowski A., Materialy Eletroniczne 7, (1974).
39. Taczanawski A., Testing of metal to ceramic seal parameters. ONPMP Research Report No 15 (1972).
40. Taczanowski A., Wlosinski W., Kulesza T. Metal to ceramic seals. Paper presented on RWPG conference on November 1971 (paper 3/72).
41. Twentyman M.E., Jour. of Materials Science 10 (1975).
42. West M.E., Cray T.L., Chimia i Technologia Silikatow, 5(1959).
43. Wlosinski W., Olesinska W., Kujawa E.: Wykorzystanie techniki sitodruku w obudowachdo mikroelektroniki. Mikroelektroniczna technika warstwowa. Wyd. WSJ Rzeszów 1973, s. 187-191.
44. Wlosiński W., Materialy Elektroniczne, 1(1972).
45. Wlosiński W., Olesinska W., Maliszewski B., Materialy Elektroniczne, 4 (1973).
46. Wlosinski W., Adamiec M., Jakowlew B.,Maliszewski B., Muszkat W., Olesinska W. m Monoliryczne obudowy do uladow scalonych duzej skali integracji., Sprawozdanie z prac ONPMP (1975).

prac ONPMP(1975). ONPMP Research Report.
47. Wlosiński W., Olesińska W., Piela E., Opracowanie technologiczno-konstrukcyjne obudów do diod mocy. Sprawozdanie z

prac ONPMP 1975. ONPMP Research Report.
48. Wlosiński W., Materialy Elektroniczne, 1(1975)
49. Wlosiński W. Szklo i Ceramika, 7(1975).
50. Wlosiński W., Zjawiska dyfuzyjne w granicznych warstwach polaczeń ceramika-metal w aspekcie optymalizacji technologii, Prace wlasne ONPMP, Warszawa 1976 (w druku). Investigation Report (in print).
51. Zalwski E., Sprawozdanie z prac ONPMP (1972). ONPMP Research Report.